TRANSIENT RESPONSE OF HEATED SANDWICH COMPOSITE STRUCTURES WITH DIFFERENT CORE MATERIALS

GEÇİCİ REJİMDE UYGULANAN ISITMANIN FARKLI ÇEKİRDEK MALZEMESİNE SAHİP SANDVİÇ KOMPOZİT YAPILARIN DİNAMİK KARAKTERİNE ETKİSİ

ENES ERKAN KISA

ASSOC. PROF. DR. BİLSAY SÜMER

Supervisor

Submitted to

Graduate School of Science and Engineering of Hacettepe University

as a Partial Fulfilment to the Requirements

for the Award of the Degree of Master of Science

in Mechanical Engineering.

2020

To my lovely wife, Elif Bürümlü Kısa

ABSTRACT

TRANSIENT RESPONSE OF HEATED SANDWICH COMPOSITE STRUCTURES WITH DIFFERENT CORE MATERIALS

Kısa, Enes Erkan
M.S., Department of Mechanical Engineering
Supervisor: Assoc. Prof. Dr. Bilsay Sümer

July 2020, 129 pages

Sandwich composite structures are widely preferred in modern aircraft exterior and interior structures because of their lightweight and high strength capability. Aircraft structures might be exposed to harsh thermal environments during their operational life arising from aerodynamic heating, solar radiation or engine. The exposure to thermal environment affects the mechanical properties and modal parameters of aircraft structures.

In this study, the effects of core structure on dynamic characteristic of sandwich composite structure is examined under transient thermal condition by using the thermal experimental modal analysis method. As test specimens, seven sandwich composite test plates are manufactured from aluminum, nomex and glassfiber core materials, which have different core structure parameters. The transient thermal environment is applied to one face of the test plate while the structure is excited with white noise vibration excitation. The responses of the test plates are recorded during heating process, and then analyzed by MATLAB to define modal parameters of the test plates at different temperature values.

The test results showed that, under transient thermal environment, as the core cell size increased, the natural frequency decrease rate of the test plate increases and the damping of structure became more sensitive to temperature. The first natural frequency of the hexagonal and the OX-Core affected in same rate, but in the end of the test period, the second mode of the OX-Core was equal to initial value while the third mode decreased more than the third mode of hexagonal core. The damping ratio of the hexagonal core was more sensitive to thermal environment than the Ox-Core damping ratio. The study on the effect of core thickness showed that, the dynamic characteristics of sandwich structure became more sensitive to thermal environment as the core thickness increased. The change rate of natural frequencies and damping ratios were the highest for the thickest core. The results also showed that, each core material type affected from thermal environment differently and the dynamic characteristics of the test plate with Nomex core was the most sensitive while the glassfiber core affected less than the other core materials when heated with 3 °C/s heating rate. As the heating rate decreases, the change rates in natural frequency decrease for Nomex while increase for glassfiber and aluminum core. The change in glassfiber core is lower than other cores at each heating rate. The FRF responses of each test plates decreased under the effect of transient thermal environment.

Keywords: vibration analysis, sandwich composite structure, honeycomb core, experimental modal analysis, thermal modal analysis

ÖZ

GEÇİCİ REJİMDE UYGULANAN ISITMANIN FARKLI ÇEKİRDEK MALZEMESİNE SAHİP SANDVİÇ KOMPOZİT YAPILARIN DİNAMİK KARAKTERİNE ETKİSİ

Kısa, Enes Erkan
Yüksek Lisans, Makina Mühendisliği Bölümü
Tez Yöneticisi: Doç. Dr. Bilsay Sümer

Temmuz 2020 , 129 sayfa

Sandviç kompozit yapılar, düşük ağırlık ve yüksek mukavemet kabiliyeti nedeniyle modern hava taşıtlarının iç ve dış yapılarında sıklıkla tercih edilmektedir. Hava taşıtları, operasyonel koşullar altında, aerodinamik ısınma, solar ışıma yada motor kaynaklı zorlayıcı termal koşullara maruz kalabilmektedir. Fakat termal koşullara maruz kalan yapıların mekanik özelliklerini ve modal parameterlerini etkileyebilmektedir.

Bu çalışmada, çekirdek yapısının termal koşullar altında sanviç kompozit yapıların dinamik karakterine etkisi deneysel termal modal analiz yöntemi ile incelenmiştir. Bu amaçla, aluminyum, Nomex ve cam lifi malzemeleri kullanaraak farklı çekirdek yapılarına sahip yedi adet sandviç kompozit plaka üretilmiştir. Hava taşıtlarının yaşaması muhtemel bir geçici rejimli termal koşul, test plakalarının bir yüzüne uygulanırken, plakalar beyaz gürültü ile tahrik edilmiştir. Uygulanan tahriğe yapıların tepkileri kaydedilmiştir ve MATLAB paket programı kullanılarak kaydedilen veri çözümlenerek, yapının modal parametreleri farklı sıcaklıklarda tespit edilmiştir.

Çalışma sonuçlarında, geçici rejimli termal koşul etkisiyle birlikte, çekirdek hücre boyutunun artmasıyla doğal frekans düşüş oranınının arttığı ve yapının sönümleme katsayısının sıcaklık değişimine daha hassas olduğu gözlemlenmiştir. Altıgen ve OX-Core hücre şekline sahip çekirdek yapıların ilk doğal frekasnının aynı oranda etkilendiği ama test sonunda OX-Core hücre yapısına sahip yapının üçüncü doğal frekansı daha çok azalırken, ikinci doğal frekans değeri değişiklik göstermemiştir. Altıgen hücre yapısının sönümleme katsayısı, termal koşullar altında, OX-Core yapısının sönümleme oranından daha hassastır. Çekirdek kalınlığının dinamik karaktere etkisinin gösterildiği çalışmada, çakirdek kalınlığı arttıkça yapının dinamik karakterlerinin daha çok etkilendiği, doğal frekans ve sönümleme oranındaki değişikliğin en kalın çekirdek yapısına sahip plakada en fazla olduğu gözlenmiştir. Çalışma ayrıca çekirdek malzemesinin, termal koşullar altında yapının dinamik karakterine farklı oranlarda etkilediğini, 3 °C/s ısıtma oranında ısıtıldığında, nomex çekirdek malzemesinin dinamik karakter değişim oranlarının en fazla cam yünü çekirdek malzemesinin dinamik karakter değişim oranının da en az olduğu göstermiştir. Isıtma oranı düşürüldükçe Nomex malzeme dinamik karakter değişim oranlarının azaldığı, diğer malzemeler için ise arttığı ve tüm ısıtma oranlarında en az etkilenen çekirdek malzemesinin cam yünü olduğu gösterilmiştir. Her test plakasının frekans tepki fonksiyon büyüklüğünün, geçici rejimli ısıtma etkisi ile birlikte azaldığı gösterilmiştir.

Anahtar Kelimeler: titreşim analizi, sandviç kompozit yapı, balpeteği çekirdek, deneysel modal analiz, termal modal analiz

ACKNOWLEDGMENTS

First of all, I would like to express my thanks to my academic advisor Assoc. Prof. Dr. Bilsay Sümer for his priceless guidance and motivation provided me during the thesis study. I would also thank to my thesis committee members, Assoc. Prof. Dr. Çağlar Başlamışlı, Assist. Prof. Dr.Ing. Okan Görtan, Assist. Prof. Dr. Selçuk Himmetoğlu and Assist. Prof. Dr. Emrecan Söylemez who provided valuable feedbacks and suggestions.

I would like to thank Okan İspir, Umut Susuz, Evren Sakarya, Mustafa Sercan Karcı and Aysun Doğangün and my teammates in "Aeroelasticity and Structural Dynamics" team in Turkish Aerospace for their technical advices and motivation provided me during the thesis study and my graduate education.

I would like to express special thanks to my parents, Birgül and Erol. They have always supported and motivate me throughout my educational life. I always feel their love and support by me.

I am sure about that I would not complete my thesis study without support of my lovely wife, Elif Bürümlü Kısa. I am very grateful for her love and endless support.

TABLE OF CONTENTS

List of Tables

TABLES

List of Figures

FIGURES

LIST OF ABBREVIATIONS

EMA	Experimental Modal Analysis
DMA	Dynamic Mechanical Analysis
PEEK	Polyether Ether Ketone
CCM	Cell Core Model
OCCM	Orthotropic Continuum Core Model
FRF	Frequency Response Function
ECG	Euro-Composites Glassfiber
FEA	Finite Element Analysis
CLPT	Classical Laminate Plate Theory
CMC	Ceramic Matrix Composite
FEM	Finite Element Model
FFT	Fast Fourier Transform
kW	kiloWatt

CHAPTER 1

INTRODUCTION

1.1 Motivation and Problem Definition

Composite materials have an importance in aeronautical industry and the usage rate in primary, secondary and interior structural parts of aircrafts is increasing continuously. Composites are combined materials formed by the bonding of minimum two materials to meet a mechanical and structural requirement. These combined materials could be any engineering materials. In aeronautical industry, special carbon or glass based fabric layers are mostly preferred to produce composite structures. Composite structures provide high strength and stiffness to weight ratios and have better fatigue performance against isotropic materials [9].

Composite structures have advantage in manufacturing process and they can be manufactured in complex geometries by using less number of rivets and fasteners. This deduce to weight of structure and increase the flight performance and maneuverability of air vehicles. In addition, the weight saving in aircraft design is an effective parameter to lower the fuel consumption rate. These advantages of composite materials make them one of the most popular aircraft structural material. For example, the "Airbus A350 XWB" is a civil aircraft and more than %50 of structural parts produced from composite materials 1.1.

One of the most valued composite material types is the sandwich composites. A sandwich composite structure produced by connection of a core material with face sheets by adhesives or brazing. In a sandwich construction, the face sheets take the bending loads while core structure provides high shear and compressive strength. In engineering application, the core structure could be in three different forms; honeycomb,

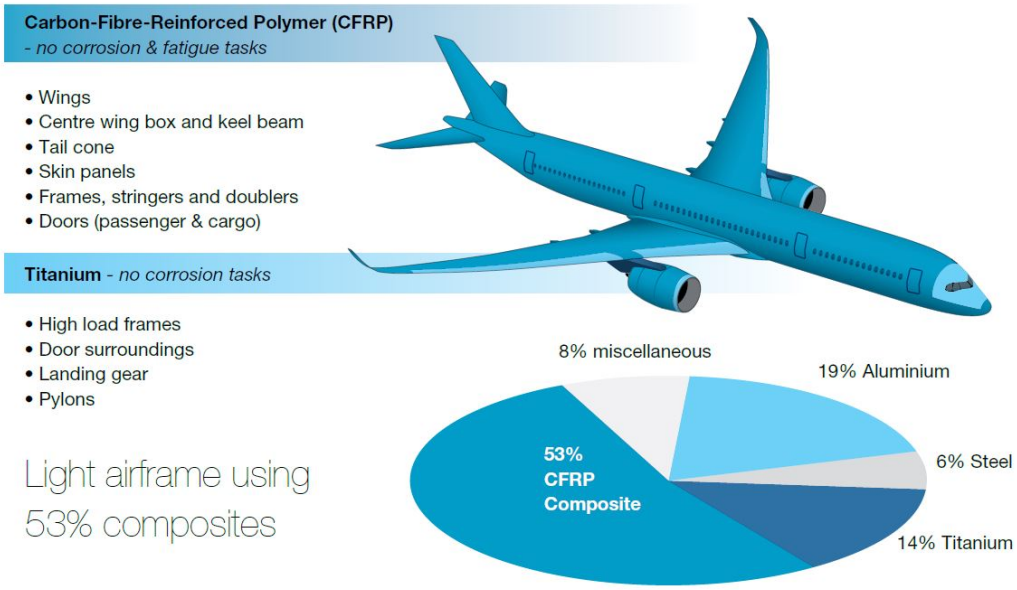

Figure 1.1: The composite material usage in Airbus A350 XWB [1]

foam and balsa[10]. The honeycomb form is the most popular core structure in aeronautical industry because of their high strength-to-weight ratio and applicability on curved surfaces. Honeycomb core structures can be manufactured from aluminum, stainless steel and titanium, KRAFT paper (softwood), KEVLAR® (para- aramid), NOMEX® (meta-aramid), TYVEK® (high density polyethylene), plastic foams, or fiberglass[10]. The honeycomb core is named because of hexagonal cell geometry shape. They can be produced in different cell shapes to response specific needs.

In addition to their mechanical advantages, the sandwich composite structures could provide thermal insulation, high noise insulation and high vibration damping, magnetic shielding, fire and water resistance, corrosion resistance or impact energy absorption when using with appropriate core materials.

The capabilities of sandwich composites are make them suitable for primary and secondary structural elements of aircrafts. Especially, the sandwich composite structures are widely preferred in aerodynamic surfaces [5]. During operational life, the aircraft structures could face with harsh thermal and dynamic conditions. Aerodynamic friction, solar radiation and engine could increase temperature of structures and with increasing temperature, the mechanical properties of the components of sandwich structures could change[10] . The change in mechanical properties directly affects

the stiffness of the structure and modal parameters of sandwich structures change. If the changes in modal parameters are not well defined in design phase, it could increase the risk of resonance, flutter or any other aeroelastic problems.

In this study, the effects of core structure on modal characteristic of sandwich composite structure is examined under transient thermal condition by using the Experimental Modal Analysis (EMA) method. As test specimens, seven sandwich composite test plates are manufactured which have different core structures but the same carbonfiber face sheets. The selected core materials are widely preferred in the aeronautical industry.

1.2 Proposed Methods and Models

In this study, an experimental modal analysis (EMA) method is used under elevated thermal environment, which simulates aircraft thermal environments. With this method, the modal parameters like natural frequency and damping ratio of sandwich composite plates with different core materials are investigated at increasing thermal environment and the changes in modal parameters are presented. To use in test, three different sandwich composite plates are produced by using aluminum honeycomb, glassfiber honeycomb and nomex honeycomb core materials in 400*400 mm dimensions. Each test plate is tested by the proposed test procedure in Section 3.5 to see effect of core material on modal parameters change under elevated thermal conditions.

1.3 Contributions and Novelties

The contributions of the thesis study are:

- A new test platform and a test procedure are investigated to perform EMA under thermal environmet is developed.
- The effect of core material type on modal parameters under thermal environment is defined.

- The effect of different heating rate is compored.
- The effect of cell size on modal parameters under thermal environment is examined.
- The effect of core thickness on modal parameters under thermal environment is examined.
- The effect of cell shape on modal parameters under thermal environment is examined.

1.4 The Outline of the Thesis

The study is presented in five Chapters. In the Chapter 1 the moral of thesis and problem definition is given. The method and contributions to literature is presented. In the Chapter 2, the literature review is briefly summarized.In the Chapter 3 the methodology of the current study is summarized. The test platform and the test plates are described. The developed test and data analysis are explained in detail. In Chapter 4, the test results of each test plates are presented with related figures and tables. In Chapter 5, the study is concluded and a general discussion on the study and intended future works are given.

CHAPTER 2

LITERATURE REVIEW

The relevant literature is discussed in three sections. Firstly, the studies on heating sources of aircrafts are shown. Secondly, the effect of temperature on mechanical properties of isotropic and composite materials are summarized. Lastly, the studies on the effect of heating on modal parameters are presented.

2.1 The Heating Sources

Kaye[11], in 1950, prepared a numerical study that showed the transient temperature distribution on wing structure caused by supersonic speeds of aircraft. The study performed on a basic, wedge-shaped wing model between 1.4 to 6 Mach speeds. The numerical methods were presented by heat flow calculations in both two-dimensional and one-dimensional (normal to the chord of wing). Both methods revealed the same temperature distribution along the wing. Therefore, the one-dimensional heat flow differential equations can be applicable to calculate temperature distribution of thin wing structures at supersonic flights. The study has indicated that as the speed of aircraft increases, the temperature of the wing also increases.

Monaghan[12] conducted a study on the analytical methods for preliminary estimates of the aerodynamic heating rates in high speed flight by using intermediate enthalpy approximations. The results showed that aerodynamic heating rate increases with the increase in speed.

Van Driest[13] performed a study to show the main causes and effects of Aerodynamic Heating in 1956. In this study, it is stated that, the fluid particles that flow over

the body creates a thin layer and the kinetic energy of fluid particles turns into heat because of friction. As aircraft speed increases, the kinetic energy of flow and the transferred heat into body also increases. The aerodynamic heating affects the aerodynamic performance of aircraft. To overcome negative effects of the aerodynamic heating, several methods are proposed in the study.

Rohacs et al. [14] performed a study on small aircrafts that have small gas turbine engine to examine the infrared radiation that affects on the aircraft. In the study, the temperature distribution of aircraft skin and engine parts was measured by using infrared thermal cameras. In the results, with the effect of radiation sources, the aircraft skin temperature can reach high values.

2.2 Temperature Dependent Mechanical Properties

As stated in the literature, the temperature over the aircraft skin can be reach high values as the flight speed increases. This phenomenon arises another problem for composite aircraft structures. The mechanical properties of composite structure would change with temperature. The temperature dependent mechanical properties of composite materials can be obtained by using Dynamical Mechanical Analysis (DMA) method.

In 1950's, the effects of thermal stress on rigidity of structures were investigated by extant researches [8][9][10] . These researches showed that the increasing temperature reduces the structural rigidity and could affect modal characteristic of structures.

Daryabeigi[15] also examined the effects of adhesive thickness, thermal conductivity and emissivity on the heat transfer performance of sandwich panel in the range of 250-500K. The core and face sheets were different titanium alloys and to bond the face and core together, a polyamide adhesive film on a woven glass carrier is used. In addition to the Swann-Pittman model, the effect of adhesive layers was included to numerical calculations. The radiation and conduction were modelled by using the finite volume method. The numerical model has been also validated by the other published experiments. It was found that the adhesive layer significantly affected the heat transfer performance through the honeycomb core panel. The adhesive layer

increases the contact area between face and core wall, and provides higher thermal conductivity than the conductivity value between bare core wall-face sheet contacts. The adhesive layer has also higher emissivity rate than face sheets, which increases the radiation heat transfer between the faces. As the thickness of adhesive layer increases, the thermal conductivity also increases.

Fatemi and Lemmen[16] conducted a study on the computation of effective thermal and mechanical properties of a honeycomb sandwich panel. To calculate thermal conductivities of structure, they used an alternative method of Swann-Pittman method with Gebhart factors. In the study, they used both the detailed honeycomb sandwich structure model and the equivalent laminate structure model, which are prepared for the finite element analysis. It was shown that equivalent laminate structure exhibited the same thermal and thermomechanical behaviors with the detailed model. They show the heat not only through the thickness conducted but also through to lateral direction of panel.

Melo and Radford[17][18] performed an experiment with DMA method to inspect temperature dependent viscoelastic properties of unidirectional fiber reinforced PEEK/IM7 composite structure. It was demonstrated that, in the transverse direction, the property of elastic modulus did not change and the other mechanical properties such as elastic modulus in lateral direction, shear modulus and Poisson's ratio decrease with increasing temperature in the test temperature range. The test was conducted on the 8-plied specimen between 20-120 °C temperature range with 3°C/s temperature increase rate.

Liu and Zhao[19] have studied the role of honeycomb core geometric parameters on vibration properties of sandwich composite panels. They performed both computational and experimental methods to predict modal characteristics of the structure. They used aluminum honeycomb core with two different thickness value and aluminum face sheets to product sandwich composite structure. In computation methods, the Cell Core Model (CCM) and Orthotropic Continuum Core Model (OCCM) were used and the results were congruent with the experimental results. They stated that, the shear moduli affect the natural frequencies of the same mode by changing the mode shapes.

Aklilu, Adali and Bright[20] have examined the effects of temperature on mechanical

properties of Carbon, Glass and Hybrid Polymer composite specimens. In order to test, the specimens were heated from 25 °C to 140 °C and mechanical properties with respect to the temperature were calculated by Dynamical Mechanical Analysis method. The results indicated that, the stiffness value of test specimens decreases with the increase in temperature. In addition, damping properties of glass, carbon and glass epoxy specimens have higher damping values as the temperature increases.

2.3 Effect of Heating on Modal Parameters

In literature, the increase in temperature leads decrease the mechanical properties of structures. These changes directly affect the stiffness of structure. The stiffness is the key parameter to define modal characteristics such as natural frequencies, mode shapes and damping values. The modal characteristics of aircraft structures must be defined in design and analysis processes. The structure must be away from vibration environment of aircraft in order to avoid vibration-based failures (e.g., flutter, resonance and vibration fatigue). There are studies on the effects of thermal environment on modal parameters.

Early research on the effect of heat on the modal characteristic of structures was conducted in 1950's and these researches showed the significance of this effect to define the exact behavior of aircraft structure under actual operational conditions.

Vosteen and colleagues[21] performed an experiment on simple cantilever plate to examine the effect of heating on vibration characteristics in 1955. The study showed the changes on only the first torsion and bending mode. In the research, aerodynamic heating was simulated with carbon-rod radiators along the longitudinal edges of cantilever beam solid wing model. The encountered rapid aerodynamic heating reduced the stiffness of the wing, and non-uniform temperature distribution led to plate buckle torsionally and increased the deflection of the wing under steady-state loads while decreased the natural frequencies. The stiffness change of plate with the increasing temperature was calculated with small-deflection theory and energy method. As the temperature differences along the wing increased, theory became invalid.

Vosteen and colleagues[22] took one-step further over their previous research and

performed a test on three different wing structures to see the effect of transient heating under various heating conditions. They determined the stiffness change of the wing structures by measuring the natural frequency changes, and then performed theoretical calculations to compare test results. They see that near thermal buckling temperature values, the natural frequencies are remarkably changed.

Dryden and Duberg[23] conducted a study on the effect of aerodynamic heating on aeroelastic characteristics. It was found that, the increasing temperature created thermal stress on the structure and reduced the structural stiffness, which could influence aeroelastic behavior. For example, the "flag-waving" type flutter mode occurred because of aerodynamic heating. "General Discussion" part of the study highlighted significant effects of the aerodynamic heating on structure with the comments of Sir Arthur Hall, Dr. Von Karman and other important scientists.

Runyan and Jones[24]' experimental and analytical study also concerned with flutter of a solid wing under effect of aerodynamic heating. In study, a solid aluminum-alloy cantilever wing model was tested at 2 Mach speed at cold test condition and there was no flutter. When the test was conducted in 800 °F (426 °C), torsional stiffness decreased and a short period of flutter occurred.

In 1991, Kehoe and Snyder[25] released a thermoelastic vibration test technique procedure and applied these techniques on a test plate. As test plate, they used a rectangular 7075 aluminum plate. The test plate was hanged in front of a heat array and the plate heated on one side while experimental modal analysis was performing on the plate. The study showed that, as the temperature of the plate increases, the natural frequencies and FRF magnitudes decrease while the damping ratios increase. Later, Snyder and Kehoe[26] released an another study and performed a finite element analysis(FEA) that correlated with test results of EAL and STARS in-house programs. In the FEA, both thermal stresses and temperature dependent mechanical properties were included to analytical calculations. Two years later, Kehoe and Deaton[23] performed tests on the three same-sized test plates that manufactured with different material types. The comparisons showed that each plate resulted same outcomes.

Kim [27] developed a theoretical method to investigate vibration characteristics of initially stressed functionally graded rectangular plates, which consist metal and ce-

ramic materials in a thermal environment. In this study, the effects of the material composition ratios, the plate geometry and the temperature field on the test plates were investigated. To obtain the frequency equation of the method the Rayleigh-Ritz procedure was used. The effect of temperature on vibration characteristics of structure increases as the metal composition ratio increases.

Vangipuram and Ganesan[28] have examined the vibration and damping characteristics of sandwich composite structure under thermal loads by using finite element method. The sandwich composite structure consisted from stiff layers and isotropic core materials. In the results of study, the natural frequencies decreases with increasing temperature and mode shifts could occur at certain ply-angles. The ply angle directly affected the decrease rate of natural frequencies with increasing temperature The most effective ply angle was depend on the selected boundary conditions.

Jeyaraj Padmanabhan and Ganesan[29] presented a study on the vibration and acoustic response characteristic of an isotropic rectangular test plate with different boundary conditions in a thermal environment by using a finite element method. In the study, with increasing temperature, the vibration response of the plate increased and reach maximum when it reached to the critical buckling temperature.

Jeyeraj, Ganesan and Padmanabhan[30] presented numerical studies on the effect of thermal environment on vibration and acoustic response characteristics of a composite plate with inherent material damping. Firstly, they defined the thermal environment and the effect of increasing temperature to structure modelled as pre-stress. Then, the critical buckling temperature was defined. Under the effect of pre-stress, the natural frequencies of plate were calculated for each time step during heating and vibration response of structure is calculated. Calculations were done by FE method that based on Classical Laminate Plate Theory (CLPT). As the result of study, the vibration response of the composite structure decreased with increasing temperature.

Liu and Li[31] inspected the vibration and acoustic response of a sandwich plate that subjected to a concentrated harmonic force under thermal environment. The modal characteristics of plate were defined by using both thin plate theory and thick plate theory in order to show the effect of rotational inertia and shear deformation and the results were compared. The thin plate theory gave higher natural frequency and

lower dynamic response. In the results, it was showed that the increasing temperature decreases the vibration response and the natural frequencies and the thermal environment effected the low-frequency range much more than the high-frequency range.

Liu, Li and Liu[32] presented a study to show effect of aerodynamic heating on modal characteristic of a wing structure up to 6 Mach flight speed. An isotropic material was selected as a test plate. The study was conducted for four different cases. As result, it was observed that the natural frequency of structure was decreasing with increasing temperature while the mode shape remained same; and if a temperature gradient on the structure occurred, the mode shapes of structures changed.

Geng, Li and Li[33] performed an experimental and numerical study on the vibration and acoustic response of a clamped rectangular isotropic plate under thermal environment. According to test results, the natural frequencies of structure decreased with increasing temperature and the close vibration modes experienced mode shift between each other. In the results of numerical studies, it was stated that, the initial deflection influenced modal characteristic of structure.

Zhao and colleagues[34] constructed a test platform that can simulate the thermal and vibration environments of an aircraft during high speed, long range flight. As a test material, they used a tri-laminated composite wing structure that has metallic plate core. The test material attached to test platform and heated from both face while vibration excitation is applied. The vibration responses were measured to find the natural frequencies and vibration modes changes during heating process. In this study, it was stated that increasing temperature affected the mechanical properties of structure and for this reason, the modal characteristic of structures decreased as the material temperature increased.

Zhang and colleagues[35] inspected the effect of high thermal environment with high thermal gradient up to 900 °C on the modal characteristic structures. In study, they used Ceramic Matrix Composite (CMC) sandwich material which known as a good thermal insulator and mostly used on aerospace industry. They applied thermal condition to only one face of the structure. In addition to an experimental study, they developed a finite element analysis solver to calculate the effect of heating on the sandwich structures. They mentioned that, increasing temperature directly affected

the elastic properties of the structure and the natural frequency and the damping ratio decreased as the temperature increased.

Cheng and colleagues [36] researched the effect of radiation heating on modal characteristic of simple plate and stiffened plate. They used a test method and generated a FEA method to solve effect of heating on modal parameters. The exerted radiation heating was modelled by Monte Carlo Theory and the "MSC.Nastran" was used to solve normal mode analysis under thermal environment. In the result of research, it was observed that, the natural frequencies were decreased and the close modes were shifted with increasing temperature. In the FEA, both temperature dependent mechanical properties and thermal stress effects must be included into calculation sequences.

Li and Yu[37] performed a numerical solution to inspect vibration and acoustic responses of the three layer composite sandwich panel under high temperature environment. Test plate was simply supported. Face sheets were orthotropic and the core was 9 mm isotropic material. Analytical solution verified by a finite element analysis solution. In this analysis, firstly, thermoelastic analyses were done by using linear static solver (sol 101) to solve stress distribution and the normal mode analysis (sol 103) was performed with this pre-stress values. In the numerical solution, the governing equation was solved by Hamilton's principle; therefore, the thermal stress was handled as external loads.

Du, Geng and Li[38] presented the effect of thermal gradient on the dynamical characteristics of a laminated structure by using analytical methods for different temperature gradients and the results were compared with experimental and numerical results in the literature. It was stated that the thermal gradient led the thermal bending moment and stiffening effect on the structure. As result of the study, as the temperature gradient increased, the displacement responses and the stiffening effect also increased and this led to increase of the natural frequency of the structure.

Vio, Munk and Verstaete[39] presented a study that shows the effects of transient temperatures on the flutter behavior of wing structure with a control surface and compared the results with cold wing and steady-state temperature distribution. In the results, it was observed that, the added thermal nonlinearities into the system resulted

a smaller flutter velocity range. The steady-state temperature distribution case could lead an over design parameters for flutter analysis calculations.

Bai and friends[40] performed an experimental modal test under thermal environment on a sandwich composite plate that composed from Nomex honeycomb and woven carbon fiber skin materials. In the experiment, it was observed that, the natural frequencies of test plate decreased with increasing temperature and the modal damping value dramatically affected from temperature changes. The skin material was the major factor to affect modal parameters of test plate. During experiment, a modal shaker was used to excite structure during heating process, because, it was stated that, the impact test hammer would be dangerous in thermal environment and it can not excite structure continuously during temperature increase. In the research, in addition to the test, finite element analysis (FEA) solution was used to simulate the modal characteristic changes of structure under transient thermal environment. In the FEA, the temperature dependent mechanical properties were added to model. The correlation between the test and the FEA results diverged as mode number increased.

The studies reviewed above have highlighted the significant effects of thermal conditions on modal characteristics of the composite structures. It has been supported that as temperature increases, the natural frequencies of structures decrease while mode shapes have same pattern. The mode order may shift if the close natural frequencies exist.

In this study, the effects of core structure on modal characteristic of sandwich composite structure is examined under transient thermal condition by using the Experimental Modal Analysis (EMA) method. As test specimens, seven sandwich composite test plates are manufactured which have different core structures but the same carbonfiber face sheets. The selected core materials are widely preferred in the aeronautical industry.

CHAPTER 3

METHODOLOGY

In this chapter, a brief information on composite materials and Experimental Modal Analysis will be given. Then the test platform is introduced. The test and data analysis procedure will be described.

3.1 Composite Materials

A composite material is made by combining two or more materials to meet a specific mechanical property. Although the usage of composite materials in modern structures is increased in the last decades, the historical background of composite materials reach to 1500 BC. The Mesopotamian and Egyptian settlers mixed mud and straw to build durable and strong buildings. [41]. This invention lead an improvement in building structural materials and the societies had better accommodation and fortified defense walls in time. In 13th century, Mongols were used composite technology in their bows which are extremely powerful weapons and this helped Chengis Khan to achieve a domination over other nations and from a different viewpoint, the composite structures formed the today's geopolitical locations of countries [2]. Figure 3.1 shows the content of a Mongolian bow.

Modern composite materials are produced by yawing the fiber materials in an orientation pattern with epoxy filling. Each layer that tape or fabric fiber called as lamina and stacking of lamina in an orientation called as laminate as shown in Figure 3.2 and 3.3. Laminate composites are produced which as strong as steel with very low-density values. The mechanical properties of composite structure mainly affected by the fiber material, orientation and epoxy rate [42].

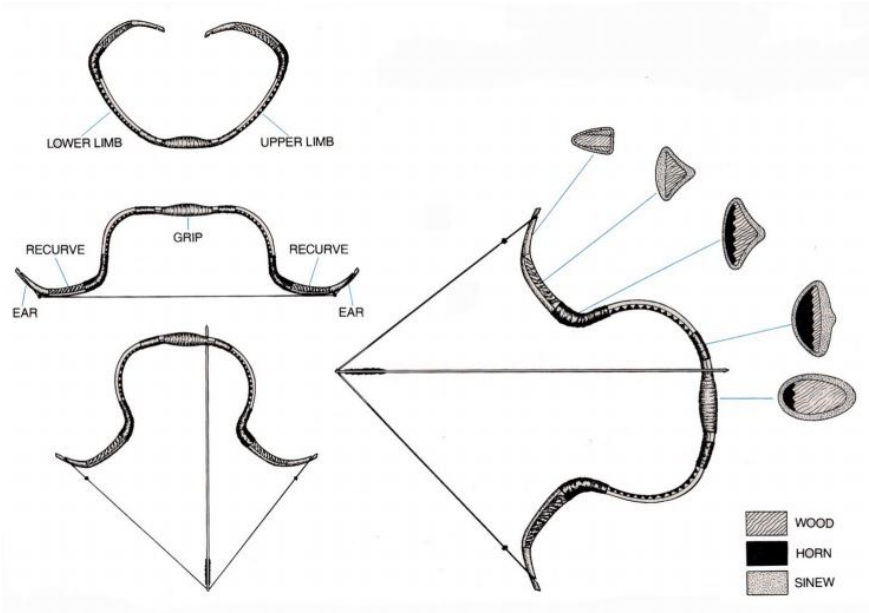

Figure 3.1: A Historical Composite Bow [2]

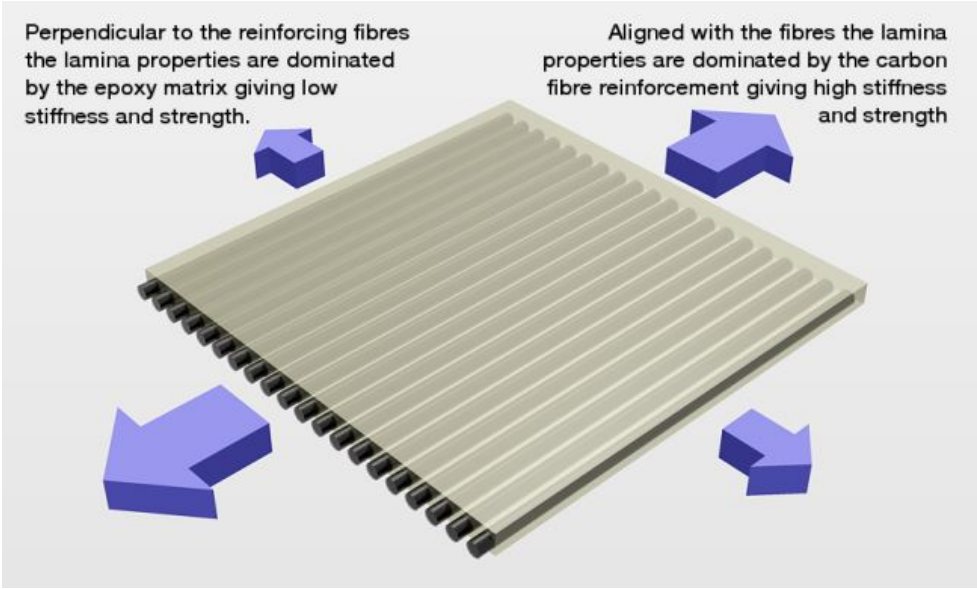

Figure 3.2: Lamina Directions [3]

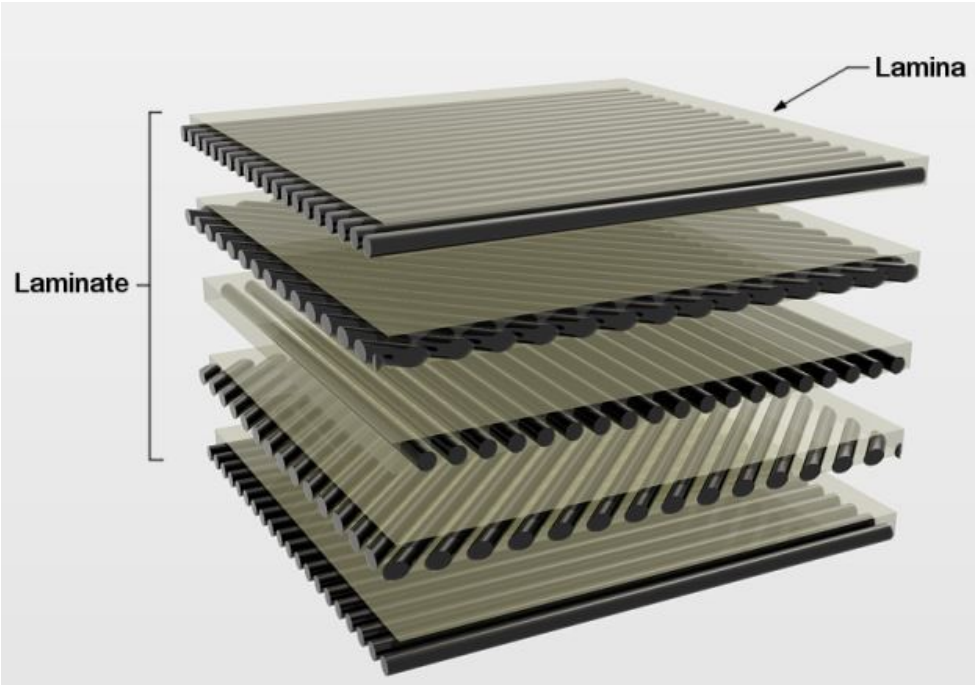

Figure 3.3: The Lay Out of a Laminated Composite [3]

In a composite lamina, the fibers are the major load carrying members [43] and the fibers in a composite lamina can be oriented as unidirectional or woven (See Figure 3.4). In unidirectional type, the fibers are arranged in only direction and their longidutional strength performance is much higher than transverse direction. The strength value in transverse direction is depend on matrix material performance other than fibers and by stacking UD laminas in different orientation, the composite structure strength in required direction can be improved. The woven type is produced by kneading and woving fibers in a pattern and woven composite lamina has high strength in both transverse and longidutional direction.

3.2 Sandwich Composite Materials

Sandwich composite material is a form of laminated composite. They are built by bonding of two composite face sheets to a special core structure with adhesives. The core structure would be in many different forms; however, the honeycomb structure form is mostly preferred in engineering applications. The honeycomb core is named after by its geometrical shape and Figure 3.5 shows geometry of a hexagonal honey-

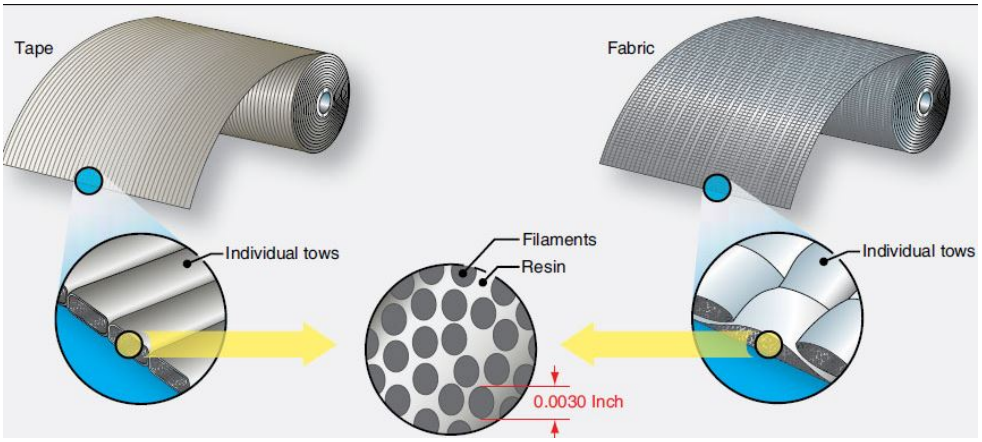

Figure 3.4: The Tape and Fabric layer [4]

comb core. However, by advancing of composite technology, new honeycomb core models with different cell geometry can be designed for specific purposes as shown in Figure 3.6. For example, Ox-Core honeycomb cells are in rectangular to give flexibility to structure in one direction for the application on curved structure.

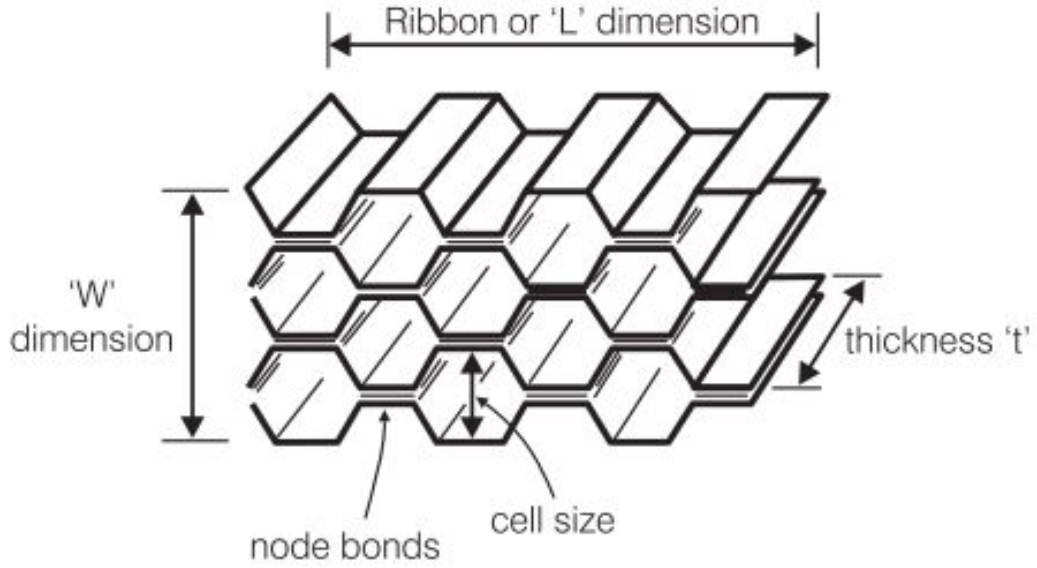

Figure 3.5: The Hexagonal Core Structure [5]

The honeycomb sandwich structure have nearly similar load carry behavior of I-beams (See Figure 3.7). While the face sheets carry tension loads, the core structure resists shear loads. The sandwich composites can provide high bending stiffness to

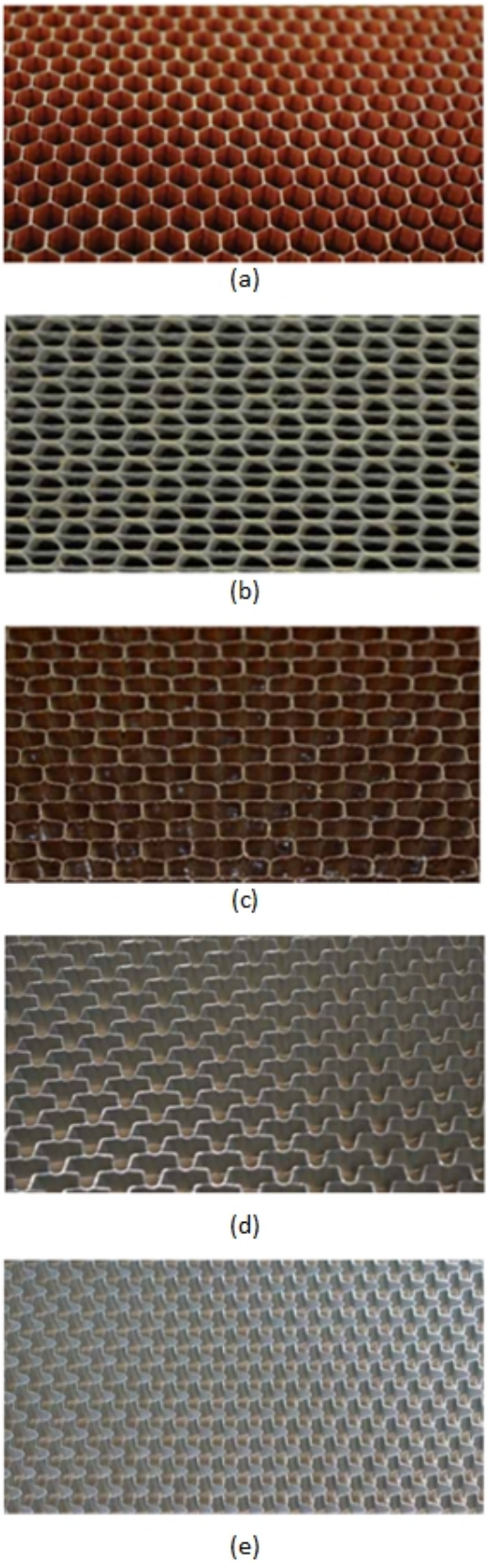

Figure 3.6: a) Hexagonal Core b) Reinforced Hexagonal Core c) OX-Core d) Flex-Core e) Double-Flex Core [5]

structure in a cost-efficient way and Figure 3.8 shows the basic correlation between thickness of the core and the effect on stiffness and weight of structure. The material of core structure give additional advantage to structure which depend on application area of structure. For example, glassfiber and Nomex core are good thermal insulator while the aluminum core is a good thermal conductor.

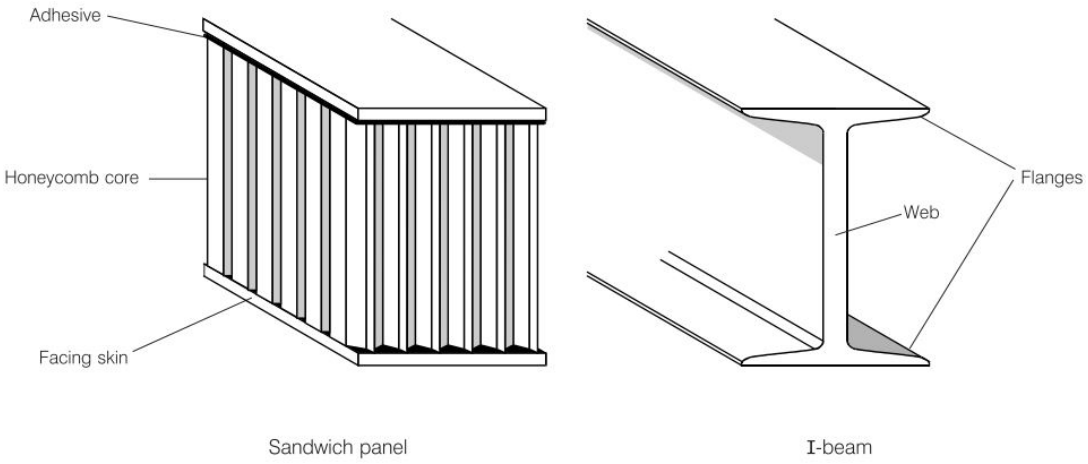

Figure 3.7: Hexagonal Core vs. I-Beam Structure[6]

	Solid Material	Core Thickness t	Core Thickness 3t
	t	2t	4t
Stiffness	1.0	7.0	37.0
Flexural Strength	1.0	3.5	9.2
Weight	1.0	1.03	1.06

Figure 3.8: The Effect of Core Thickness on Stiffness and Weight [7]

The face sheet material of sandwich structure could be metal, plywood, carbonfiber, glassfiber or aramid. Each material has its own advantages and metal, carbonfiber and glassfiber sheets or the stacking combination of them mainly preferred in aeronautical industry.

The adhesive layers play important role to keep unity of face sheets and core structure. It also has an effect on shear load carry performance of structure [44].

The application of composite structures can be seen in any engineering industry from wind energy to sports equipment. Figure 3.9 shows a typical application of composite structures on a jet aircraft.[6]

Figure 3.9: The Composite Parts of A Jet Aircraft [6]

The aircraft components in Figure 3.9 are;

1. Radar Transparent Radome: Epoxy or BMI prepreg or RTM resins and woven preforms made of glass or quartz
2. Foreplane Canard Wings: Epoxy carbon prepregs
3. Fuselage Panel Sections: Epoxy carbon prepregs. Non-metallic honeycomb core and HexBond™ adhesives
4. Leading Edge Devices: Epoxy carbon and glass prepregs

5. Fin Fairings: Epoxy glass and carbon prepregs
6. Wing Skins and Ribs: Epoxy carbon and glass prepregs
7. Fin Tip: Epoxy/quartz prepregs
8. Rudder: Epoxy carbon prepreg
9. Fin: Epoxy carbon/glass prepreg
10. Fin: Flying Control Surfaces: Epoxy carbon and glass prepregs. Honeycomb core material and HexBond™ adhesives [6].

3.3 Experimental Modal Analysis

Modal analysis is an efficient engineering method to define a structural design in terms of modal parameters namely natural frequency, damping and mode shape. This method can be performed either numerically or experimentally.

In theory, a good conducted numerical and experimental modal analysis presents same results. The each analysis method have advantages. While the numerical method does not require any test instrumentation, the experimental method require qualified expensive experiment tools. To use experimental method, the structure must be produced. The numerical method can be performed in design phase to prevent any unacceptable modal parameter.

To perform modal analysis numerically, structure must be modelled numerically, too. For this reason, Finite Element Method (FEM) is generally preferred for modelling of complex structures. The numerical modal analysis plays an important role on early phase of design process. It helps to define modal parameters of structure and by this way; resonance, flutter or any other vibration based damage mechanism can be prevented on early stage of design phase. The modelled structure, which meets with design requirements, must be experimentally tested to verify the numerical model. Figure 3.10 shows the schema of FEM validation process.

To perform modal analysis experimentally, the Experimental Modal Analysis (EMA) is an efficient method. EMA is a modal testing method that define modal parameters

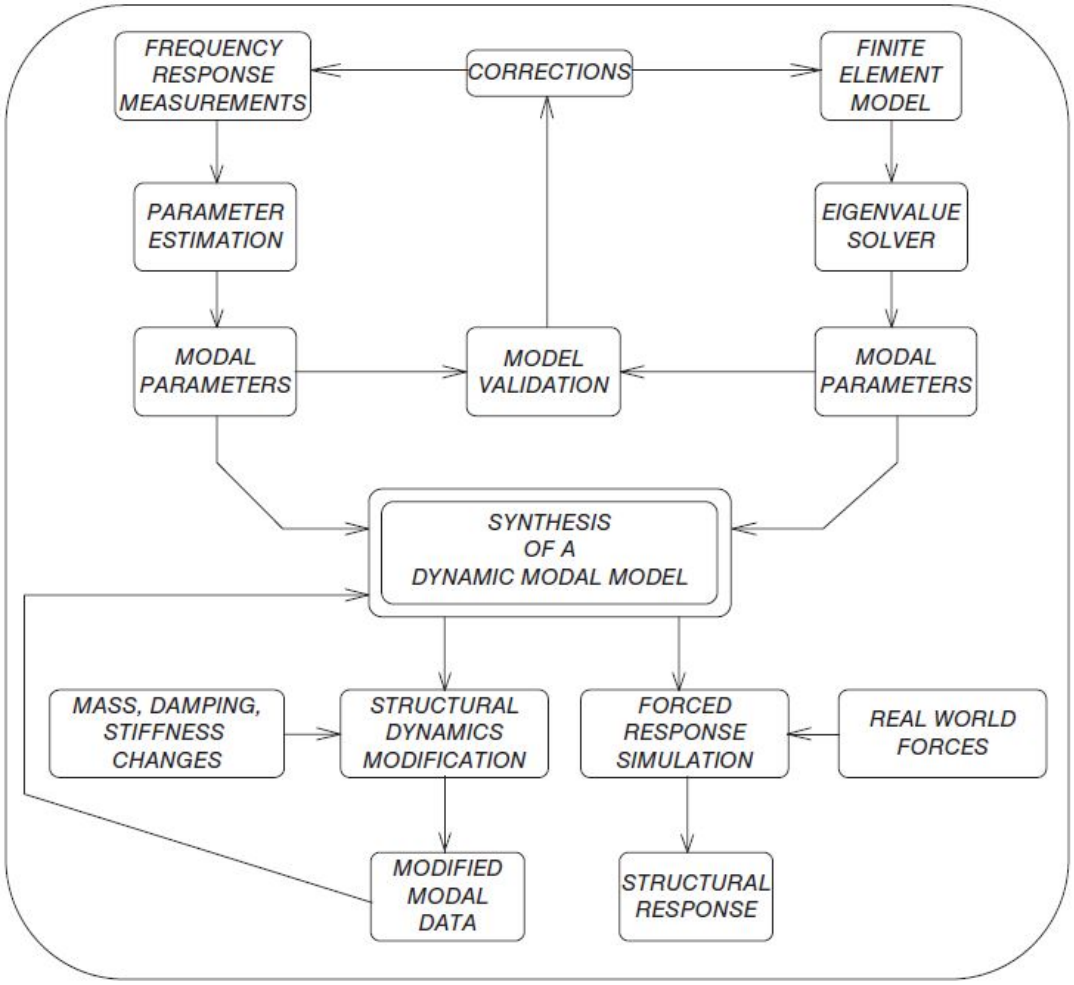

Figure 3.10: Model Verificatin Process of Dynamic Model [8]

of physical structure by using modal testing instruments.

Dynamic Testing Agency divide the EMA in the levels according to its accuracy, application and results [45]. During the test planing, pay attention on selection of required level is important. These levels are:

- Level 0: estimation of natural frequencies and damping factors; response levels measured at few points; very short test times.
- Level 1: estimation of natural frequencies and damping factors; mode shapes defined qualitatively rather than quantitatively.
- Level 2: measurements of all modal parameters suitable for tabulation and mode shape display.
- Level 3: measurements of all modal parameters, including normalized mode shapes; full quality checks performed and model usable for model validation.
- Level 4: measurements of all modal parameters and residual effects for out-of-range modes; full quality checks performed and model usable for all response-based applications, including modification, coupling and response predictions.

The quality of EMA is depended on the quality of measured data and the analysis of data. The main output of EMA is Frequency Response Function (FRF) and it shows the frequency dependent response of structure with respect to unit input and the mode shape of structure can be build up by the help of FRFs that obtained from different locations on structure [46].

A FRF can be generated using measured force input and response of a structure in time domain. There are different parameters that effect input and response of the structure. Detailed information on the calculation process of FRF is given in Section 3.6.

First of all, a boundary condition must be given to structure. Generally, in EMA, a free-free boundary condition is established by hanging the structure with bungee cords. This boundary condition does not create any pre-stress on structure and the

actual modal parameters that is independent from any effect of boundary condition can be obtained.

The input force that excite the system can be measured by force transducers. However, the excitation can be applied to structure by using different tools in different waveforms. The selection of excitation method and waveform is depend on application. The waveform is the excitation function that excite structure physically and the selection of excitation function is the main factor to selection of excitation method. The widely prefered excitation methods are the impact hammer and modal shaker. The impact hammer is a hammer shaped tool that excite structure with very short duration impulsive excitation. The excited mode range can be changed by using different hammer tip materials. A modal shaker can excite a structure during a long period of time with any waveform. The waveform and excitation frequency bandwidth can be arranged by signal generator. The excitation location must be selected away from all node lines to excite all modes in frequency of interest. The node line is the geometric line that structure has zero motion along at a particular mode.

The vibration response of the structure to the given input can be measured by accelerometers. The piezoelectric type accelerometers are mostly preferred for EMA. The accelerometers generate electric charge proportional to exposed vibration and measure the acceleration of response. Accelerometers can be found in various specifications and the selection of accelerometer must be done by considering the mass of accelerometer, frequency range, and measure sample rate. As like force transducers, the accelerometers must not be placed on node lines.

There are several reference books with more comprehensive coverage of experimental modal analysis, particularly Ewins' Book (2000)[47] and Avitabile's Book[8].

3.4 Test Platform

To perform the thermal modal tests, a unique experimental test platform is required to perform the thermal modal analysis. The manufacturing and construction processes are held in the Mechanical Engineering Department of Hacettepe University. The test platform consists of four parts and they are;

1) Test Chasis

2) Heat Array

3) Test Plates

4) Instrumentations

3.4.1 Test Chasis

Test chassis is a rectangular prism frame and carry all parts of test platform. It must be mechanically strong enough to carry all parts and rigid enough to perform experimental modal analysis.

Figure 3.11: The Chassis of the Test Platform

The test chassis is constructed by using aluminum K10 sigma profiles. Sigma profile provide high moment of inertia with low weight value and can be easily assembled together without any permanent connection method like welding.

3.4.2 Heat Array

In Section 2, the major heat sources of aircrafts under operational conditions are explained. To simulate the heat sources, a heat array is assembled to narrow side of test platform. The heat array consists parallel-arranged 13 quartz lamp and can supply in total 9.1 kW power in to the test environment and it is shown in Figure 3.12. The output power of each quartz lamp is constant, therefore, to adjust required heating rate, the test plate is hanged into a convenient distance.

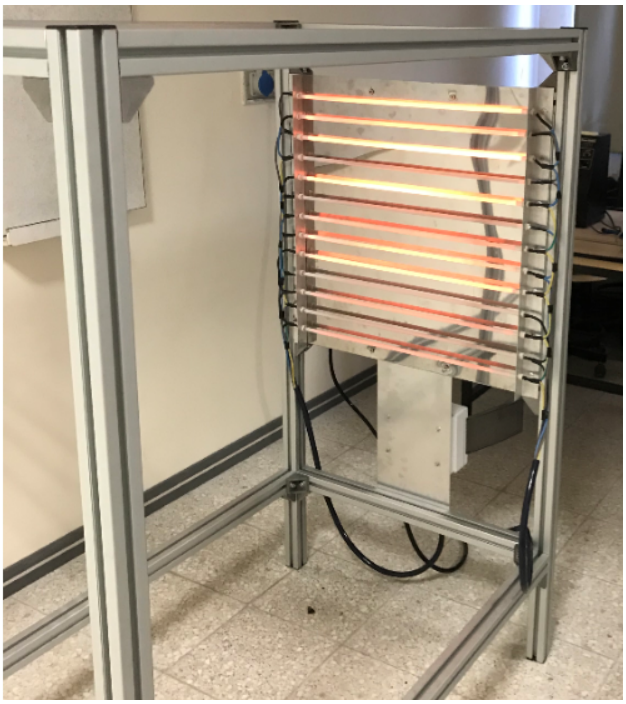

Figure 3.12: The Heat Array of the Test Platform

3.4.3 Test Plates

Main contention of the thesis study is researching the effect of honeycomb core to modal characteristic changes of sandwich composite structures under thermal envi-

ronment. There are many different core materials in different cell type and geometrical parameters. In this study, seven different honeycomb cores are selected from widely preferred core materials of current and future aircraft and aerospace projects. They are Nomex, Glassfiber and Aluminum (See Figure 3.13) Each core are uniform in quality, free from any foreign material and any defects. There is no any excessive node bond or cell wall failures on honeycombs.

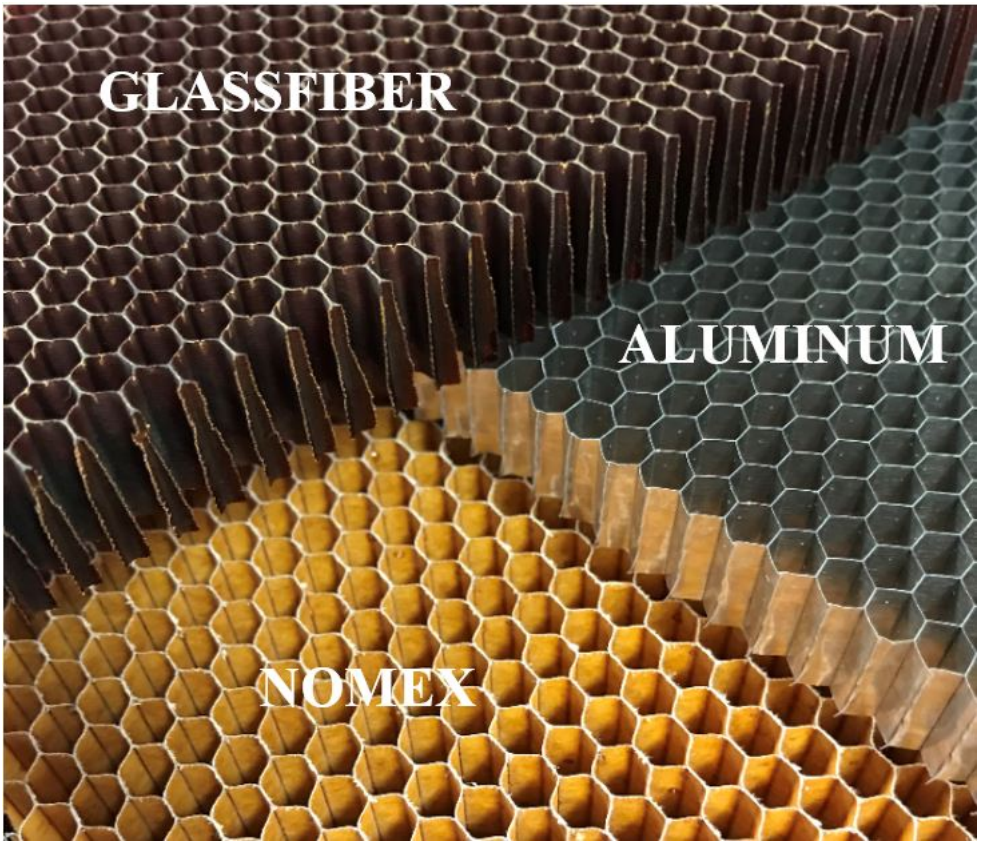

Figure 3.13: The Selected Core Materials

Each core parameters are shown in Table 3.1.

The honeycomb core mechanical properties are different in each direction. Therefore, one ply carbonfiber composite layer is lay on each face of honeycombs. In structural applications, at least three ply composite layer on each face required. Only one ply is applied on each face of the test plates to reduce the effect of face sheets. The carbonfiber composite layer mechanical properties depends on fiber directions. In this study, to reduce the anisotropic effect of mechanical properties of face sheet material,

Table 3.1: The Core Materials of the Test Plates

Core Materials	Core Material Type	Core Shape	Core Cell Size	Core Thickness
Test Plate #1	Aluminum	Hexagonal	4.8 mm	12.7 mm
Test Plate #2	Aluminum	Hexagonal	6.4 mm	12.7 mm
Test Plate #3	Nomex	Hexagonal	4.8 mm	12.7 mm
Test Plate #4	Nomex	OX-Core	4.8 mm	12.7 mm
Test Plate #5	Glassfiber	Hexagonal	4.8 mm	12.7 mm
Test Plate #6	Glassfiber	Hexagonal	4.8 mm	14.5 mm
Test Plate #7	Glassfiber	Hexagonal	4.8 mm	16.0 mm

the Hexply AGP-193-PW/8552S RC40 plain-woven prepreg carbonfiber is selected, which used in structural elements of most of aircraft projects. The mechanical properties of carbonfiber layer are equal in each fiber direction.

The lay up process of the composite sandwich plates are done in Turkish Aerospace by qualified personals. Each prepreg layer is bonded to core faces by using FM300K film adhesive the test plates are cured in autoclave at 180 °C for 2 hours (See Figure 3.14).

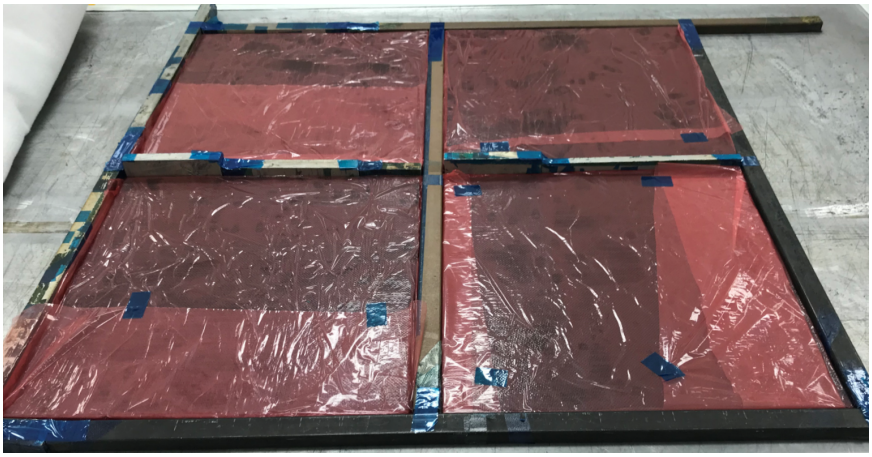

Figure 3.14: The Lay up Process of the Test Plates

3.4.3.1 Aluminum Honeycomb Composite Sandwich Structure

Aluminum honeycombs are PAMG-XR1 5056 aerospace grade aluminum honeycomb cores with corrosion resistance. The PAMG-XR1 5056 widely preferred in aerodynamic surfaces like trailing edges, leading edges, fuselage components, helicopter rotor blades and missile wings. These structural applications of PAMG-XR1 5056 are possible aircraft parts that would be faced with aerodynamic heating in real service conditions. It provides high strength with low-weight value and has high thermal conductivity rate. [48]

3.4.3.2 Glassfiber Honeycomb Sandwich Composite Structure

Glassfiber honeycombs are ECG (Euro-Composites Glassfiber) honeycomb. The glassfiber cores are known as good insulators and widely preferred in structural parts that exposure high temperature values. They are well-suited core materials for heat shields, fairings, radomes, aircraft structural parts and other assemblies that face elevated temperature in aircraft service life. [49].

3.4.3.3 Nomex Honeycomb Sandwich Composite Structure

Nomex honeycombs are HRH-10 aramid honeycomb with different core geometry which produced by aramid fiber material. Nomex cores are good thermal and electrical insulators, they have good resistance performance to water and fungus and they are self-extinguishing materials. Most of commercial aircrafts use Nomex cores in their interior panels and the exterior structures that could face with high aerodynamic heating phenomena like radome, helicopter blades, flaps etc. In this study, a hexagonal and an OX-core Nomex cores are used. The OX-Core is a special hexagonal honeycomb that has been formed by over expanded in the W direction and has a rectangular cell shapes that is used for curved structures, providing a rectangular cell shape that facilitates curving or form in the L direction. Nomex cores can be manufactured in hexagonal and OX-core [50].

3.4.4 Instrumentation

In EMA, the instrumentation plays an important role on excitation and recording of the data to define modal parameters of structure. Figure 3.15 and Figure 3.16 show the instrumentation schema and the test setup of the study.

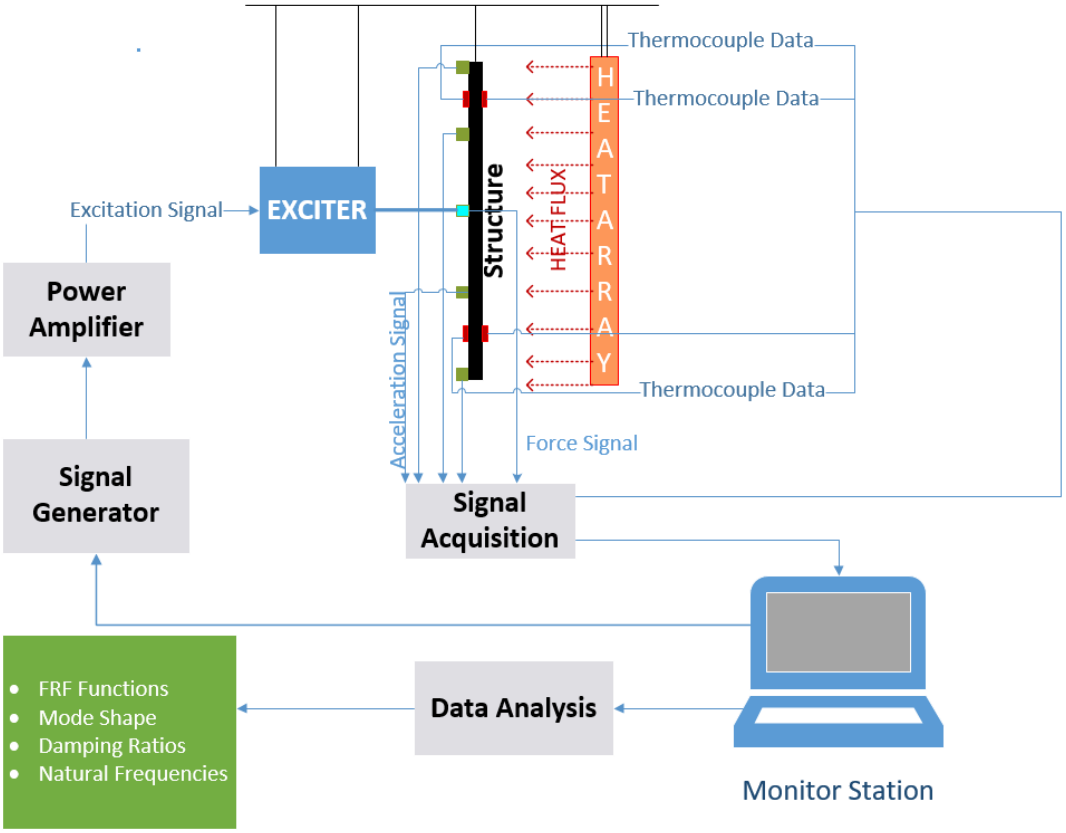

Figure 3.15: The Illustration of the Instrumentation of the Experimental Setup

The accelerometers are mounted on unheated face of the test plate before mounting to the experimental setup. There are many different ways to mount accelerometers. Thermal environment and structure of test plate cause many striction for the mounting process. Mounting with stud is the most effective method. The low thickness of face sheets and the perforated structure of core materials is not suitable to apply stud. Wax and double-sided tapes can easily affected by thermal environments and losses adhesive strength as the temperature increases. Therefore, Cyanoacrylat adhesives that can stand high temperature values are used to mount accelerometers and force transducer. The thermocouples are mounted on structure with Flashbreaker tape.

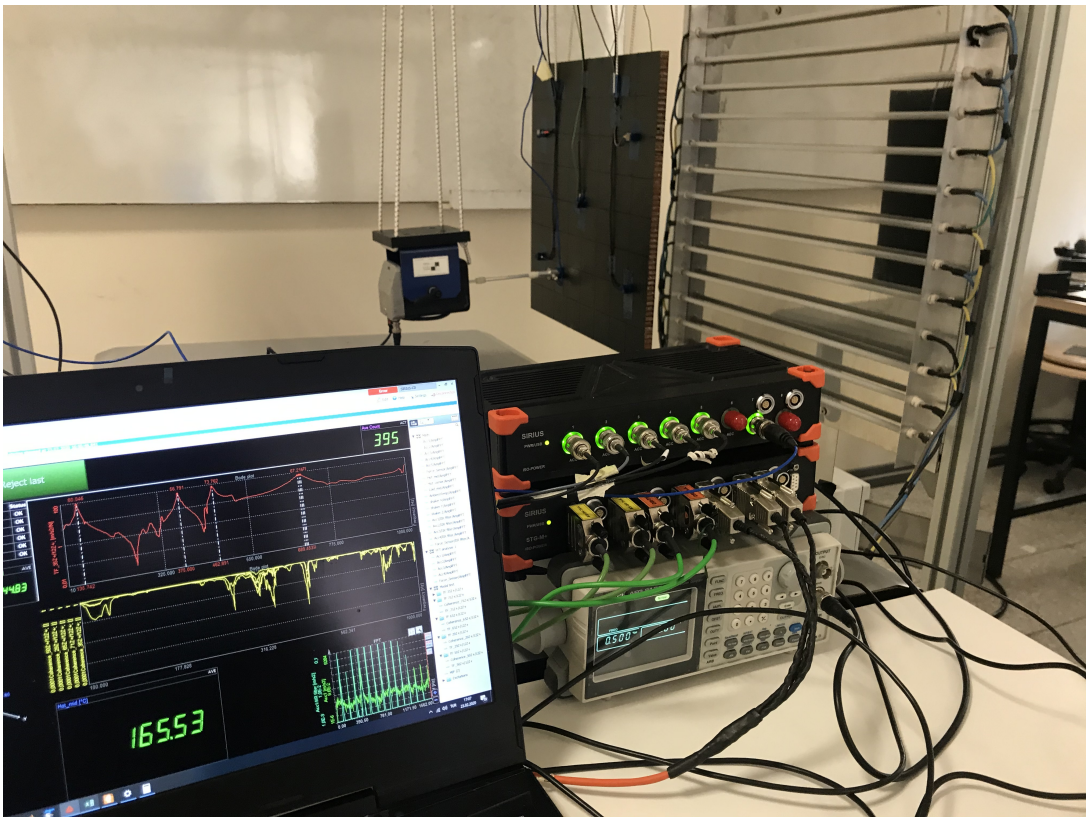

Figure 3.16: The Test Setup

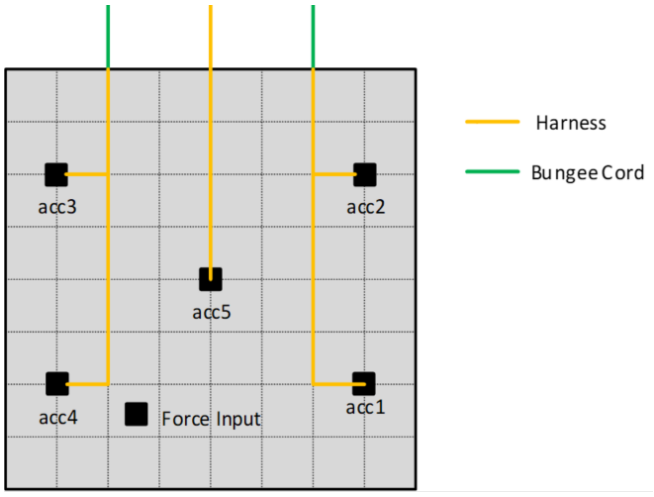

Figure 3.17: The Accelerometer Mounting on the Test Plates

3.5 Test Procedure

A modal test procedure is, which utilizing the experimental modal analysis method, is applied To inspect effect of the core material type on the change of modal parameters under the thermal environment. Each sandwich composite plate is tested individually where the procedure is the same for every plate.

The test is planned to conduct with free-free boundary conditions to reduce effect of any boundary conditions under thermal environment. Therefore, a verification process is required to show that the free-free condition is achieved. First of all, a modal test, with utilizes hammer impact test method, is conducted on a soft sponge to obtain modal parameters of the each test plates. During hammer impact modal test, only one accelerometer is used on each plate for minimum test weight and rubber hammer tip is used to prevent any impact damage that would damage core structure. Secondly, the test plates are hanged on the test platform using the bungee cords and placed parallel to the heat array.

The bungee cords are attached on face sheets with special Flashbreaker tapes that can stand high temperature up to 200 °C. Another impact modal test is performed to check effect of bungee cords. As a result of the test, the natural frequencies of the hammer impact test on soft sponge and bungee cords are equal. This procedure shows that the taped bungee cords provide free-free boundary condition to the test plates.

The first step of the test procedure is recording of the ambient temperature and humidity. It is important to conduct tests on the same ambient conditions. The ambient temperature affects the heat loss of the test plates and as it decreases, more heat transferred to ambient from the test plates during the test. The ambient humidity directly effects the mechanical properties of face sheets and core materials except aluminum core. Moreover, high humidity may cause oxidation of aluminum based core materials.

In the next step, the test plates and platform are visually checked to verify that there is no any defect on the test plates and all instrumentation equipment are mounted in perfect condition. If there are any defect on the test plates or any problem on test platform, it must be noted down to the test procedure form before the test and this

procedure must be repeated after the each test.

After the check and control steps, the experimental modal test under thermal condition is performed. Thermal modal test is repeated under different heating rates, which are 1 °C/s, 2 °C/s 3 °C/s respectively. During the test, the temperature value of heated face is increased up to 150 °C that is below the glass transition temperature of the test materials. The excitation method of test is important to get modal parameters for each temperature values. Therefore, a broadband flat excitation is applied to test plates with white noise profile. The test is repeated at least 5 times for each heating rate to increase accuracy of the test results.

3.6 Data Analysis Procedure

The force input, response and temperature data of the test plates during modal testing are recorded by DEWESOFT SIRIUS data acquisition system (DAQ) and data analysis of the modal test data is done using a mathematical software (MATLAB). DAQ has also modal data analysis capability. A new data analysis solver is prepared specific to this work to see effect of transient thermal environment on vibration response. In this section, the data analysis procedure is explained. The data analysis process schema is given in Figure 3.18.

The frequency range of interest is selected to cover the expected first three natural frequency of the test plates. According to Nyquist Theory, the sampling rate of data must be at least two times higher than the interested frequency range to avoid the aliasing. For this reason, the data collection of the test data is recorded by 4000 Hz sampling rate that is at least two times higher of third natural frequency of the test plates.

The input and response data is divided into the data parts for every 20 °C temperature steps of the hot surface as shown in Figure 3.20. The temperature step is arranged to get long enough data to increase the resolution of FRFs, and to see effect of more temperature values on the FRFs. Therefore, it is assumed that, the modal parameters of the test samples are constant during temperature increment steps.

The test plates are excited with broadband flat spectrum force data and the exposed thermal environment lead a spurious trend in recorded data [51]. For this reason, the trend removal is applied to the each data parts.

It is important to see effect of the thermal environment on modal parameters, which requires a fine frequency resolution, 1 Hz frequency resolution is used in this work. The calculation of FRF from short time test data with 1 Hz resolution could increase the statistical error of response function [52]. Thus, there are some data editing methods to extend the length of data without manipulating the characteristic of vibration data.

The test data is divided into the data segments. Each segment will be used to compute

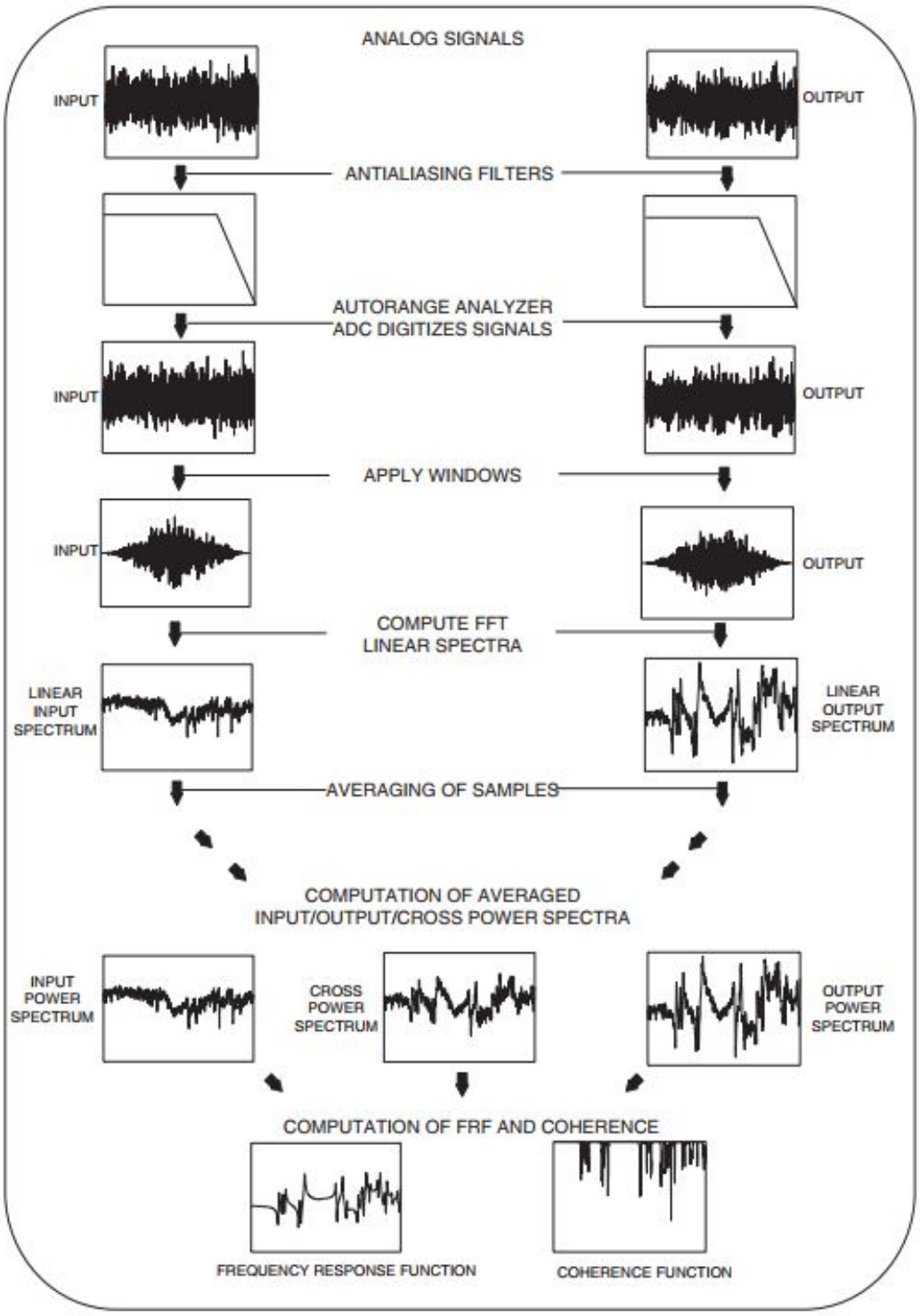

Figure 3.18: Computation Steps of Frequency Response Function (FRF) [8]

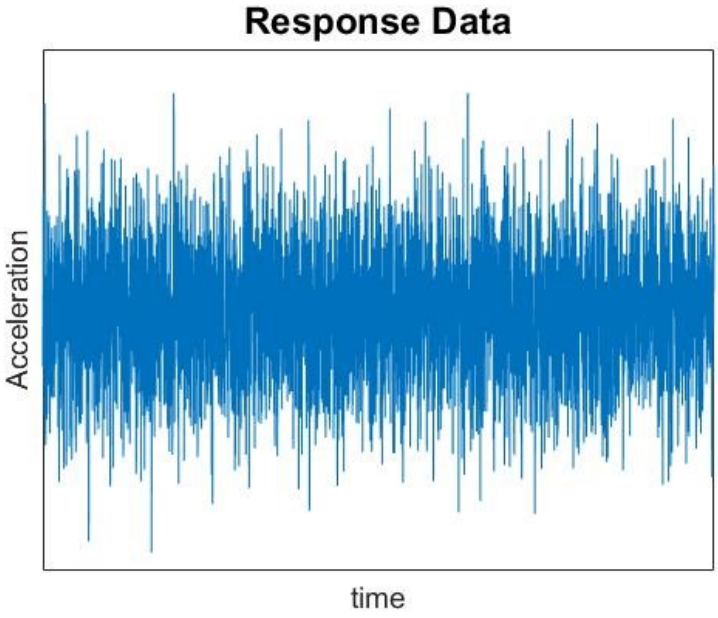

Figure 3.19: A Sample Data for the Acceleration Response

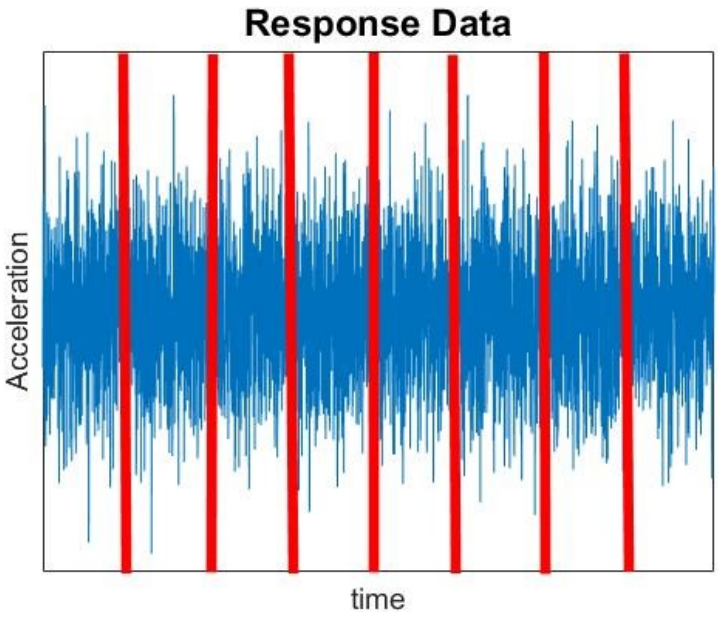

Figure 3.20: Dividing of the Sample Data into Data Parts

Fast Fourier Transform (FFT) and the averaged power spectrum of test data will be calculated using averaging of segments. FFT is a fast numerical method to represent data in frequency domain and it requires less calculation than distcrite Fourier transform.

FFT application on data segment could lead a side-lobe leakage error, which is smearing of energy through ends of data segment. To overcome the leakage, a window function is applied to each data segment. There are many type of windowing and the Hanning window is the best option for a random signal (see Figure 3.21). After the hanning window, the sample data that is shown in Figure 3.19 has a trend like in Figure 3.22.

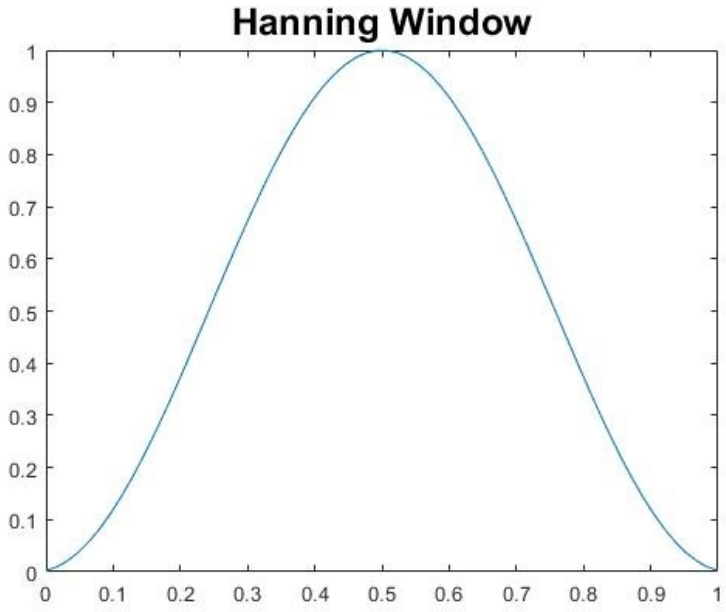

Figure 3.21: The Hanning Window

The windowing application leads a data loss at the ends of data segments. The overlapping process is preferred to reduce the data loss as the result of windowing and the overlapping also helps to extend the data length.

FFT is applied to each edited data segments and the average is used to found power spectra of input and response data. The last step of data analysis process is calculation of Frequency Response Functions (FRF) of the test plates. Frequency Response Function (FRF) is simply the ratio between the spectra of input force and the spectra

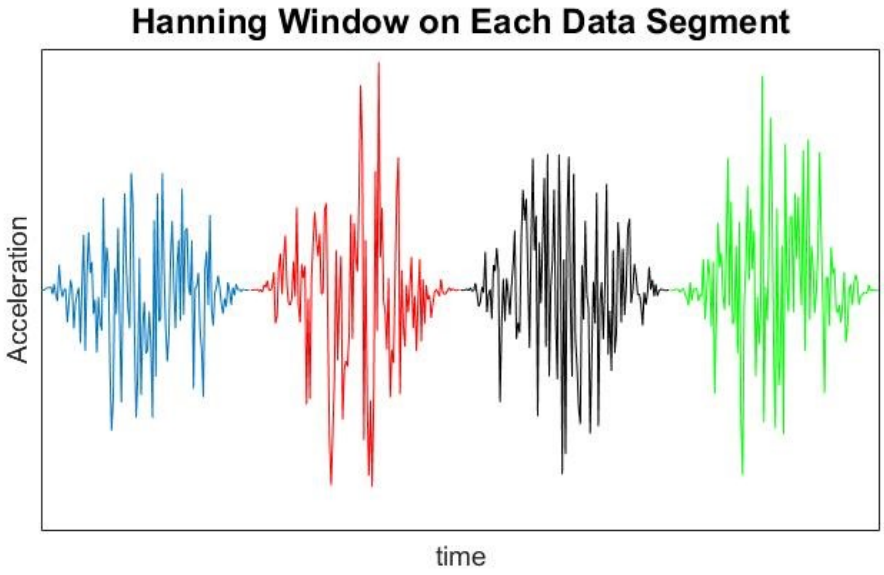

Figure 3.22: Application of Hanning Window to Data Segments

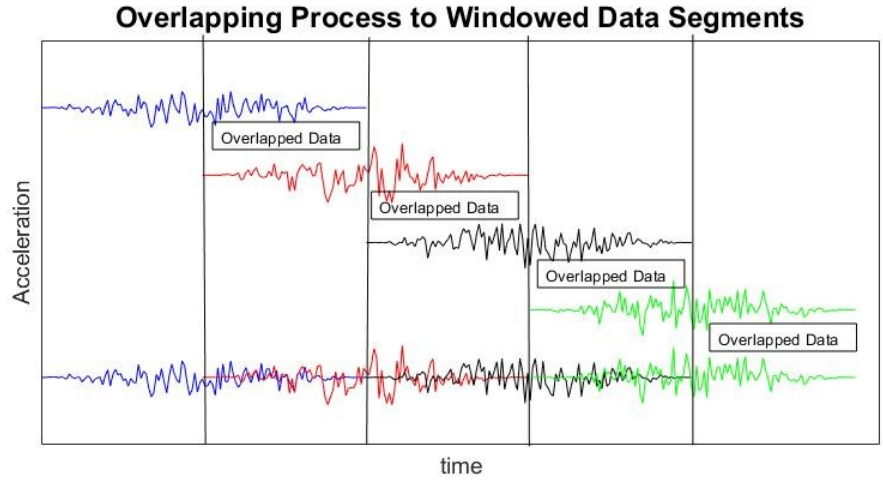

Figure 3.23: The Overlapping Process

of structural response. FRFs present all the modal parameters of the test plates but it could require a curve fitting application to reduce data to extract modal parameters.

The amplitude of absolute FRFs shows the natural frequency of the test plate while the imaginary amplitudes of the modes presents the mode shapes. The damping requires a step further calculation on FRF peak at mode points. In this study half-power bandwidth method is used to calculate damping ratios. The half-power bandwidth method uses the frequency bandwidth between the neighbor points on FRF mode peak that have -3 dB of mode amplitude.

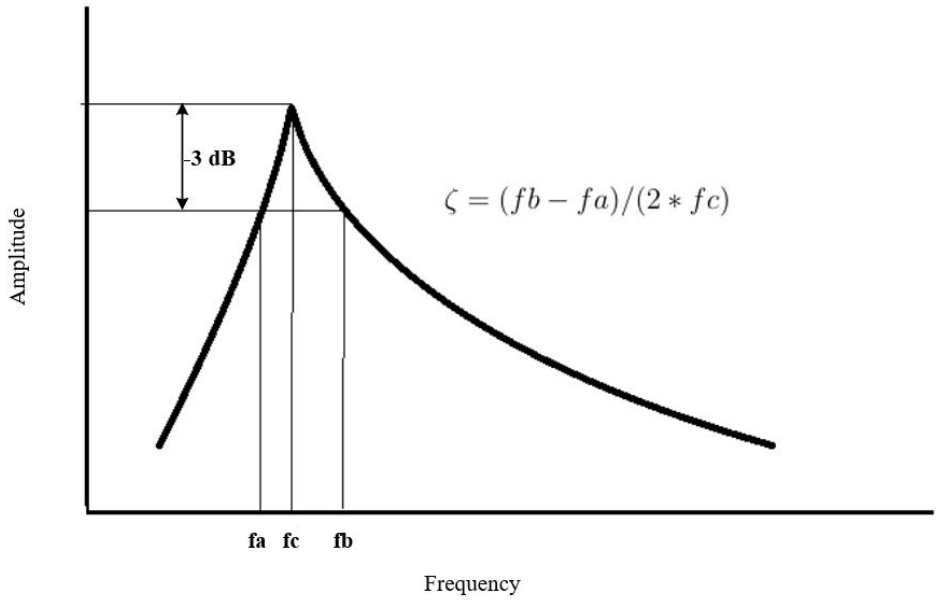

Figure 3.24: The Half-Power Bandwidth Method

CHAPTER 4

EXPERIMENTAL RESULTS

In this Chapter, the test results of each test plate are presented. The test results are compared to see the effect of the transient thermal environment on the modal parameters of different core structure.

4.1 Model Verification of the Test Platform and Plates

4.1.1 Numerical Modal Analysis of the Test Plates

As stated in Chapter 3.3, the modal analysis can be performed by experimentally and numerically and in ideal conditions, both method give same results.

The finite element method (FEM) of composite plates are modelled in MSC.Patran by shell elements. Both skin and core structure are modelled as the 2D orthotropic material and lay up configuration of composite is modelled by using the PCOMP card. The accelerometers are modelled as lumped masses at the location of mounting.

The modal analysis of FEM is performed in MSC.NASTRAN and to visualize mode shapes, MSC.PATRAN is used. In the results of analysis, the first three-mode shape is inspected and compared with the hammer impact test results. Each test plate has same geometrical shape and boundary conditions. Therefore, all the test samples have same mode shapes with different natural frequencies. Figure 4.1 presents the first three mode shape of the test plates and Table 4.1 shows the natural frequencies of each test plate according to modal analysis results.

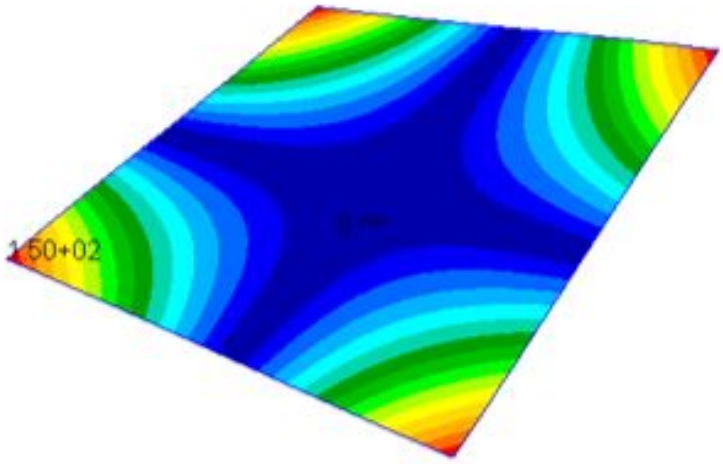

A) First Mode

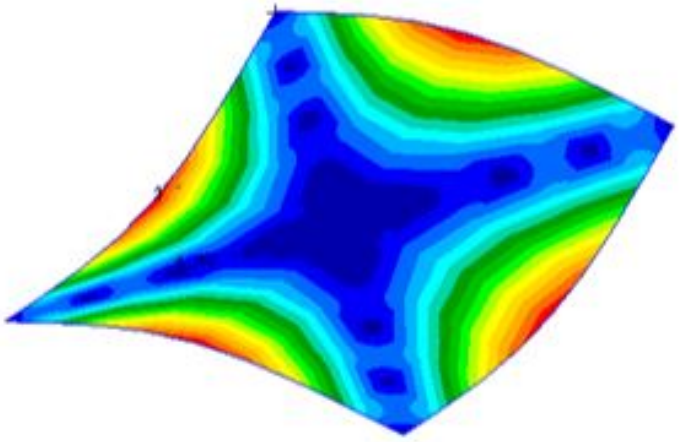

B) Second Mode

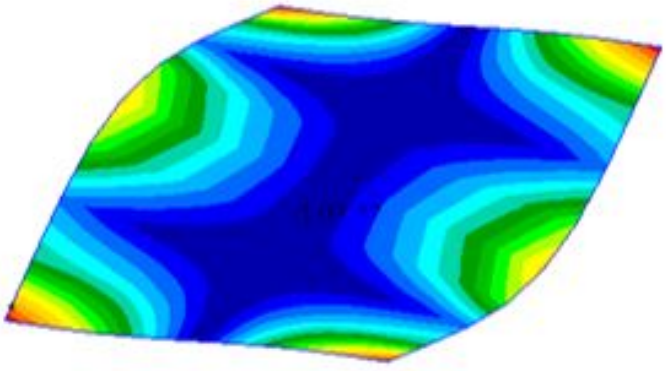

C) Third Mode

Figure 4.1: The Mode Shapes of Test Plates According to FEA

Table 4.1: The Natural Frequencies of the FEM

Natural Frequency(Hz)	**First Mode**	**Second Mode**	**Third Mode**
Test Plate 1	149.88	456.35	572.47
Test Plate 2	148.28	403.60	505.10
Test Plate 3	159.66	440.89	522.12
Test Plate 5	143.27	406.89	505.12
Test Plate 6	155.88	441.20	560.95
Test Plate 7	160.74	449.15	555.22

4.1.2 Hammer Impact Test Results

The hammer impact test is an effective and fast modal testing method to define modal parameters of structure. As seen in Figure 4.2, a hammer shaped impulse excitation tool is used to excite structure from different points and an accelerometer records the vibration response of the structure. The structure could be placed either on a sponge or suspended by elastic ropes to simulate free-free boundary condition.

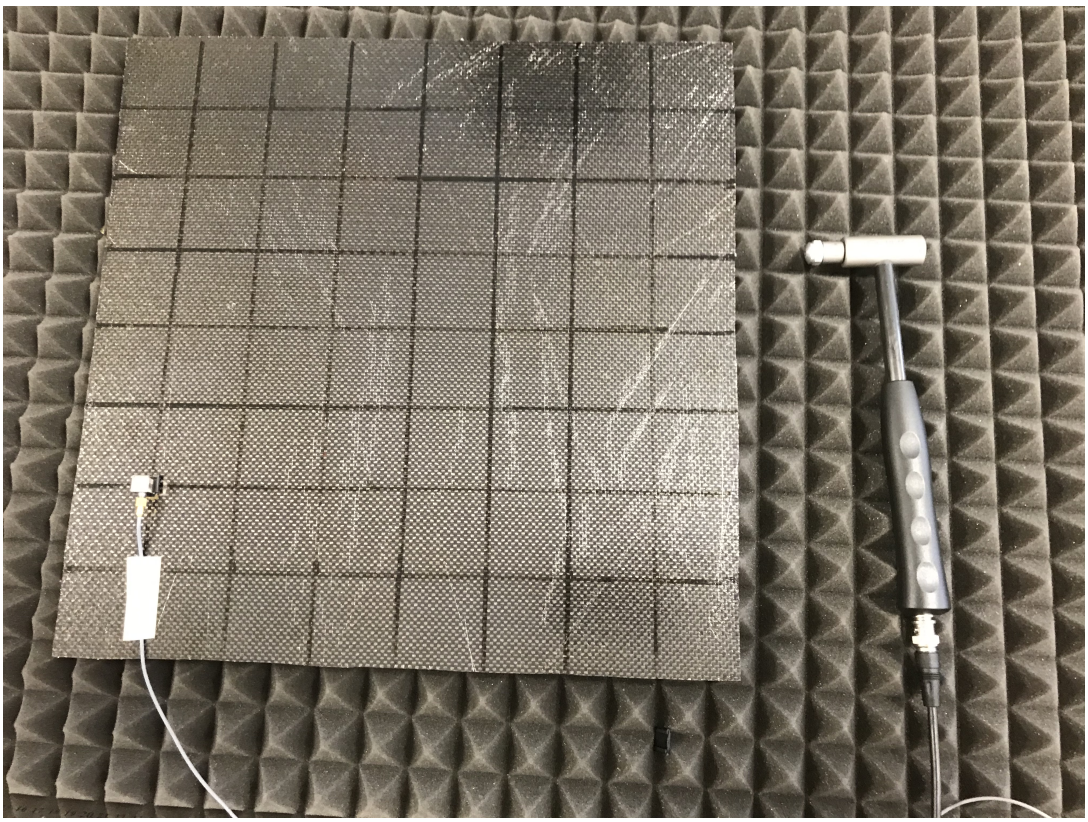

Figure 4.2: The Hammer Impact Testing Tools

During the Hammer Impact Test period, a digital signal analyzer (DEWESOFT SIRIUS) is used to get the natural frequencies, the damping ratios and the mode shapes of the test plates. At least one point excitation is required to get the natural frequencies and the damping ratios to get mode shape of the test plate, the test must be repeated on the different location on the test plate. To get response from different locations, the excitation application point or accelerometer mounting location may be changed to different location of the test plate.

The modal parameters of the test plates according to the hammer impact test results for each test plates are tabulated in Table 4.2 and 4.3. The first three mode shapes of the test plates are shown in Figure 4.3.

Table 4.2: The Hammer Impact Test Results: The Natural Frequencies

Natural Frequency (Hz)	**First Mode**	**Second Mode**	**Third Mode**
Test Plate 1	153.32	442.38	555.56
Test Plate 2	146.48	391.60	500.98
Test Plate 3	157.23	428.83	516.60
Test Plate 4	146.48	381.84	470.70
Test Plate 5	144.53	408.20	500.00
Test Plate 6	153.32	429.69	545.90
Test Plate 7	158.81	437.50	549.80

Table 4.3: The Hammer Impact Test Results: The Damping Ratios

The Damping Ratio	**First Mode**	**Second Mode**	**Third Mode**
Test Plate 1	0.028	0.013	0.011
Test Plate 2	0.025	0.030	0.017
Test Plate 3	0.024	0.020	0.015
Test Plate 4	0.060	0.046	0.020
Test Plate 5	0.060	0.049	0.025
Test Plate 6	0.055	0.034	0.033
Test Plate 7	0.047	0.030	0.015

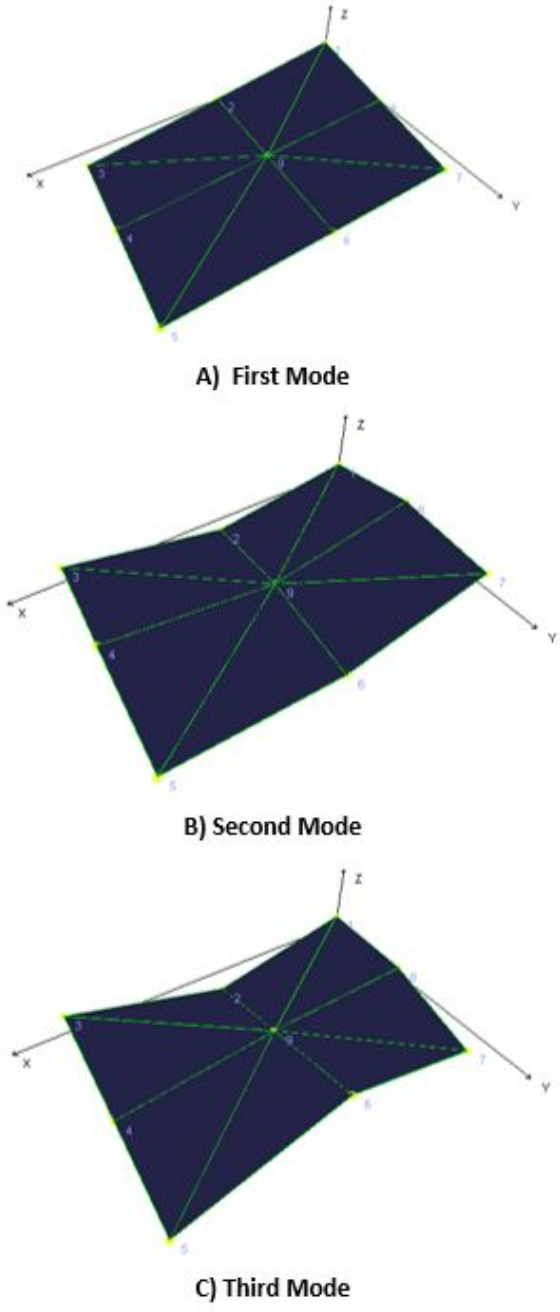

Figure 4.3: The Mode Shapes of Test Plates According to Hammer Impact Test

4.2 The Test Results of Sandwich Composite Plates with Aluminum Honeycombs

The effect of cell size on the modal parameters of sandwich composite structure on elevated thermal environment is examined by using two aluminum hexagonal cores with different cell sizes, which are the test plate 1 and 2. Both core have same core thickness, cell wall thickness and cell geometry. The test plate 1 also is used to examine the effect of core material type and it is tested with three different heating condition.

4.2.1 The Test Results of the Test Plate 1

The test plate 1 is an aluminum honeycomb and the temperature difference between faces are very low. As the heating rate decreases, the temperature difference between faces also decreases. Therefore, with the heating rate 2 °C/s and 1 °C/s, the unheated surface temperature reaches 120 °C before the heated surface reaches 150 °C. This situation lead a limitation on test temperature range. The accelerometers have maximum operational temperature value 120 °C and after this value, the noise in response data increases. Therefore, the modal parameters of aluminum plates are shown for heated surface temperature between 30 °C and 130°C except for the test that conduct with 3 °C/s heating rate.

4.2.1.1 3 °C/s Heating Rate

Figure 4.4 presents the temperature change during the test period.

During the test period, the frequency response functions (FRF) are calculated for every 20 °C temperature increase and the Figure4.5 shows the spectrogram of the FRFs. The spectrograms show the FRF at each temperature increament steps.

Figure 4.6 and Figure 4.7 present the changes in the FRFs of the test plate 1 when heated with 3 °C/s heating rate.

In Figure 4.8 the change in FRF amplitude of the first natural frequency is presented.

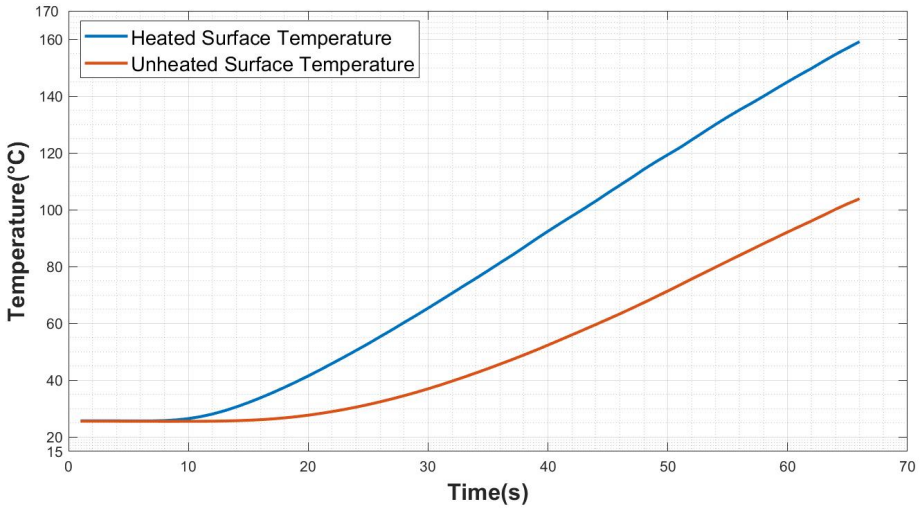

Figure 4.4: The Temperature Values of the Test Plate 1 (3 °C/s heating rate)

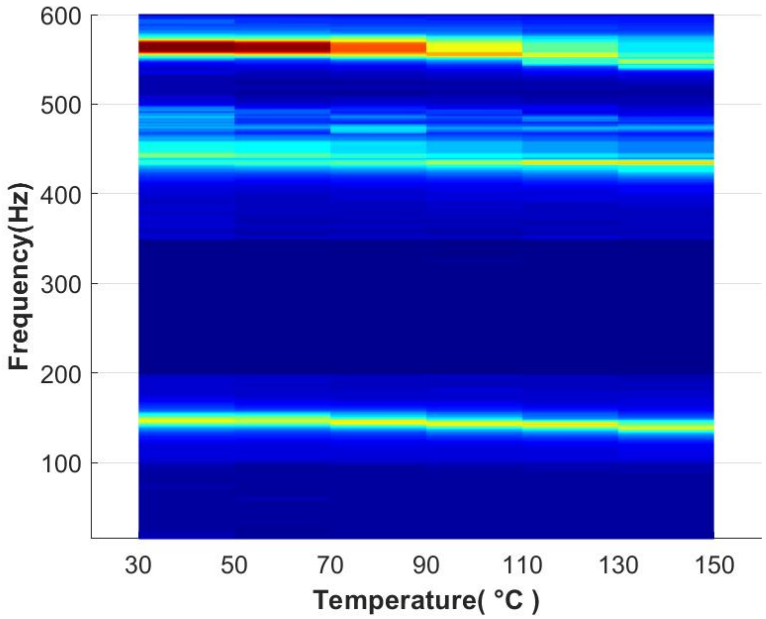

Figure 4.5: The Spectrogram of the Temperature Dependent FRF changes of the Test Plate 1 (3 °C/s heating rate)

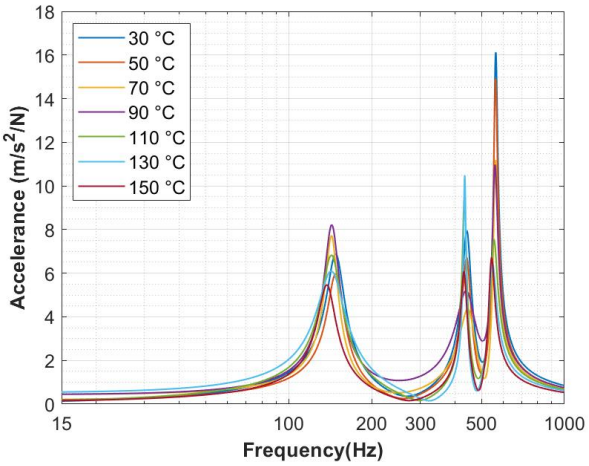

Figure 4.6: The FRFs of the Test Plate 1 under the Elevated Temperature (3 °C/s heating rate)

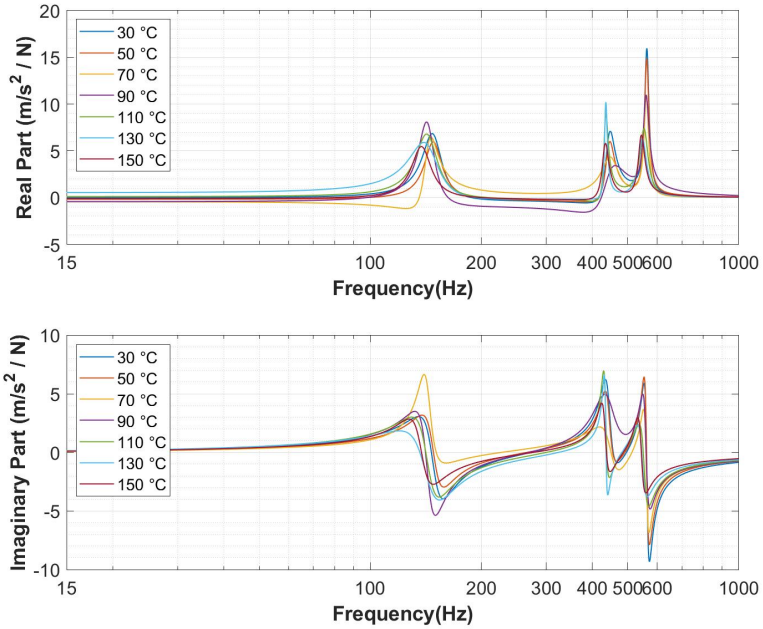

Figure 4.7: The Real and Imaginary Part of FRFs of the Test Plate 1 under the Elevated Temperature (3 °C/s heating rate)

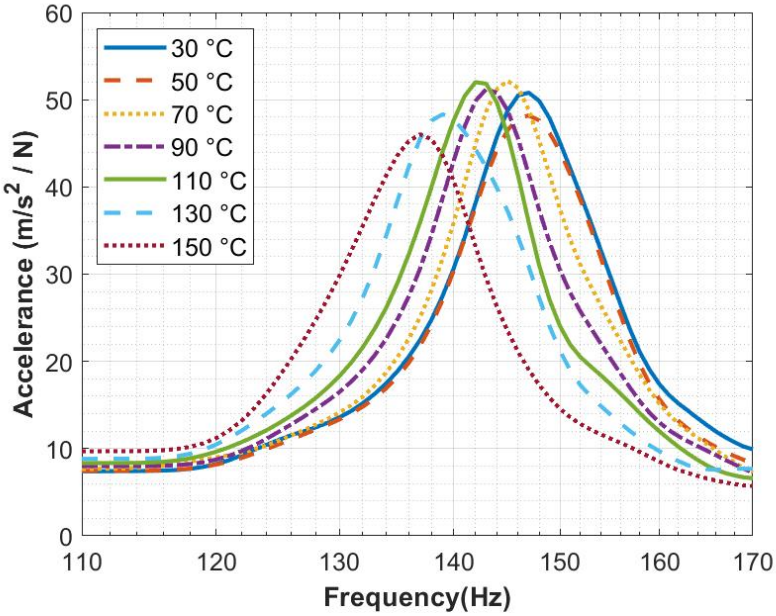

Figure 4.8: The Changes of the First Mode of the Test Plate 1 (3°C/s heating rate)

Table 4.4 shows the values of first three natural frequencies at every 20 °C and the Figure 4.9 shows the trend of change in natural frequencies when the test plate 1 is heated with 3 °C/s heating rate. The change rate column shows the percent change of the initial frequency at the end of test period.

Table 4.4: The Natural Frequencies of the Test Plate 1 with respect to Temperature (3 °C/s heating rate)

Natural Frequency (Hz)	**30 °C**	**50 °C**	**70 °C**	**90 °C**	**110 °C**	**130 °C**	**150 °C**	**Difference**
First Mode	148.44	148.47	145.18	143.37	142.26	139.32	137.84	-7%
Second Mode	443.30	443.13	449.61	442.15	434.19	435.03	432.92	-2%
Third Mode	562.98	562.02	561.16	559.20	553.37	546.71	542.88	-4%

Table 4.5 and Figure 4.10 present the changes of damping ratios.

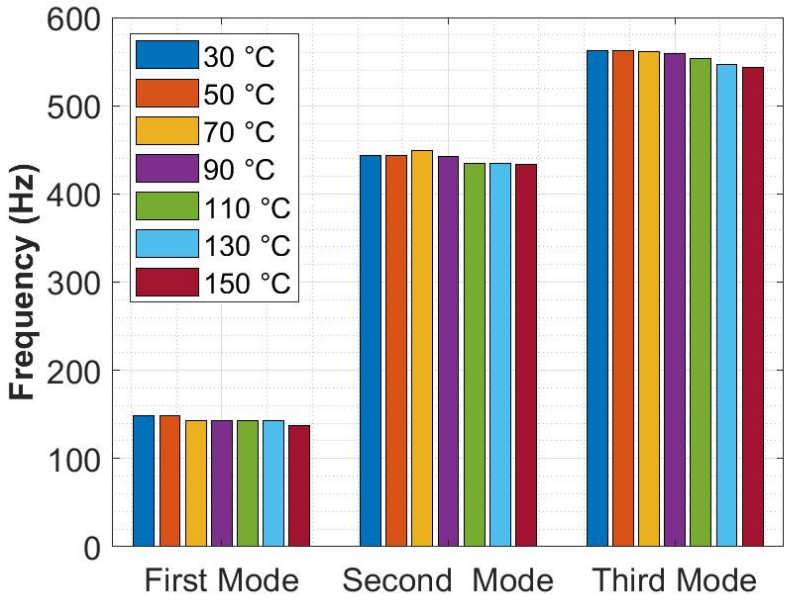

Figure 4.9: The Natural Frequencies of the Test Plate 1 with respect to Temperature (3 °C/s heating rate)

Table 4.5: The Damping Ratios of the Test Plate 1 with respect to Temperature (3 °C/s heating rate)

3 °C/s	**30 °C**	**50 °C**	**70 °C**	**90 °C**	**110 °C**	**130 °C**	**150 °C**	**Change Rate**
First Mode	0.076	0.068	0.052	0.062	0.085	0.115	0.076	0%
Second Mode	0.037	0.035	0.067	0.082	0.017	0.011	0.026	-29%
Third Mode	0.017	0.017	0.017	0.023	0.031	0.031	0.025	50%

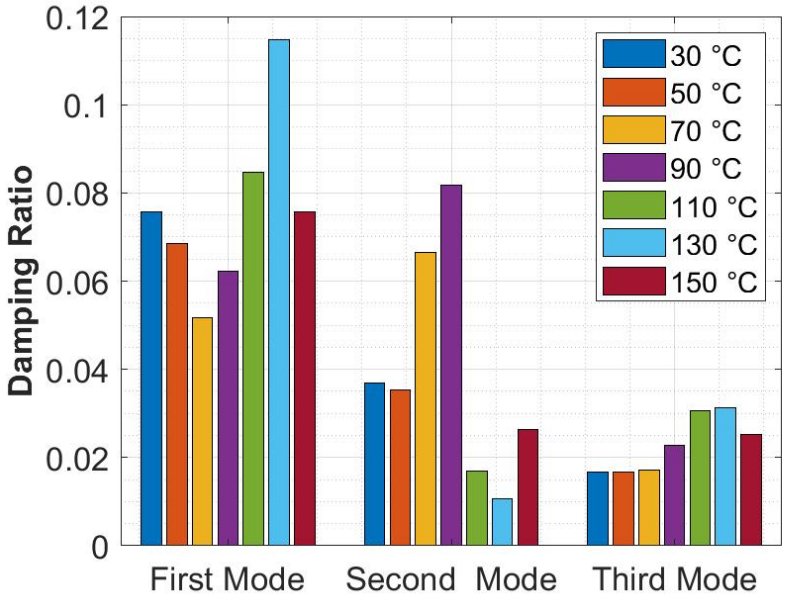

Figure 4.10: The Damping Ratios of the Test Plate 1 with respect to Temperature (3 °C/s heating rate)

4.2.1.2 2 °C/s Heating Rate

In this condition, the heated surface heated with 2 °C/s heating rate and when the unheated surface reaches nearly 120 °C, the test stopped. The duration of this test condition is 61 seconds. The temperature difference between faces reaches up to 20 °C.

During test period, the frequency response functions (FRF) are calculated for every 20 °C temperature increase and the Figure4.12 shows the spectrogram of the FRFs.

Figure 4.13 and Figure 4.14 present the changes in the FRFs of the test plate 1 when heated with 2 °C/s heating rate.

In Figure 4.15 the change in FRF amplitude of first natural frequency is presented.

Table 4.6 shows the values of first three natural frequencies at every 20 °C and Figure 4.16 shows the trend of change in natural frequencies when the test plate 1 is heated with 2 °C/s heating rate. The change rate column shows the percent change of the initial frequency at the end of test period.

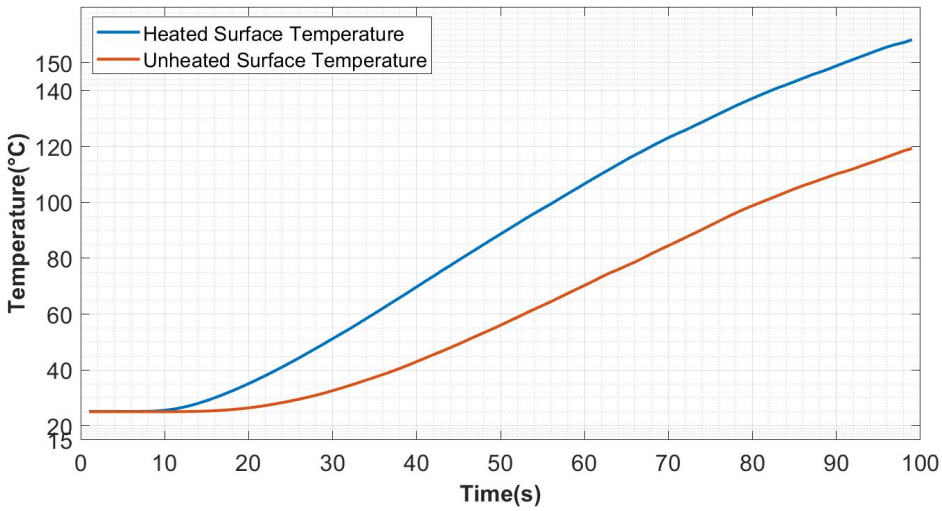

Figure 4.11: The Temperature values of the Test Plate 1 (2°C/s heating rate)

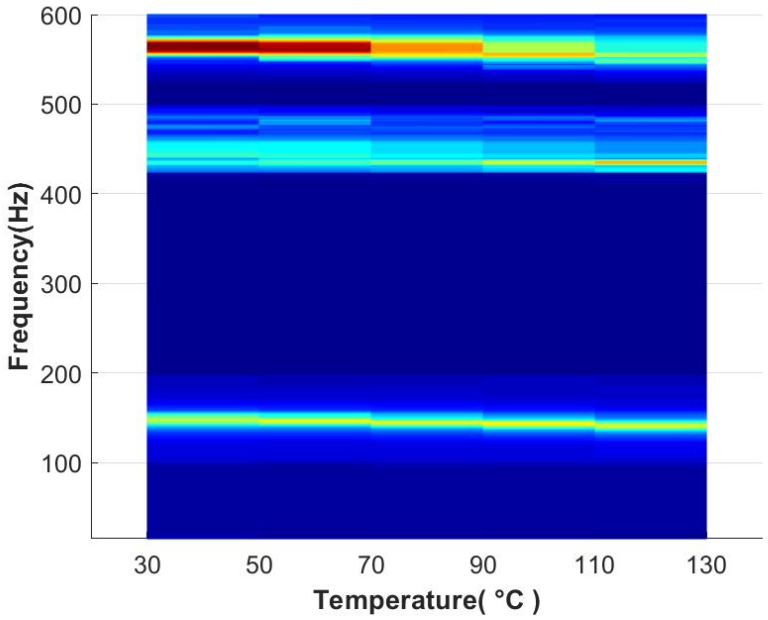

Figure 4.12: The Spectrogram of the Temperature dependent FRF changes of the Test Plate 1 (2°C/s heating rate)

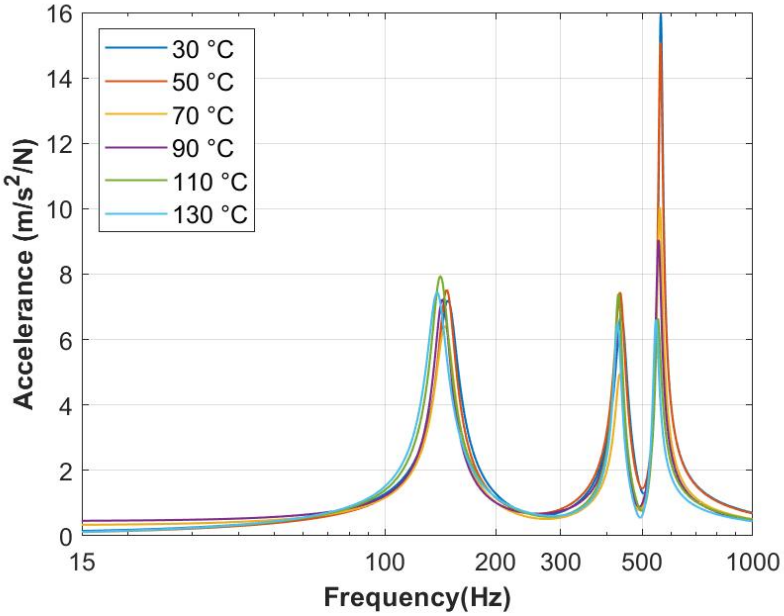

Figure 4.13: The FRFs of the Test Plate 1 under elevated Temperature (2°C/s heating rate)

Table 4.6: The Natural Frequencies of the Test Plate 1 with respect to Temperature (2 °C/s heating rate)

Natural Frequency (Hz)	**30 °C**	**50 °C**	**70 °C**	**90 °C**	**110 °C**	**130 °C**	**Change Rate**
First Mode	149.12	147.52	144.64	143.99	142.42	139.30	-7%
Second Mode	448.57	444.24	447.14	434.97	434.21	430.07	-4%
Third Mode	563.18	559.10	560.82	555.86	556.69	548.05	-3%

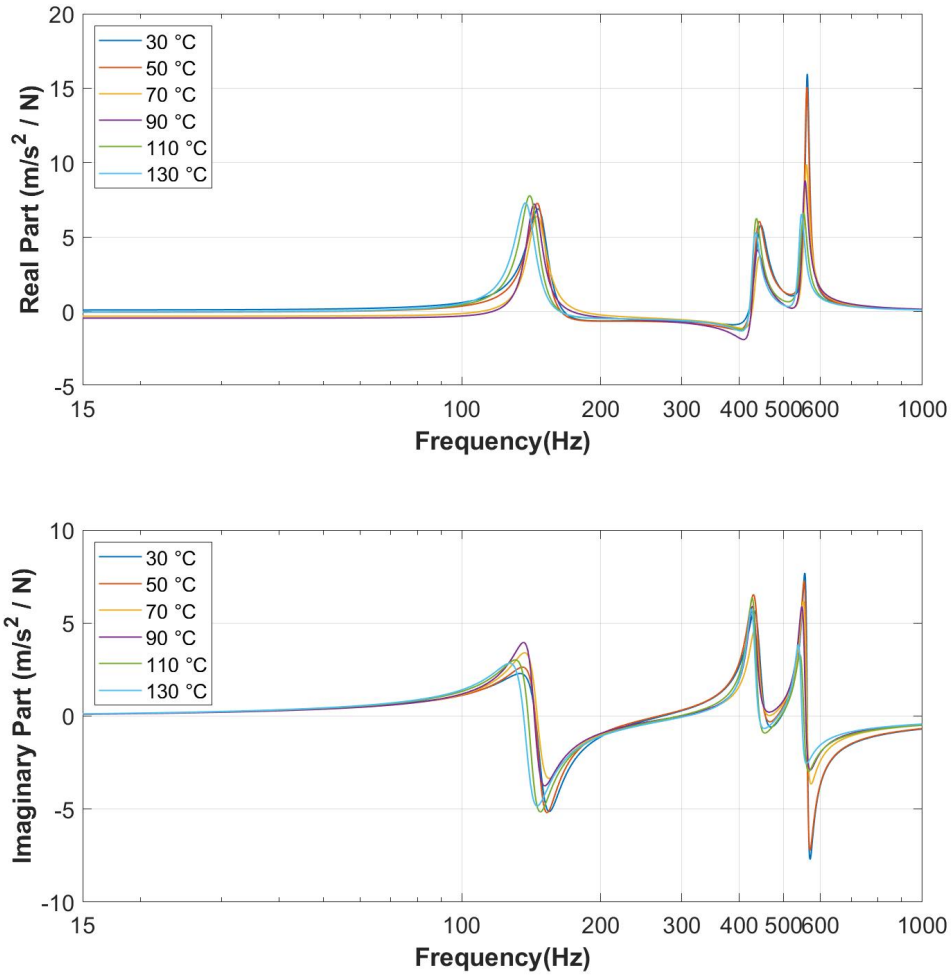

Figure 4.14: The Real and Imaginary Part of FRFs of the Test Plate 1 under Elevated Temperature (2°C/s heating rate)

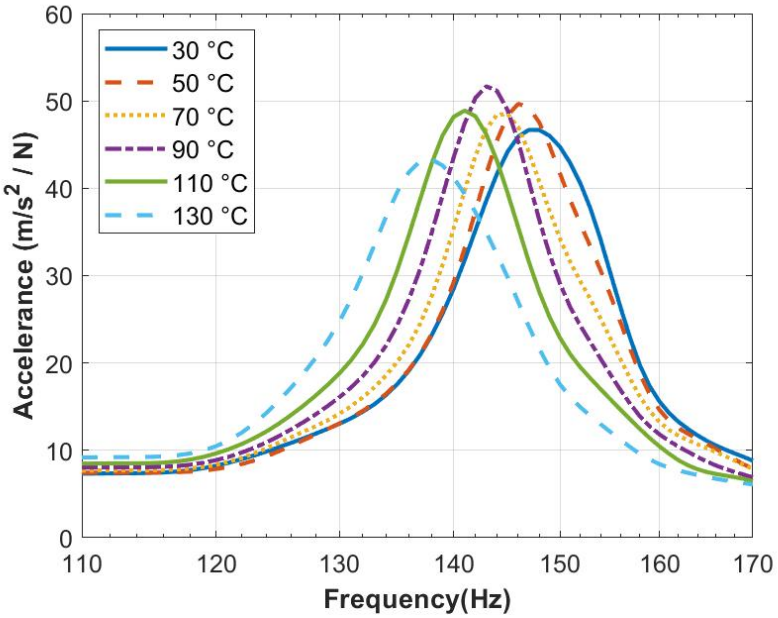

Figure 4.15: The Changes of the First Mode of the Test Plate 1 (2°C/s heating rate)

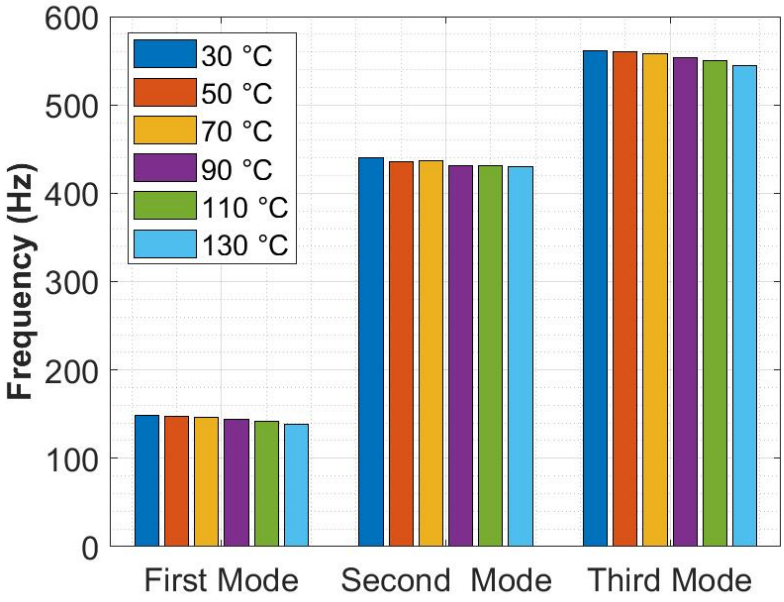

Figure 4.16: The Natural Frequencies of the Test Plate 1 with respect to Temperature (2 °C/s heating rate)

Table 4.7 and Figure 4.17 present the changes of damping ratios.

Table 4.7: The Damping Ratios of the Test Plate 1 with respect to Temperature (2 °C/s heating rate)

2 °C/s	**30 °C**	**50 °C**	**70 °C**	**90 °C**	**110 °C**	**130 °C**	**Change Rate**
First Mode	0.068	0.062	0.063	0.058	0.066	0.074	9%
Second Mode	0.059	0.068	0.081	0.052	0.048	0.044	-25%
Third Mode	0.015	0.016	0.022	0.009	0.027	0.008	-43%

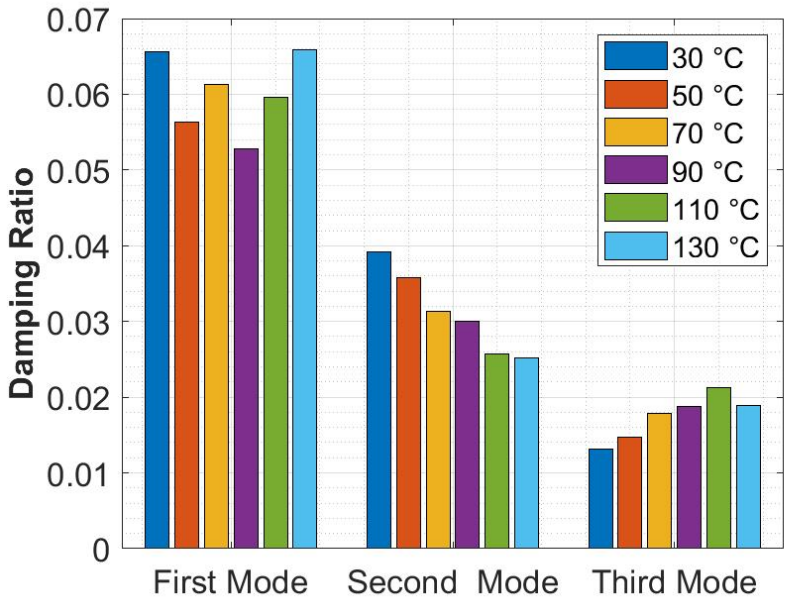

Figure 4.17: The Damping Ratios with respect to Temperature (2°C/s heating rate)

4.2.1.3 1 °C/s Heating Rate

The hot surface heated with heating rate of 1 °C/s and when the cold surface reaches nearly 120°C, the test is stopped. The duration of test is 123 seconds. The temperature difference between faces reaches up to 20 °C during the test.

The frequency response functions (FRF) are calculated for every 20 °C temperature increase and the Figure4.19 shows the spectrogram of the FRFs.

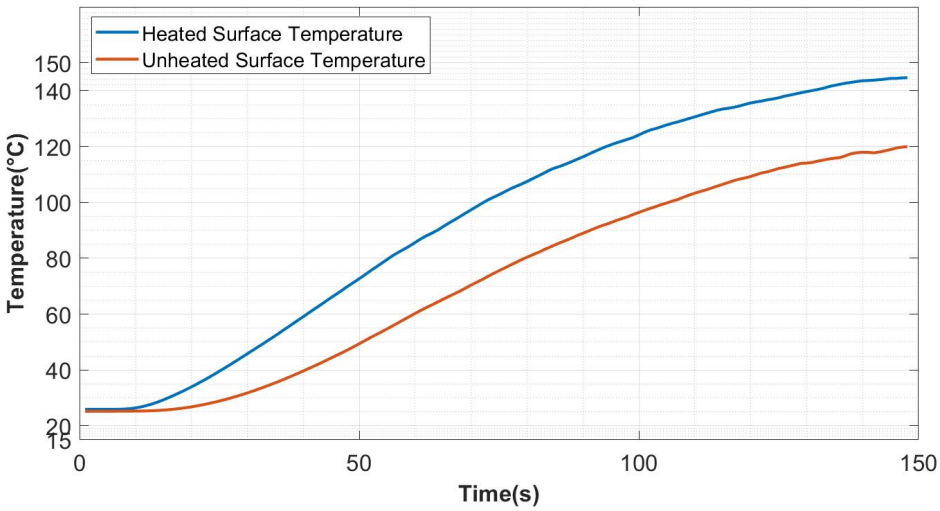

Figure 4.18: The Temperature values of the Test Plate 1 (1°C/s heating rate)

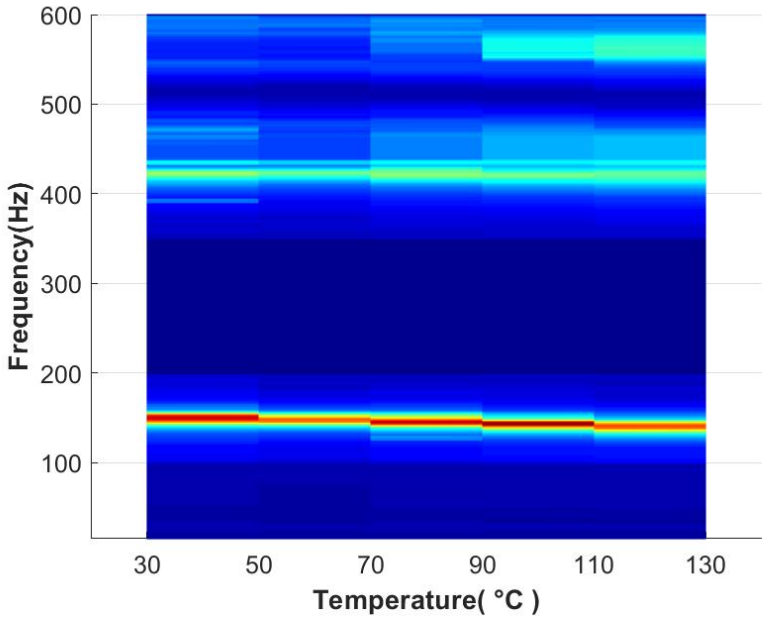

Figure 4.19: The Spectrogram of the Temperature dependent FRF changes of the Test Plate 1 (1°C/s heating rate)

Figure 4.20 and Figure 4.21 present the changes in the FRFs of the test plate 1 when heated with 1 °C/s heating rate.

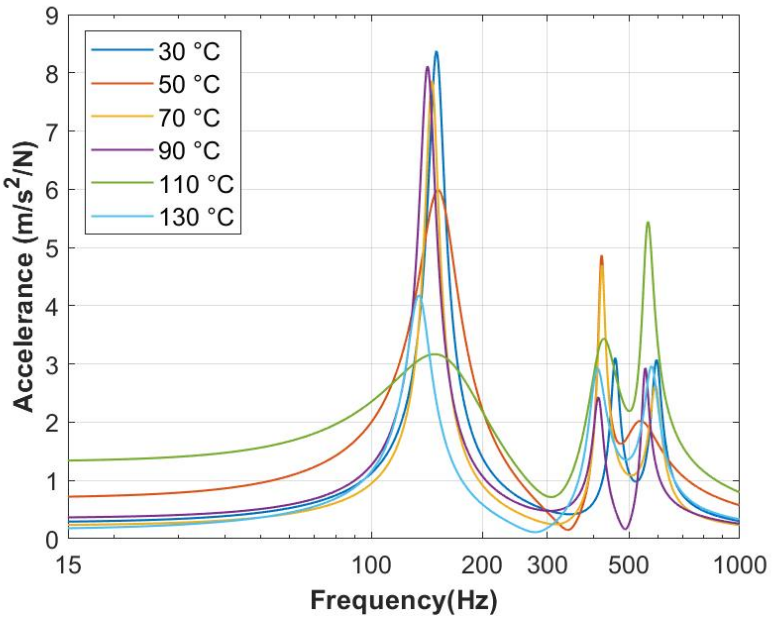

Figure 4.20: The FRFs of the Test Plate 1 under elevated Temperature (1°C/s heating rate)

In Figure 4.22 the change in FRF amplitude of first natural frequency is presented.

Table 4.8 shows the values of first three natural frequencies at every 20 °C and Figure 4.23 shows the trend of change in natural frequencies when the test plate 1 is heated with 1 °C/s heating rate. The change rate column shows the percent change of the initial frequency at the end of test period.

Table 4.8: The Natural Frequencies of the Test Plate 1 with respect to the Temperature (1 °C/s heating rate)

Natural Frequency (Hz)	**30 °C**	**50 °C**	**70 °C**	**90 °C**	**110 °C**	**130 °C**	**Change Rate**
First Mode	150.23	152.74	146.09	142.15	159.61	134.81	-10%
Second Mode	458.88	421.11	421.85	413.98	422.96	408.92	-11%
Third Mode	593.64	527.75	591.17	552.33	561.21	576.40	-3%

Table 4.9 and Figure 4.24 present the changes of damping ratios.

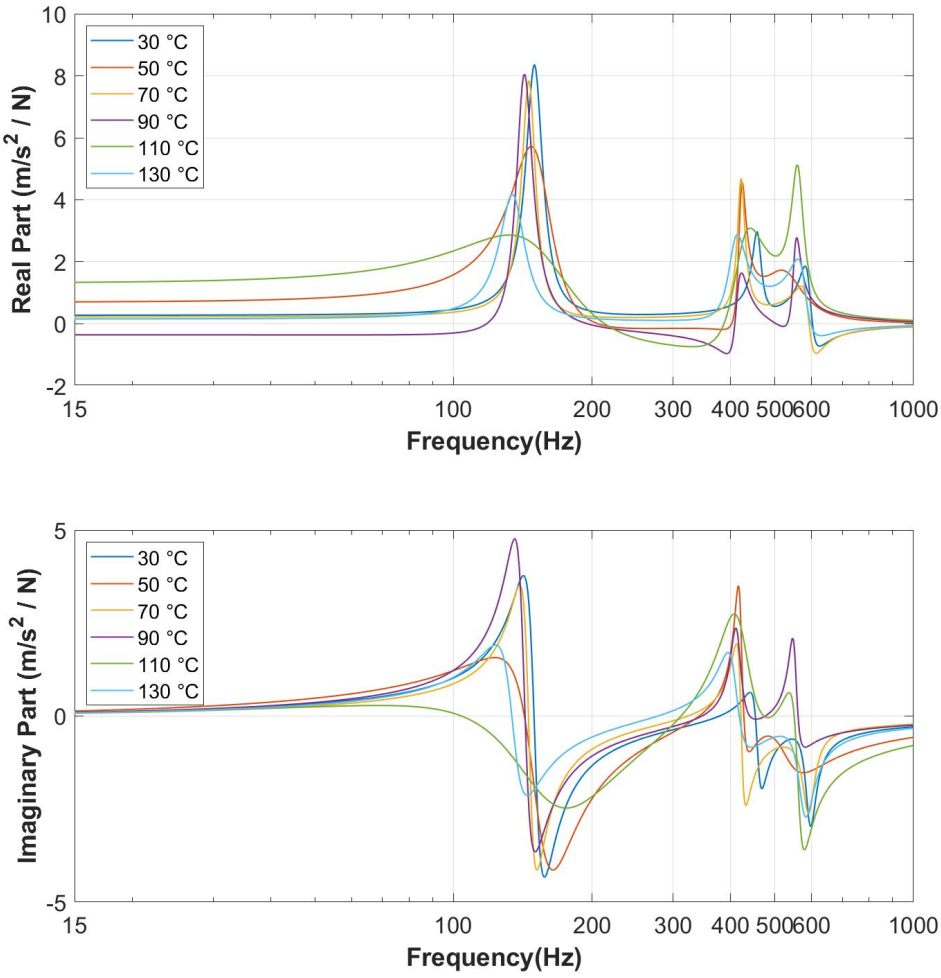

Figure 4.21: The Real and Imaginary Part of FRFs of the Test Plate 1 under the Elevated Temperature (1°C/s heating rate)

Table 4.9: The Damping Ratios of the Test Plate 1 with respect to the Temperature (1 °C/s heating rate)

1 °C/s	**30 °C**	**50 °C**	**70 °C**	**90 °C**	**110 °C**	**130 °C**	**Change Rate**
First Mode	0.052	0.129	0.043	0.051	0.340	0.079	51%
Second Mode	0.028	0.023	0.024	0.033	0.098	0.055	93%
Third Mode	0.033	0.125	0.037	0.025	0.038	0.048	46%

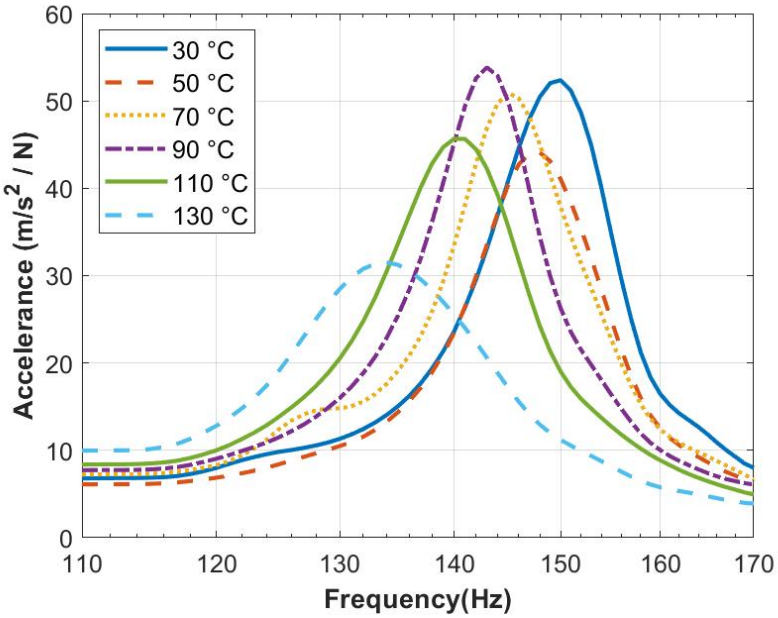

Figure 4.22: The Changes of the First Mode of the Test Plate 1 (1 °C/s heating rate)

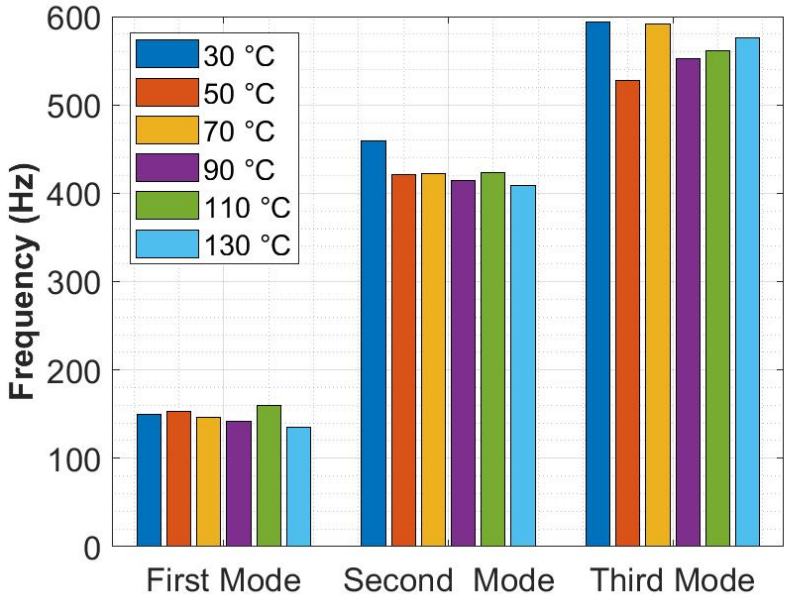

Figure 4.23: The Natural Frequencies of the Test Plate 1 with respect to the Temperature (1 °C/s heating rate)

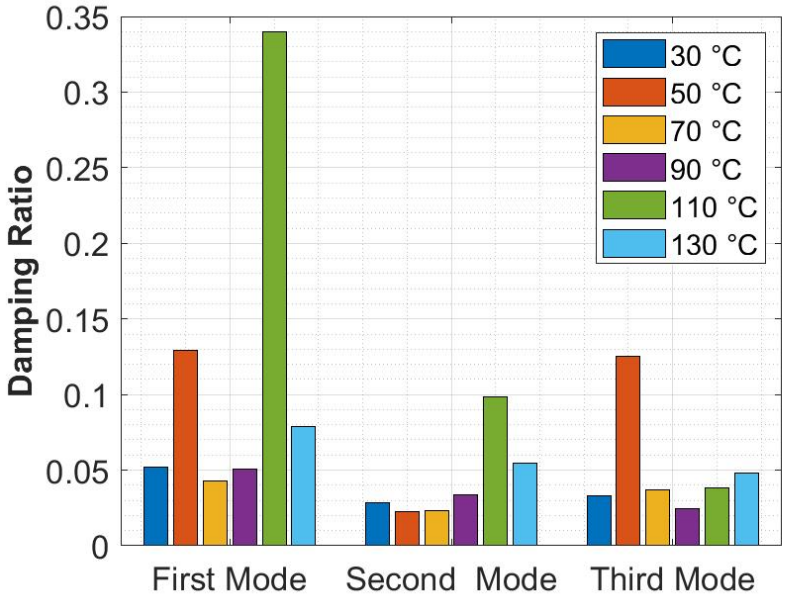

Figure 4.24: The Damping Ratios of the Test Plate 1 with respect to Temperature (1 °C/s heating rate)

4.2.2 The Test Results of the Test Plate 2

Figure 4.25 presents the temperature change during the test period.

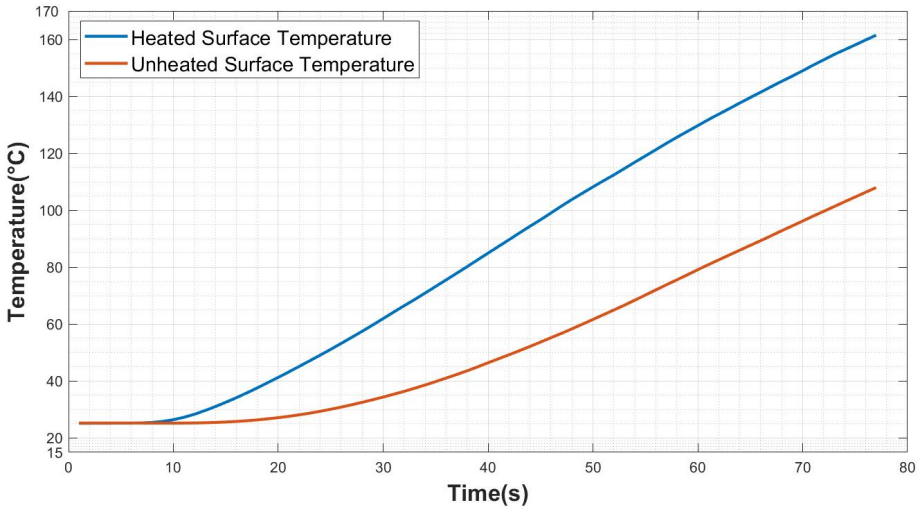

Figure 4.25: The Temperature values of the Test Plate 2 (3 °C/s heating rate)

Table 4.10 and 4.26 shows the first three natural frequencies of the test plate 2.

Table 4.10: The Natural Frequencies of Test Plate 2 under the Thermal Environment

Natural Frequency (Hz)	**30 °C**	**50 °C**	**70 °C**	**90 °C**	**110 °C**	**130 °C**	**150 °C**	**Change Rate**
First Mode	140.10	138.12	137.07	137.00	132.40	129.71	121.11	-13%
Second Mode	389.82	387.72	386.10	384.83	380.30	375.44	364.08	-7%
Third Mode	494.82	491.45	489.00	483.87	495.74	492.79	455.62	-8%

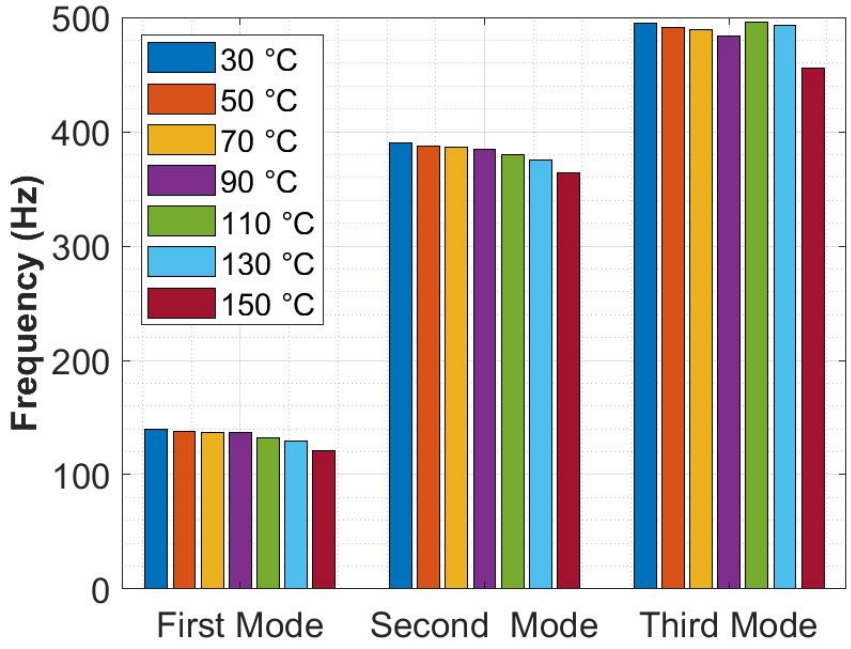

Figure 4.26: The Change of Natural Frequencies of the Test Plate 2 under the Thermal Environment

Table 4.11 and Figure 4.27 shows the damping ratios of the test plate 2.

Table 4.11: The Damping Ratios of Test Plate 2 under the Thermal Environment

3 °C/s	**30 °C**	**50 °C**	**70 °C**	**90 °C**	**110 °C**	**130 °C**	**150 °C**	**Change Rate**
First Mode	0.029	0.027	0.028	0.041	0.054	0.045	0.158	450%
Second Mode	0.037	0.025	0.025	0.014	0.024	0.031	0.034	-8%
Third Mode	0.021	0.021	0.019	0.028	0.031	0.056	0.063	204%

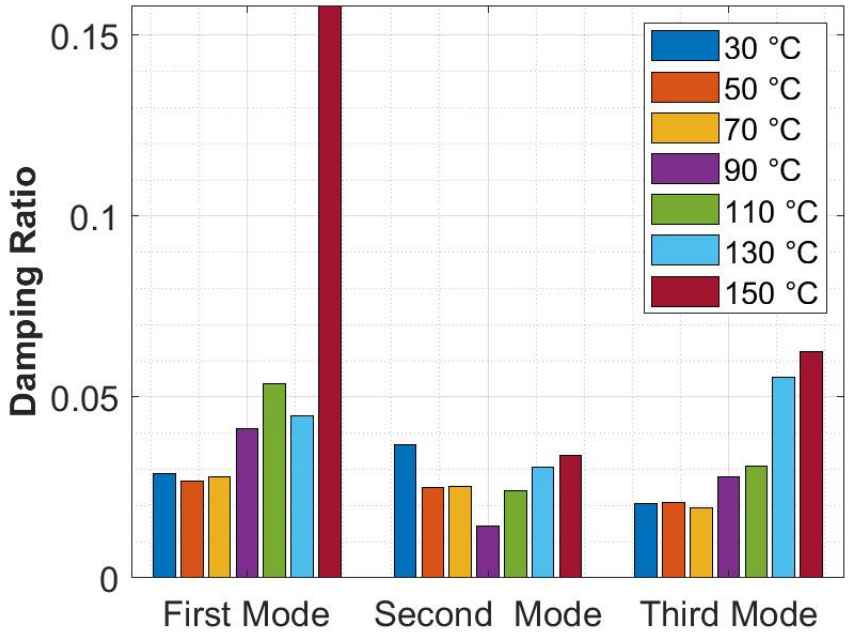

Figure 4.27: The Change of Damping Ratios of the Test Plate 2 under Thermal Environment

The vibration response amplitudes of the first natural frequency of the test plates 2 under the elevated temperature are shown in Figure 4.28.

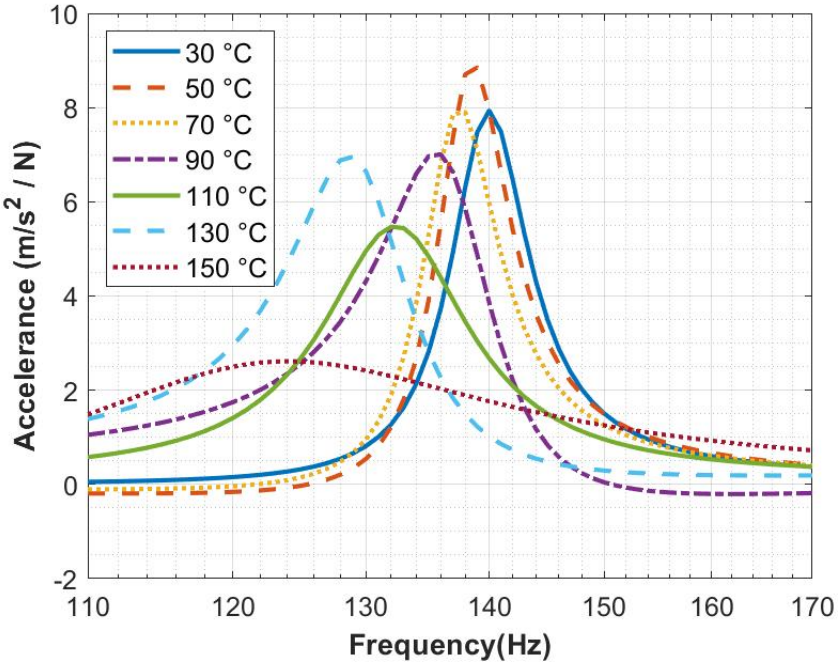

Figure 4.28: The FRF of the First Mode the Test Plate 2 under the Thermal Environment

4.3 The Test Results of Sandwich Composite Plate with Nomex Honeycombs

The effect of cell geometry on modal parameters of sandwich composite structure under the elevated thermal environment is examined by two nomex cores with different cell geometries which are the test plate 3 and test plate 4. Both core have same core thickness, cell wall thickness and cell size.

The test plate 3 is tested with three heating rate and results of each test condition is presented.

4.3.1 The Test Results of Test Plate 3

4.3.1.1 3 °C/s Heating Rate

When the heated surface heated to 160°C with 3°C/s heating rate, the unheated surface reaches nearly 35°C and the test duration is 47 seconds. The temperature differ-

ence between faces reaches up to 125°C.

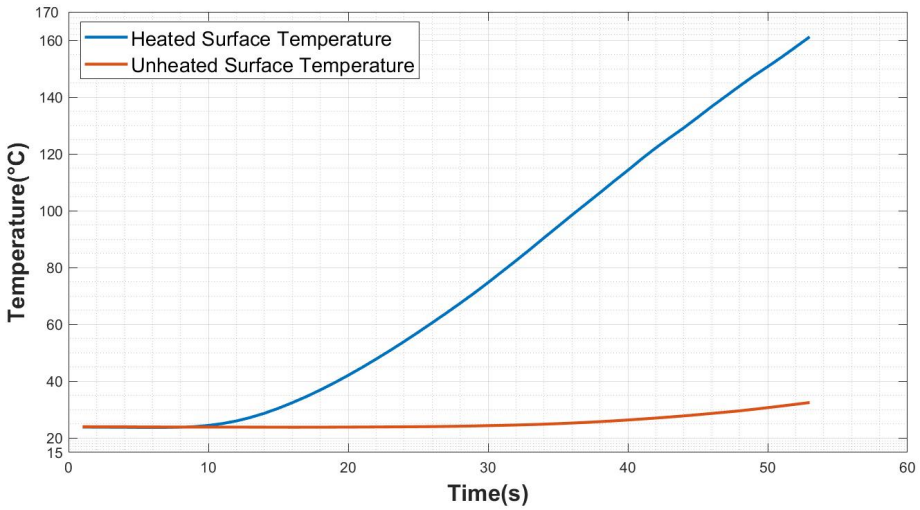

Figure 4.29: The Temperature values of the Test Plate 3 (3°C/s heating rate)

During test period, the frequency response functions (FRF) are calculated for every 20 °C temperature increase and the Figure 4.30 shows the spectrogram of the FRFs.

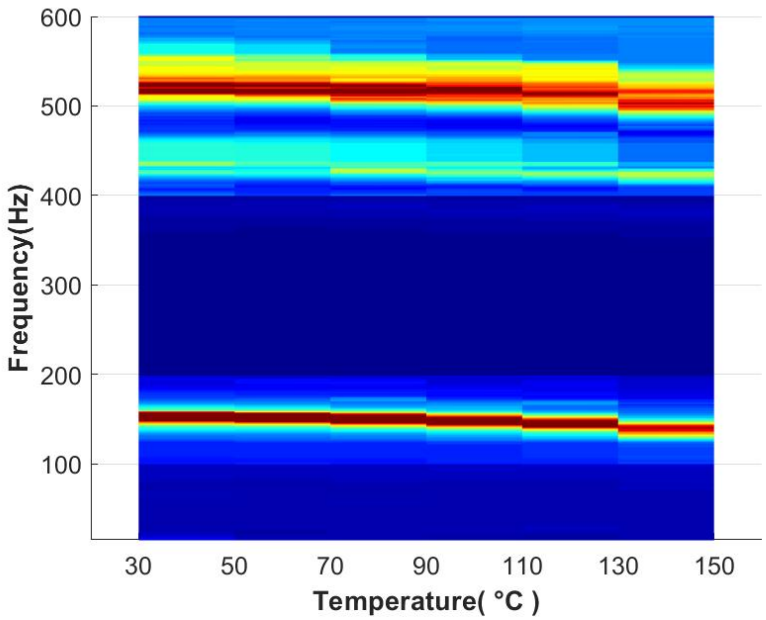

Figure 4.30: The Spectrogram of the Temperature dependent FRF changes of the Test Plate 3 (3°C/s heating rate)

Figure 4.31 and Figure 4.32 present the changes in the FRFs of the test plate 3 when

heated with 3°C/s heating rate.

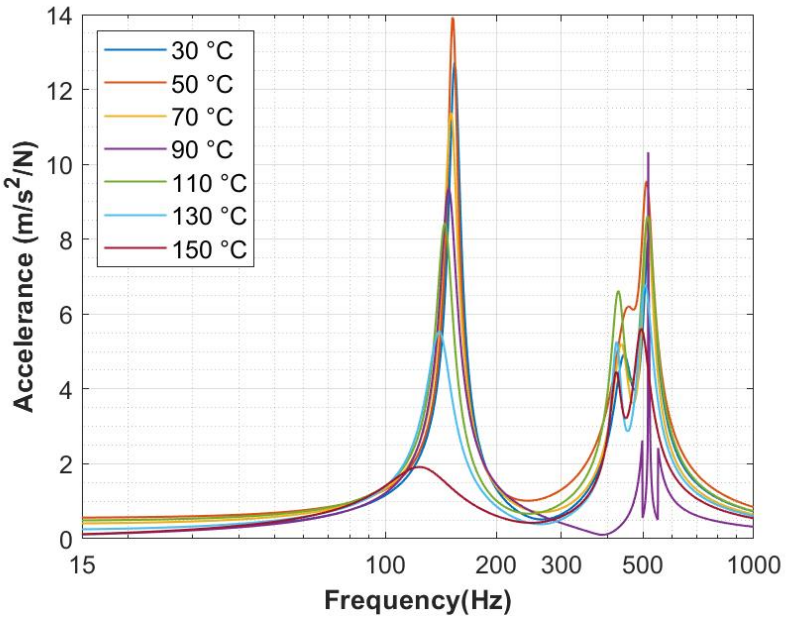

Figure 4.31: The FRFs of the Test Plate 3 under the Elevated Temperature (3°C/s heating rate)

In Figure 4.33 the change in FRF amplitude of first natural frequency is presented.

Table 4.12 shows the values of first three natural freuencies at every 20 °C and Figure 4.34 shows the trend of change in natural frequencies when the test plate 3 is heated with 3 °C/s heating rate. The change rate column shows the percent change of the initial frequency at the end of test period.

Table 4.12: The Natural Frequencies of the Test Plate 3 with respect to the Temperature (3°C/s heating rate)

Natural Frequency (Hz)	**30 °C**	**50 °C**	**70 °C**	**90 °C**	**110 °C**	**130 °C**	**150 °C**	**Change Rate**
First Mode	154.24	152.49	150.77	148.54	145.23	140.34	125.69	-19%
Second Mode	445.38	454.17	438.28	434.64	429.30	425.13	424.03	-5%
Third Mode	518.17	510.76	513.75	519.06	514.34	505.96	493.62	-5%

Table 4.13 and Figure 4.35 present the changes of damping ratios.

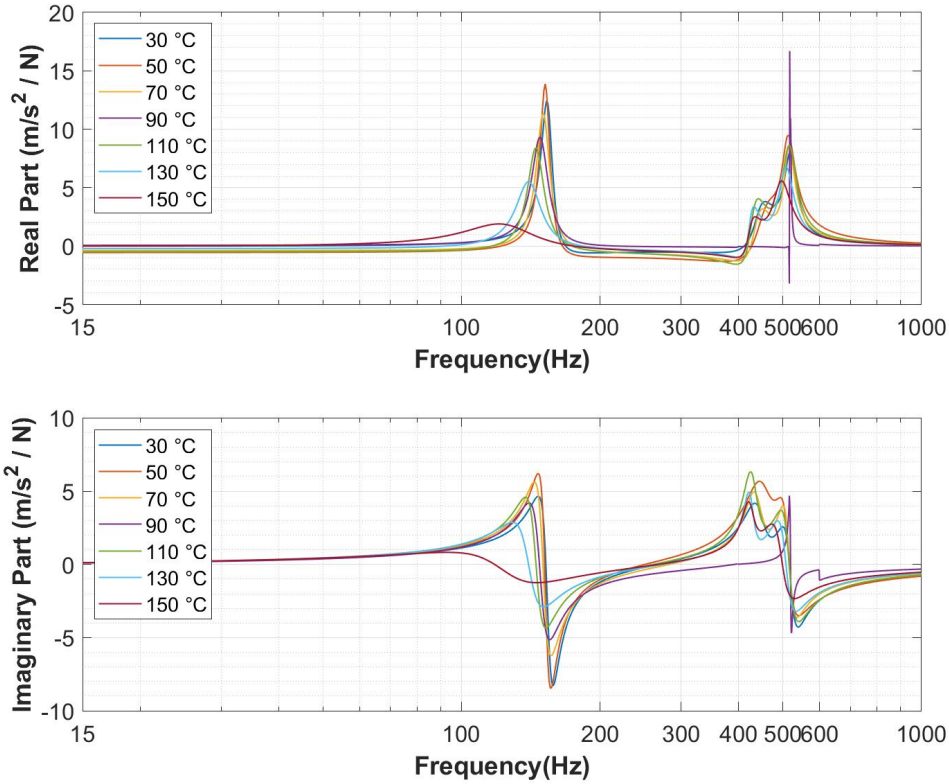

Figure 4.32: The Real and Imaginary Part of FRFs of the Test Plate 3 under the Elevated Temperature (3°C/s heating rate)

Table 4.13: The Damping Ratios of the Test Plate 3 with respect to the Temperature (3°C/s heating rate)

3 °C/s	**30 °C**	**50 °C**	**70 °C**	**90 °C**	**110 °C**	**130 °C**	**150 °C**	**Change Rate**
First Mode	0.035	0.031	0.042	0.051	0.051	0.078	0.222	536%
Second Mode	0.062	0.082	0.052	0.000	0.045	0.031	0.038	-39%
Third Mode	0.039	0.041	0.034	0.004	0.045	0.047	0.055	42%

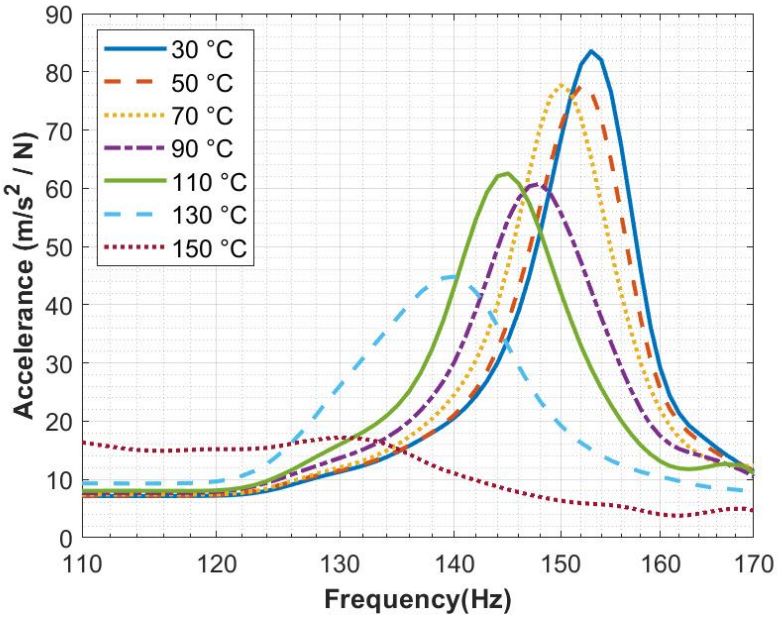

Figure 4.33: The Changes of the First Mode of the Test Plate 3 (3°C/s heating rate)

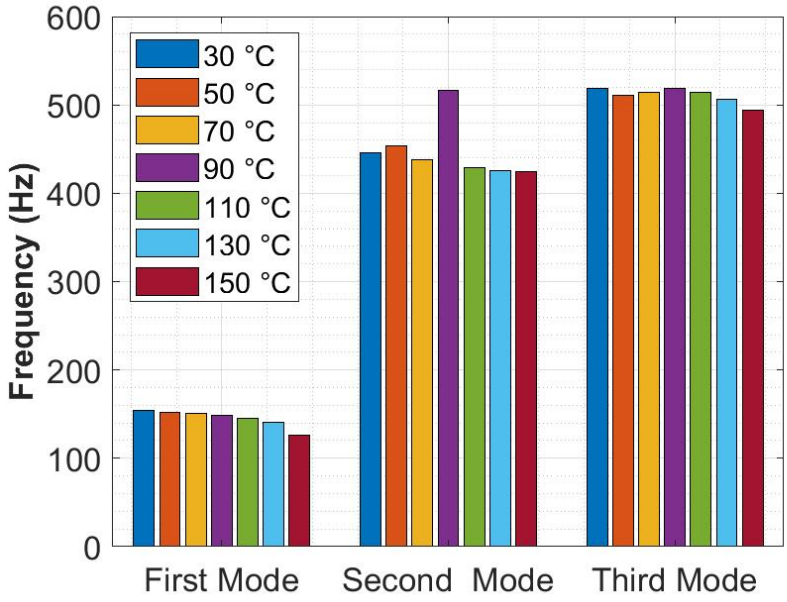

Figure 4.34: The Natural Frequencies of the Test Plate 3 with respect to Temperature (3°C/s heating rate)

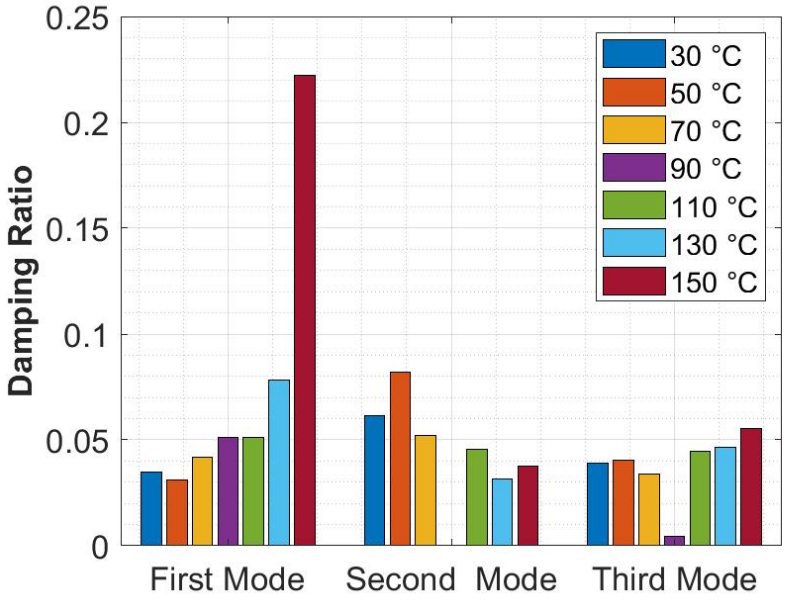

Figure 4.35: The Damping Ratios of the Test Plate 3 with respect to the Temperature (3°C/s heating rate)

4.3.1.2 2 °C/s Heating Rate

In this condition, the heated surface heated with 2°C/s heating rate and when the heated surface reaches nearly 160°C the test stopped. The duration of this test condition is 70 seconds. The temperature difference between faces reaches up to 115°C.

During test period, the frequency response functions (FRF) are calculated for every 20 °C temperature increase and the Figure 4.37 shows the spectrogram of the FRFs.

Figure 4.38 and Figure 4.39 present the changes in the FRFs of the test plate 3 when heated with 2°C/s heating rate.

In Figure 4.40 the change in FRF amplitude of the first natural frequency is presented.

Table 4.14 shows the values of first three natural freuencies at every 20 °C and Figure 4.41 shows the trend of change in natural frequencies when the test plate 3 is heated with 2 °C/s heating rate. The change rate column shows the percent change of the initial frequency at the end of test period.

Table 4.15 and Figure 4.42 present the changes of damping ratios.

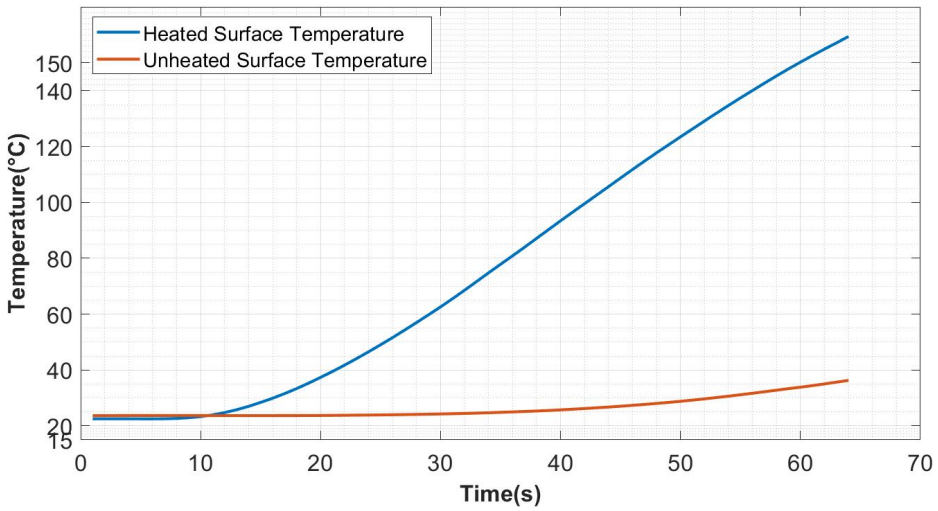

Figure 4.36: The Temperature Values of the Test Plate 3 (2°C/s heating rate)

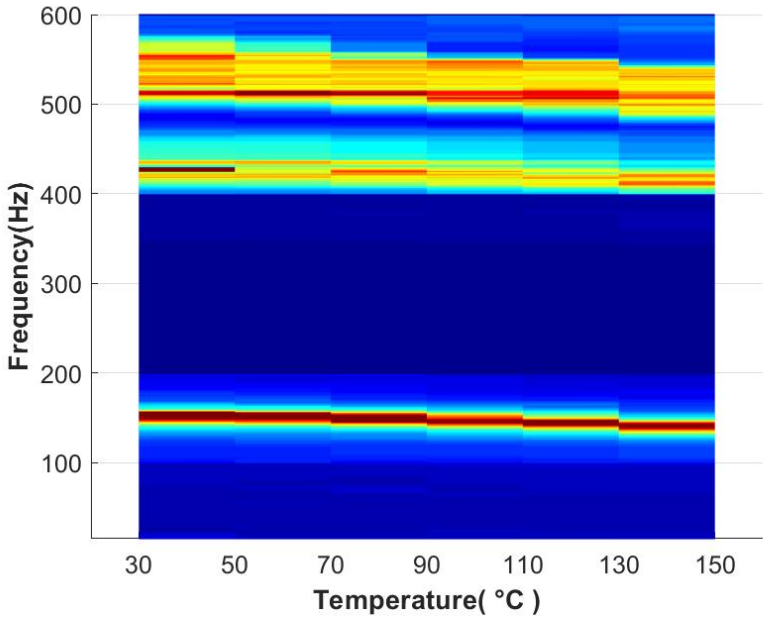

Figure 4.37: The Spectrogram of the Temperature Dependent FRF changes of the Test Plate 3 (2°C/s heating rate)

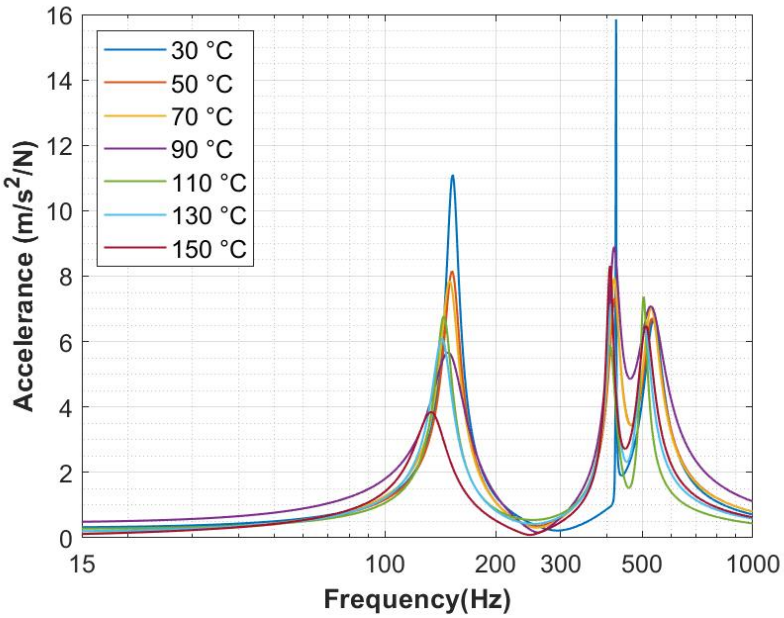

Figure 4.38: The FRFs of the Test Plate 3 under elevated Temperature (2°C/s heating rate)

Table 4.14: The Natural Frequencies of the Test Plate 3 with respect to Temperature (2°C/s heating rate)

Natural Frequency (Hz)	**30 °C**	**50 °C**	**70 °C**	**90 °C**	**110 °C**	**130 °C**	**150 °C**	**Change Rate**
First Mode	152.92	152.51	150.29	149.87	144.73	143.17	134.23	-12%
Second Mode	424.54	421.37	419.89	419.14	409.99	412.83	409.27	-4%
Third Mode	536.12	531.12	527.75	526.95	503.82	506.35	510.72	-5%

Table 4.15: The Damping Ratios of the Test Plate 3 with respect to Temperature(2°C/s heating rate)

2 °C/s	**30 °C**	**50 °C**	**70 °C**	**90 °C**	**110 °C**	**130 °C**	**150 °C**	**Change Rate**
First Mode	0.040	0.052	0.057	0.109	0.052	0.065	0.103	158%
Second Mode	0.035	0.037	0.034	0.037	0.035	0.029	0.022	-36%
Third Mode	0.060	0.061	0.057	0.089	0.022	0.042	0.051	-14%

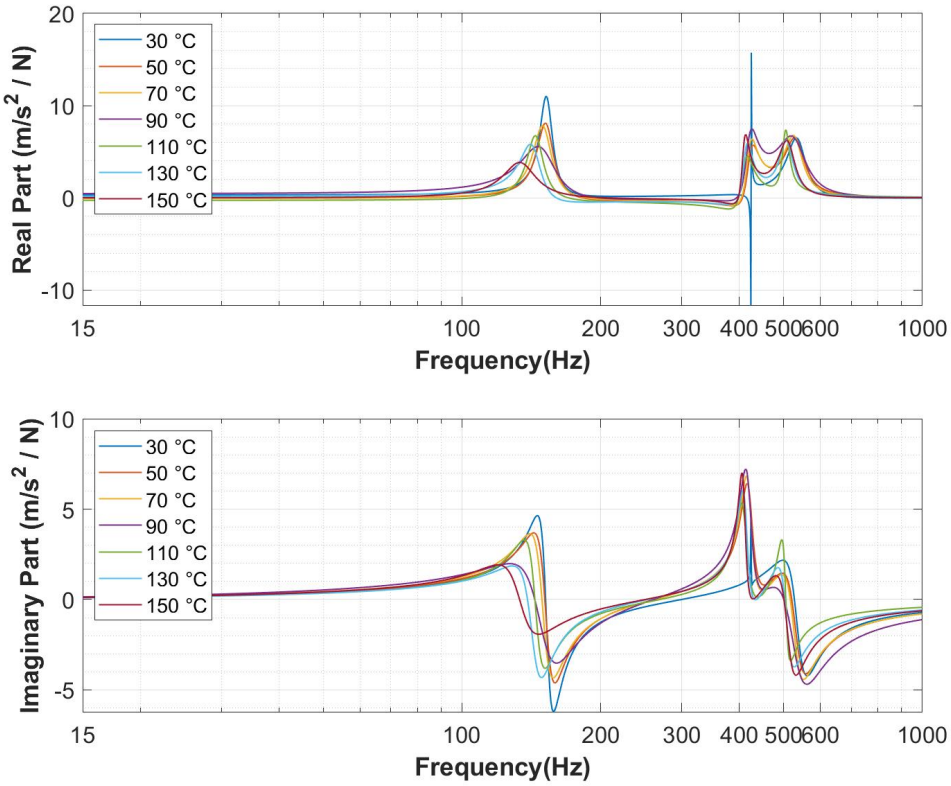

Figure 4.39: The Real and Imaginary Part of FRFs of the Test Plate 3 under the Elevated Temperature (2°C/s heating rate)

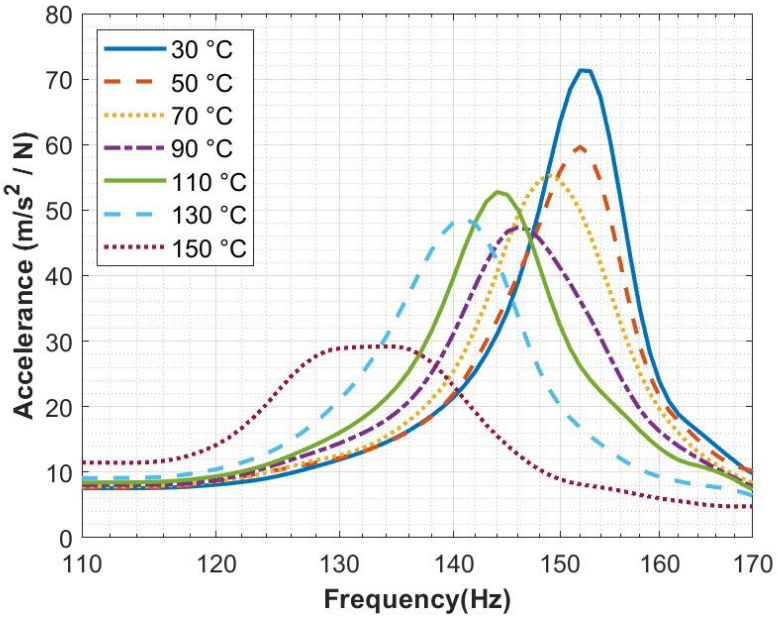

Figure 4.40: The Changes of the First Mode of the Test Plate 3 (2°C/s heating rate)

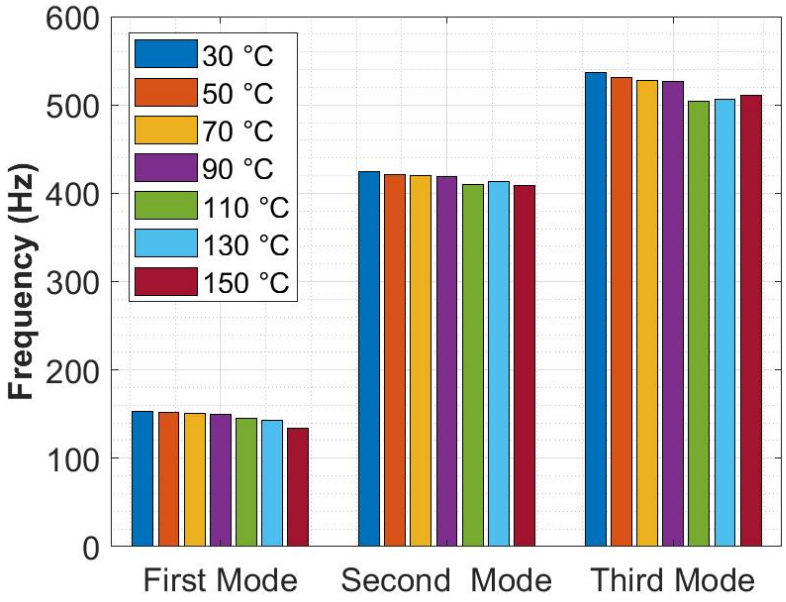

Figure 4.41: The Natural Frequencies of the Test Plate 3 with respect to Temperature (2°C/s heating rate)

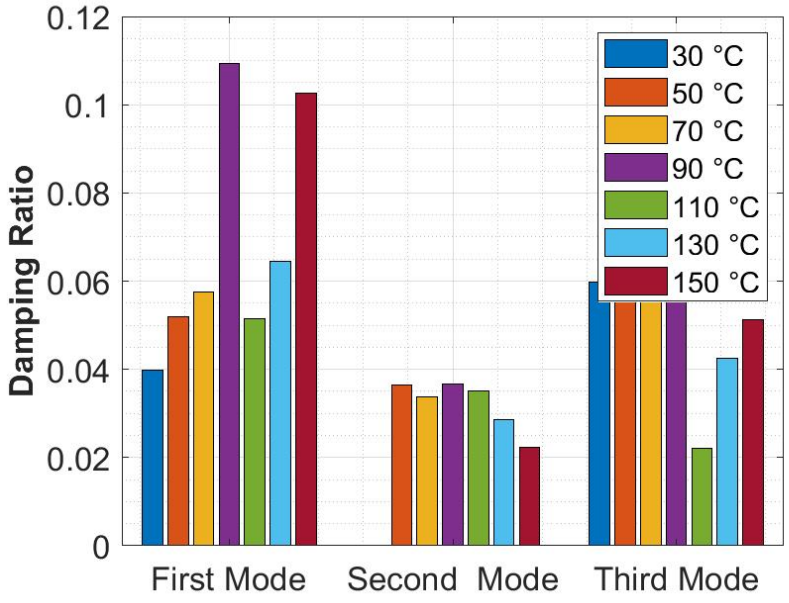

Figure 4.42: The Damping Ratios of the Test Plate 3 with respect to Temperature(2°C/s heating rate)

4.3.1.3 1 °C/s Heating Rate

In this condition, the heated surface heated with 1°C/s heating rate and when the heated surface reaches nearly 160°C the test stopped. The duration of this test condition is 141 seconds. The temperature difference between faces reaches up to 105°C.

During test period, the frequency response functions (FRF) are calculated for every 20 °C temperature increase and the Figure 4.44 shows the spectrogram of the FRFs.

Figure 4.45 and Figure 4.46 present the changes in the FRFs of the test plate 3 when heated with 1°C/s heating rate.

In Figure 4.47 the change in FRF amplitude of the first natural frequency is presented.

Table 4.16 shows the values of first three natural freuencies at every 20 °C and Figure 4.48 shows the trend of change in natural frequencies when the test plate 3 is heated with 1 °C/s heating rate. The change rate column shows the percent change of the initial frequency at the end of test period.

Table 4.17 and Figure 4.49 present the changes of damping ratios.

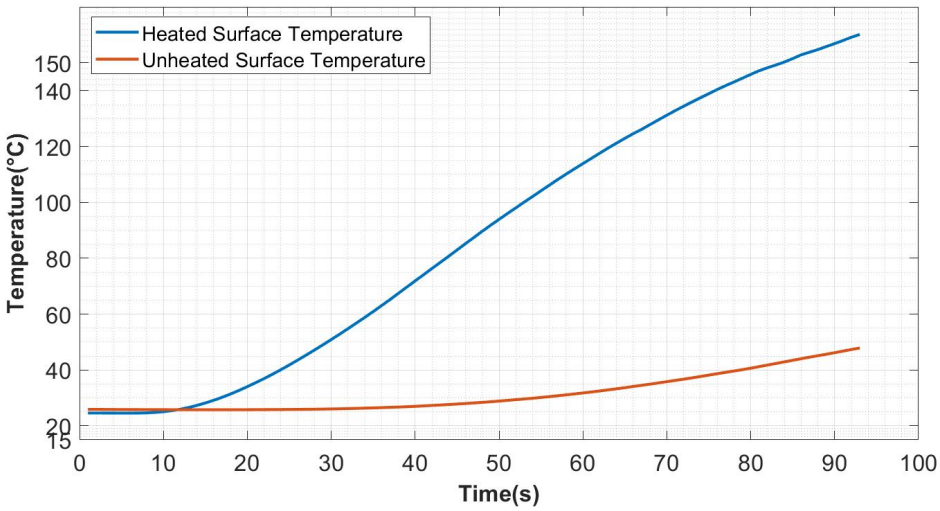

Figure 4.43: The Temperature values of the Test Plate 3 (1°C/s heating rate)

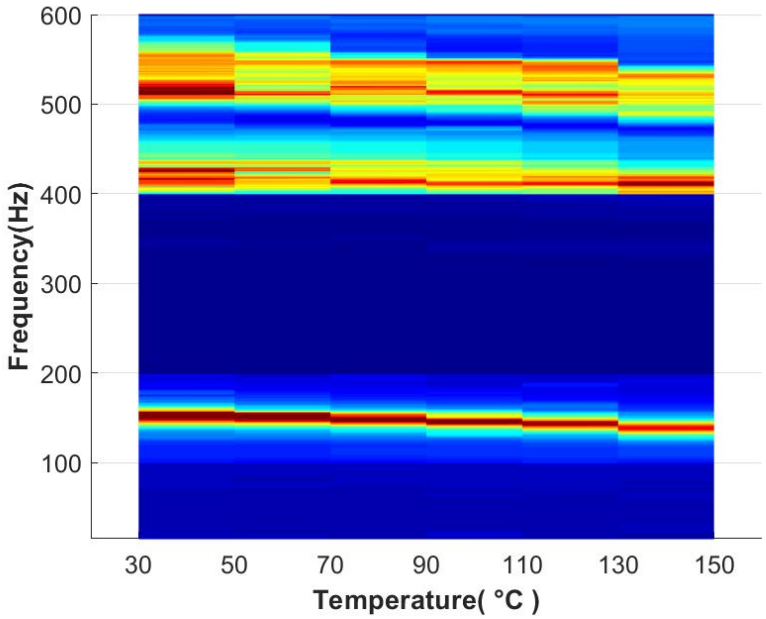

Figure 4.44: The Spectrogram of the Temperature dependent FRF changes of the Test Plate 3 (1°C/s heating rate)

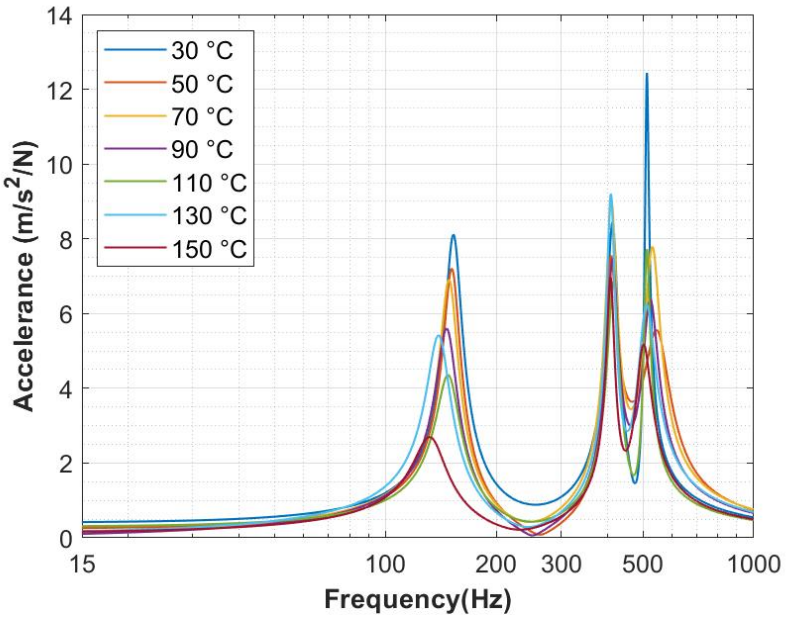

Figure 4.45: The FRFs of the Test Plate 3 under the Elevated Temperature (1°C/s heating rate)

Table 4.16: The Natural Frequencies of the Test Plate 3 with respect to Temperature (1°C/s heating rate)

Natural Frequency (Hz)	**30 °C**	**50 °C**	**70 °C**	**90 °C**	**110 °C**	**130 °C**	**150 °C**	**Change Rate**
First Mode	153.17	151.75	149.18	147.07	148.55	139.91	132.89	-13%
Second Mode	414.37	408.09	410.34	413.65	415.85	409.66	408.77	-1%
Third Mode	512.21	546.53	529.88	522.44	511.70	509.62	500.67	-2%

Table 4.17: The Damping Ratios of the Test Plate 3 with respect to Temperature(1°C/s heating rate)

1 °C/s	**30 °C**	**50 °C**	**70 °C**	**90 °C**	**110 °C**	**130 °C**	**150 °C**	**Change Rate**
First Mode	0.054	0.054	0.057	0.068	0.077	0.076	0.106	96%
Second Mode	0.036	0.036	0.034	0.035	0.035	0.026	0.025	-30%
Third Mode	0.012	0.083	0.049	0.050	0.019	0.055	0.050	301%

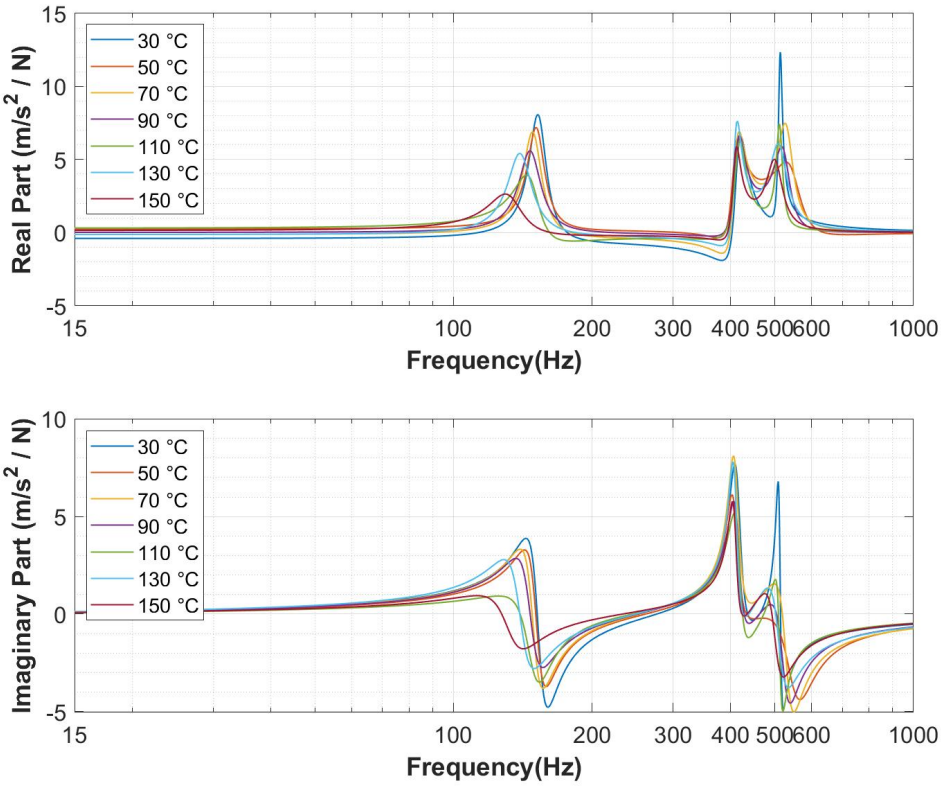

Figure 4.46: The Real and Imaginary Part of FRFs of the Test Plate 3 under the Elevated Temperature (1°C/s heating rate)

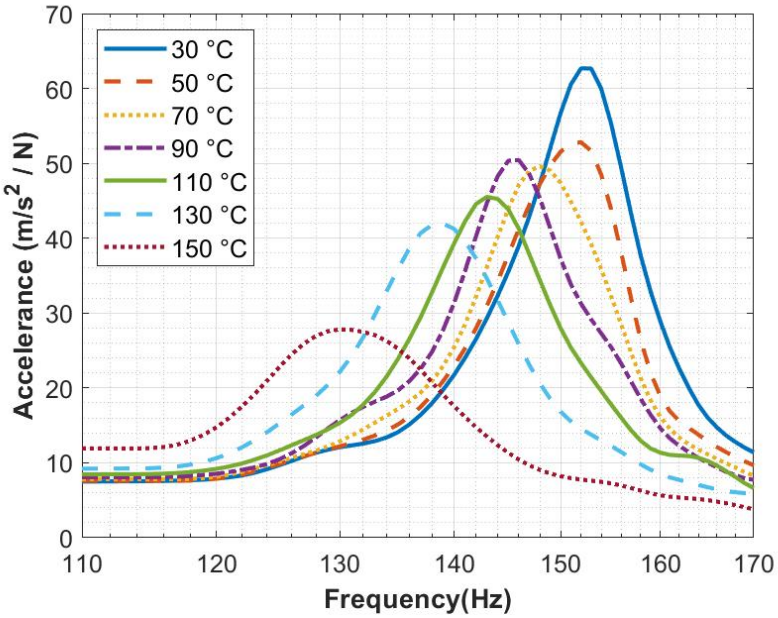

Figure 4.47: The Changes of the First Mode of the Test Plate 3 (1°C/s heating rate)

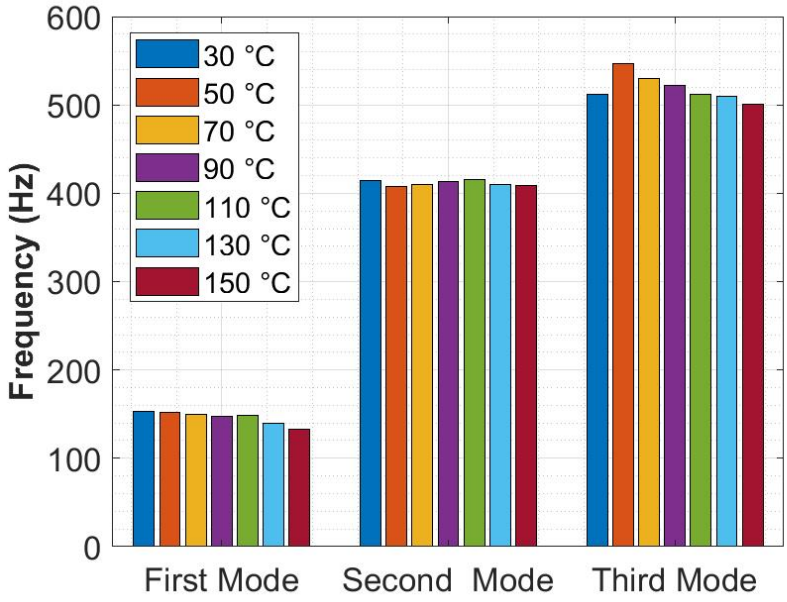

Figure 4.48: The Natural Frequencies of the Test Plate 3 with respect to Temperature (1°C/s heating rate)

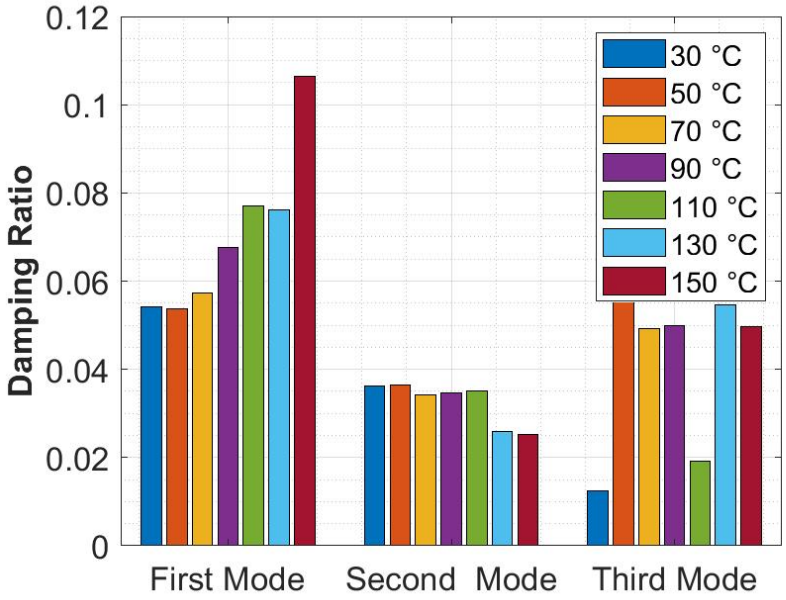

Figure 4.49: The Damping Ratios of the Test Plate 3 with respect to Temperature(1°C/s heating rate)

4.3.2 The Test Results of Test Plate 4

Figure 4.50 presents the temperature change during the test period.

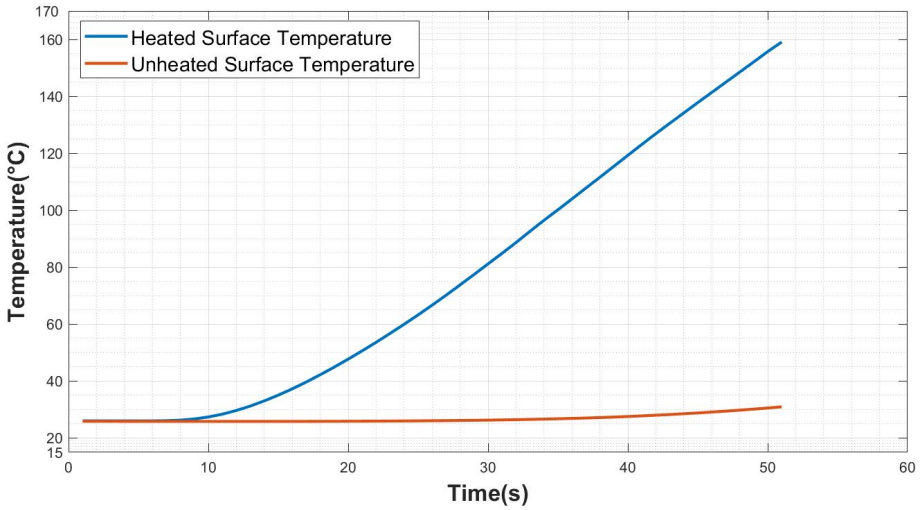

Figure 4.50: The Temperature Values of the Test Plate 4 (3 °C/s heating rate)

Table 4.18 and 4.51 shows the first three natural frequencies of the test plate 4.

Table 4.18: The Natural Frequencies of Test Plate 4 under thermal environment

Natural Frequency (Hz)	**30 °C**	**50 °C**	**70 °C**	**90 °C**	**110 °C**	**130 °C**	**150 °C**	**Change Rate**
First Mode	139.53	138.93	137.36	134.74	131.20	127.38	113.74	-18%
Second Mode	367.52	381.00	384.16	380.52	375.43	375.32	368.88	-0%
Third Mode	480.11	480.74	481.12	476.98	445.78	445.35	433.82	-10%

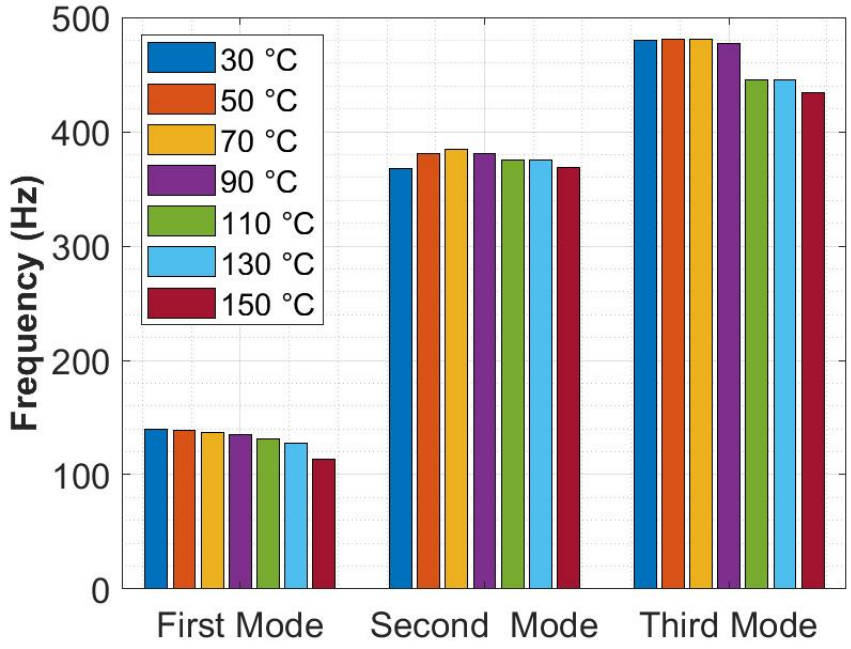

Figure 4.51: The Change of Natural Frequencies of the Test Plate 4 under Thermal Environment

Table 4.19 and Figure 4.52 shows the damping ratios of the test plate 4.

Table 4.19: The Damping Ratios of the Test Plate 4 under the Thermal Environment

3 °C/s	**30 °C**	**50 °C**	**70 °C**	**90 °C**	**110 °C**	**130 °C**	**150 °C**	**Change Rate**
First Mode	0.051	0.045	0.053	0.055	0.057	0.082	0.126	147%
Second Mode	0.041	0.037	0.032	0.029	0.047	0.058	0.070	71%
Third Mode	0.025	0.043	0.065	0.074	0.053	0.037	0.057	131%

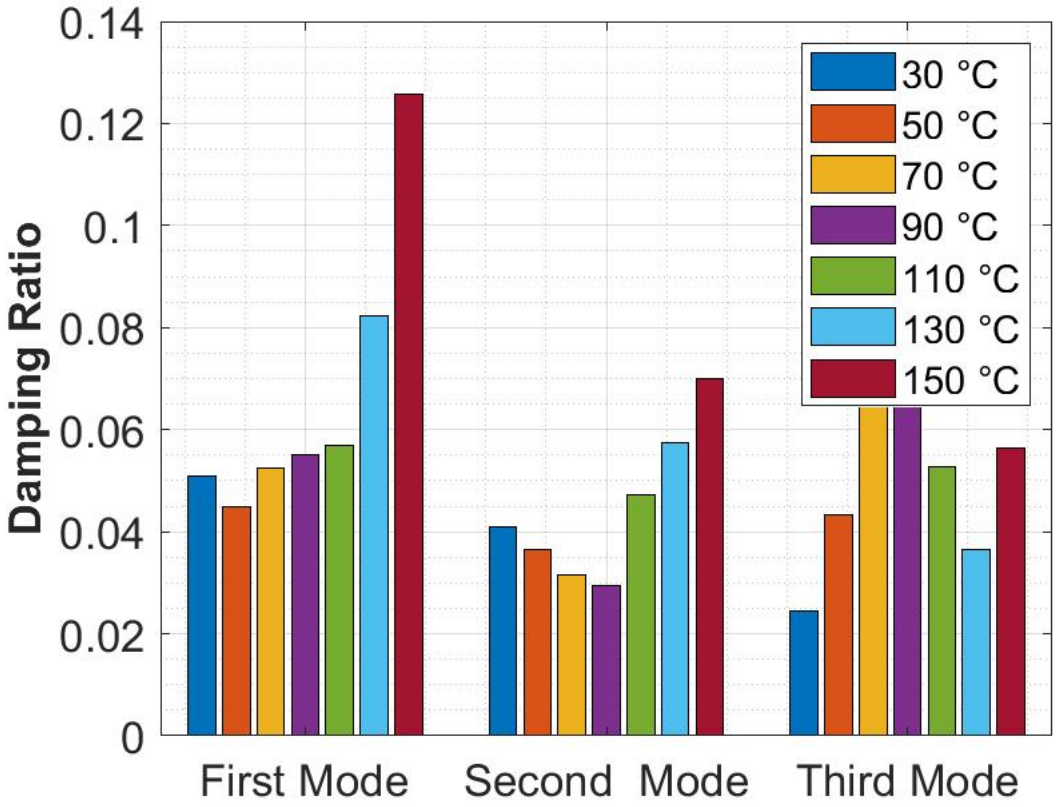

Figure 4.52: The Change of Natural Frequencies of the Test Plate 4 under Thermal Environment

The Figure 4.53 shows the FRF amplitude changes of first natural frequency of the test plate 4.

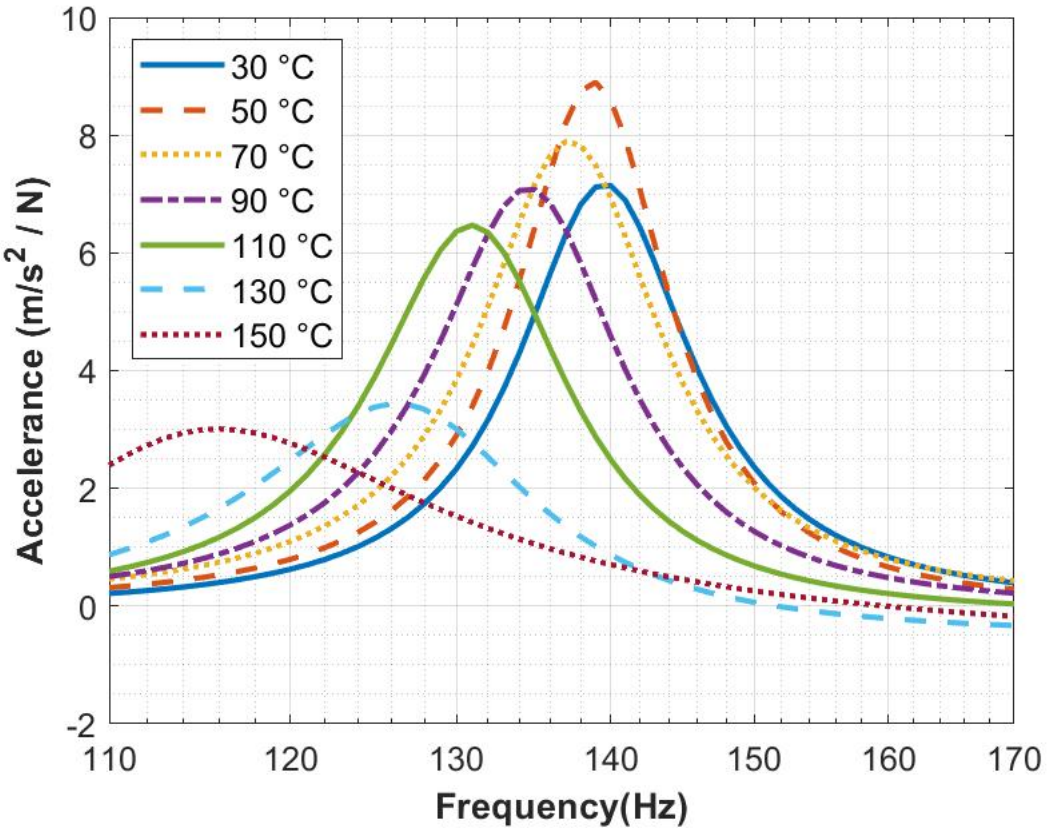

Figure 4.53: The Change of Natural Frequencies of the Test Plate 4 under the Thermal Environment

4.4 The Test Results of Sandwich Composite Plates with Glassfiber Honeycombs

The effect of core thickness on modal parameters of sandwich composite structure under transient thermal environment is examined by using three glassfiber hexagonal cores with same cell size, cell wall thickness and cell geometry. These are test plate 5, 6 and 7. The test plate 5 also is used to see the effect of core material type. The test plate 5 is tested with three different heating rates and the results of the each test plates are presented.

4.4.1 The Test Results of the Test Plate 5

4.4.1.1 3 °C/s Heating Rate

When the heated surface heated to 160°C with 3°C/s heating rate, the unheated surface reaches nearly 29°C and test duration is 47 seconds. The temperature difference between faces reaches up to 131°C.

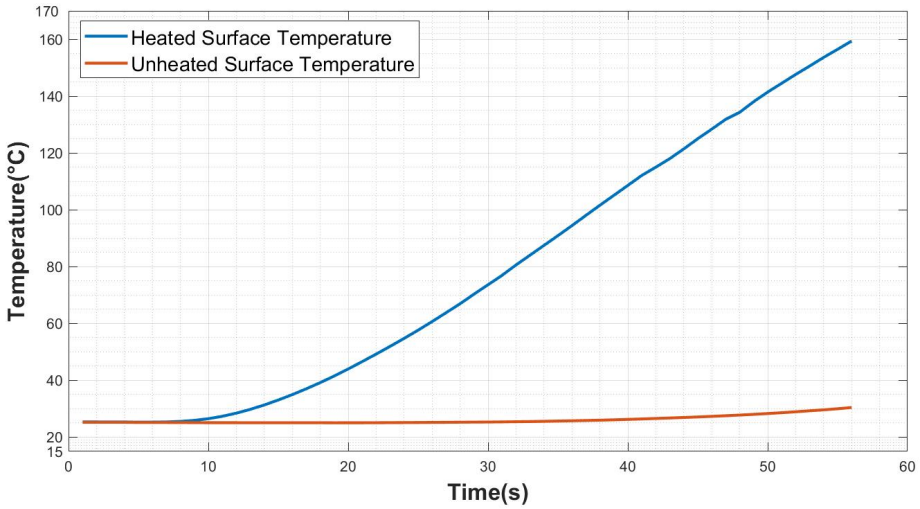

Figure 4.54: The Temperature values of the Test Plate 5 (3°C/s heating rate)

During test period, the frequency response functions (FRF) are calculated for every 20 °C temperature increase and the Figure 4.55 shows the spectrogram of the FRFs.

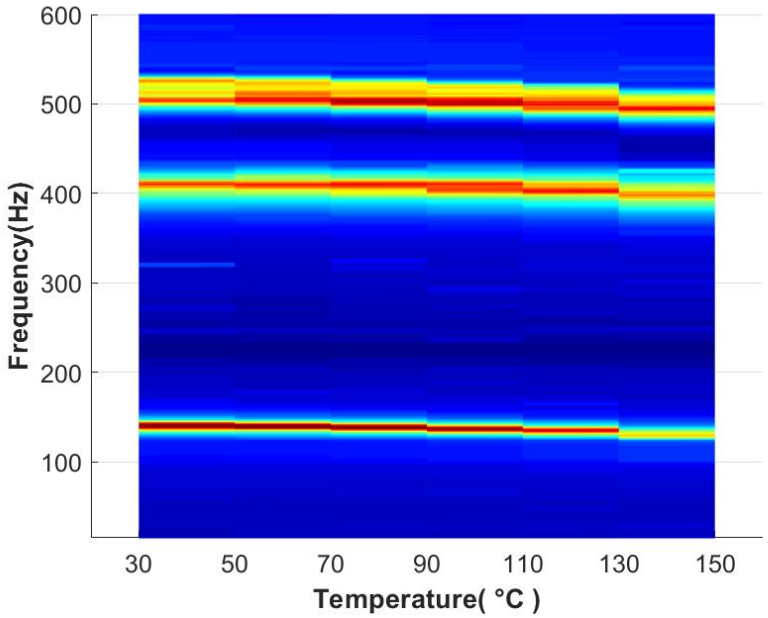

Figure 4.55: The Spectrogram of the Temperature dependent FRF changes of the Test Plate 5 (3°C/s heating rate)

Figure 4.56 and Figure 4.57 present the changes in the FRFs of the test plate 5 when heated with 3°C/s heating rate.

In Figure 4.58 the change in FRF amplitude of the first natural frequency is presented.

Table 4.20 shows the values of first three natural freuencies at every 20 °C and Figure 4.59 shows the trend of change in natural frequencies when the test plate 5 is heated with 3 °C/s heating rate. The change rate column shows the percent change of the initial frequency at the end of test period.

Table 4.20: The Natural Frequencies of the Test Plate 5 with respect to Temperature (3°C/s heating rate)

Natural Frequency (Hz)	**30 °C**	**50 °C**	**70 °C**	**90 °C**	**110 °C**	**130 °C**	**150 °C**	**Change Rate**
First Mode	140.81	139.90	138.93	137.27	135.62	132.33	131.03	-7%
Second Mode	411.18	410.35	408.99	408.67	406.33	401.49	392.98	-4%
Third Mode	507.17	502.50	500.12	501.16	498.01	493.40	483.06	-5%

Table 4.21 and Figure 4.60 present the changes of damping ratios.

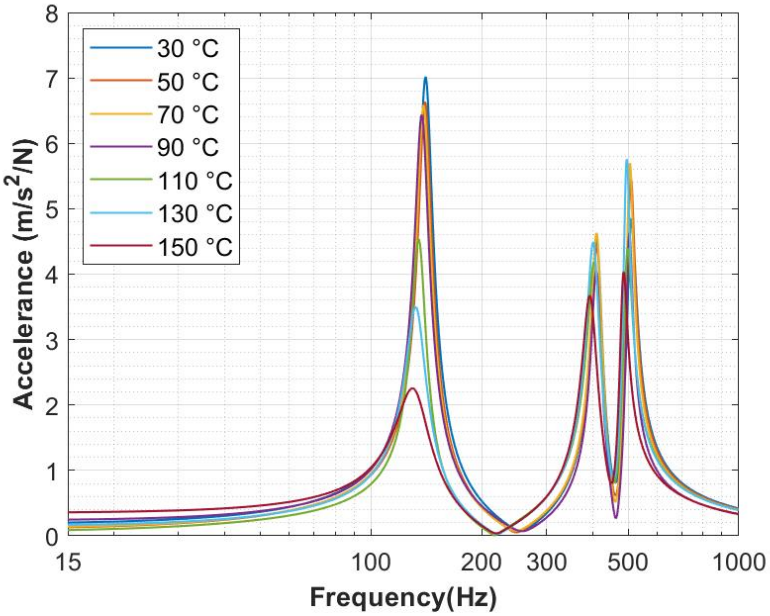

Figure 4.56: The FRFs of the Test Plate 5 under the Elevated Temperature (3°C/s heating rate)

Table 4.21: The Damping Ratios of the Test Plate 5 with respect to Temperature(3°C/s heating rate)

3 °C/s	**30 °C**	**50 °C**	**70 °C**	**90 °C**	**110 °C**	**130 °C**	**150 °C**	**Change Rate**
First Mode	0.058	0.052	0.053	0.053	0.056	0.063	0.077	34%
Second Mode	0.033	0.037	0.033	0.033	0.035	0.042	0.048	46%
Third Mode	0.029	0.023	0.020	0.023	0.024	0.022	0.024	-17%

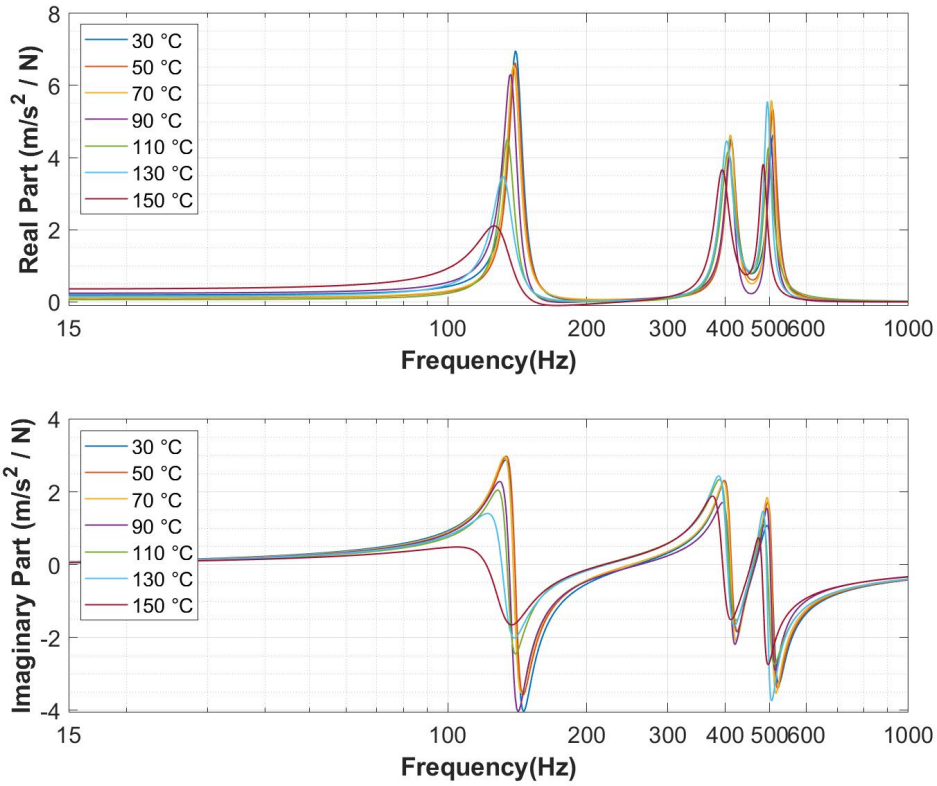

Figure 4.57: The Real and Imaginary Part of FRFs of the Test Plate 5 under Elevated Temperature (3°C/s heating rate)

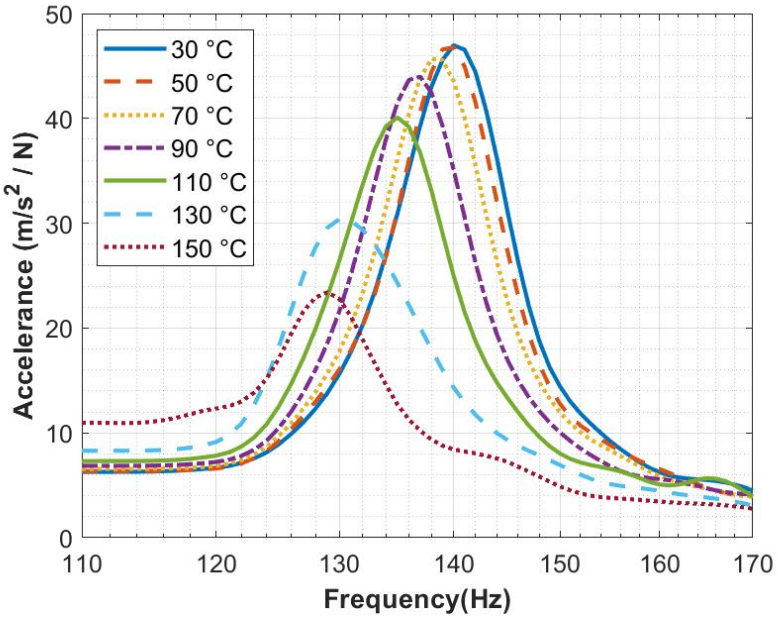

Figure 4.58: The Changes of the First Mode of the Test Plate 5 (3°C/s heating rate)

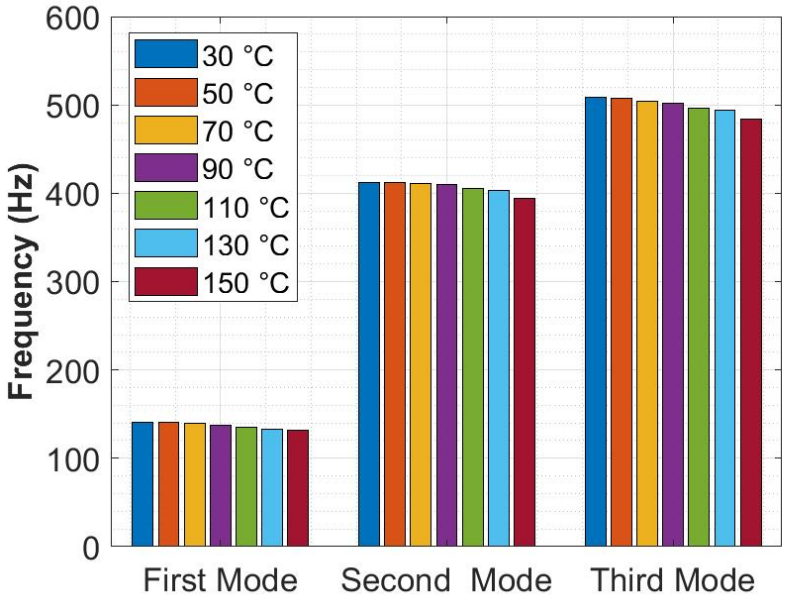

Figure 4.59: The Natural Frequencies of the Test Plate 5 with respect to Temperature (3°C/s heating rate)

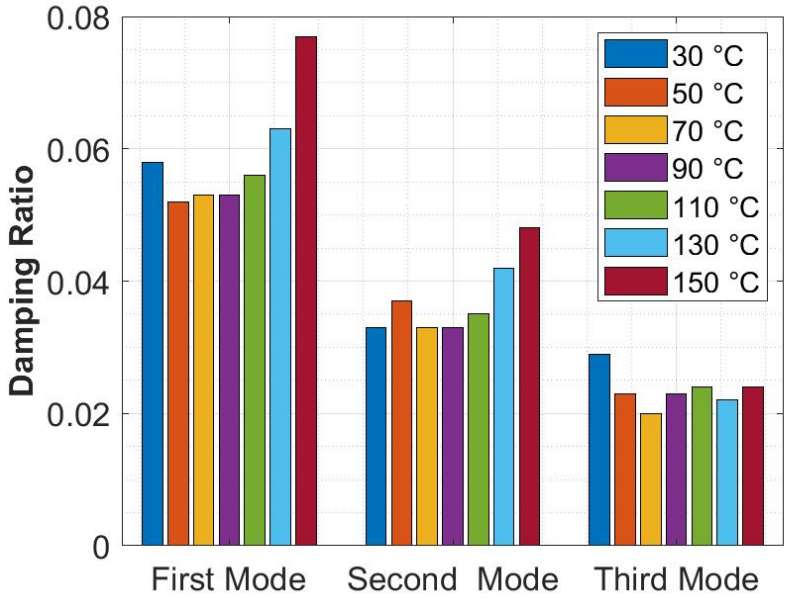

Figure 4.60: The Damping Ratios of the Test Plate 5 with respect to Temperature (3°C/s heating rate)

4.4.1.2 2 °C/s Heating Rate

In this condition, the heated surface heated with 2°C/s heating rate and when the heated surface reaches nearly 160°C the test stopped. The duration of this test condition is 70 seconds. The temperature difference between faces reaches up to 123°C.

During test period, the frequency response functions (FRF) are calculated for every 20 °C temperature increase and the Figure4.62 shows the spectrogram of the FRFs.

Figure 4.63 and Figure 4.64 present the changes in the FRFs of the test plate 5 when heated with 2°C/s heating rate.

In Figure 4.65 the change in FRF amplitude of first natural frequency is presented

Table 4.22 shows the values of first three natural freuencies at every 20 °C and Figure 4.66 shows the trend of change in natural frequencies when the test plate 5 is heated with 2 °C/s heating rate. The change rate column shows the percent change of the initial frequency at the end of test period.

Table 4.23 and Figure 4.67 present the changes of damping ratios.

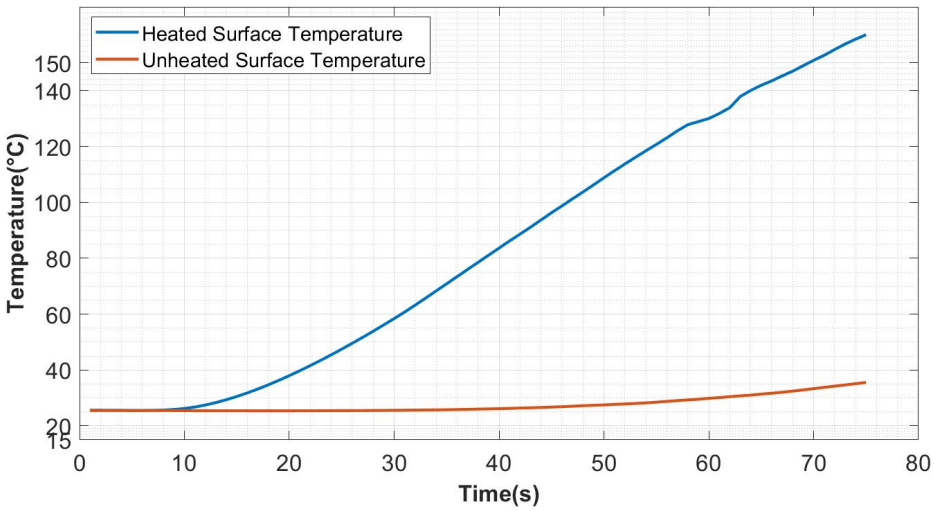

Figure 4.61: The Temperature values of the Test Plate 5 (2°C/s heating rate)

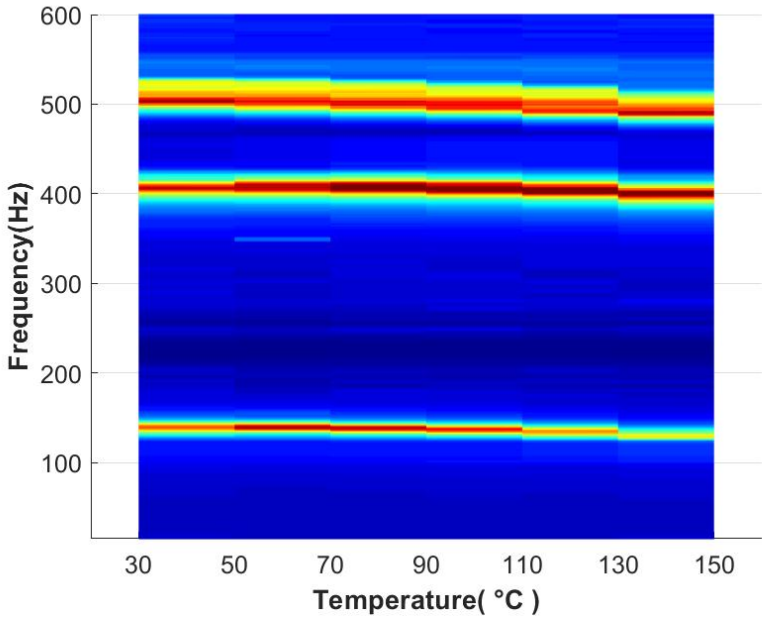

Figure 4.62: The Spectrogram of the Temperature Dependent FRF changes of the Test Plate 5 (2°C/s heating rate)

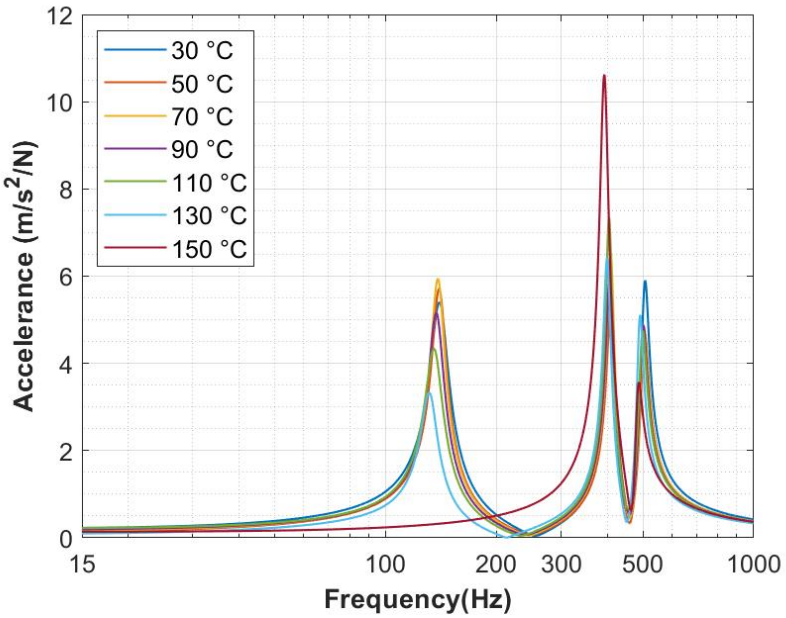

Figure 4.63: The FRFs of the Test Plate 5 under elevated Temperature (2°C/s heating rate)

Table 4.22: The Natural Frequencies of the Test Plate 5 with respect to Temperature (2°C/s heating rate)

Natural Frequency (Hz)	**30 °C**	**50 °C**	**70 °C**	**90 °C**	**110 °C**	**130 °C**	**150 °C**	**Change Rate**
First Mode	140.43	140.08	139.00	137.68	135.76	131.79	129.17	-8%
Second Mode	409.31	409.96	409.21	407.79	405.11	400.31	393.17	-4%
Third Mode	505.49	503.89	501.90	499.72	497.48	489.89	483.82	-4%

Table 4.23: The Damping Ratios of the Test Plate 5 with respect to Temperature(2°C/s heating rate)

2 °C/s	**30 °C**	**50 °C**	**70 °C**	**90 °C**	**110 °C**	**130 °C**	**150 °C**	**Change Rate**
First Mode	0.058	0.046	0.045	0.049	0.056	0.052	0.160	176%
Second Mode	0.027	0.026	0.023	0.025	0.021	0.024	0.028	6%
Third Mode	0.026	0.027	0.026	0.025	0.026	0.021	0.022	-15%

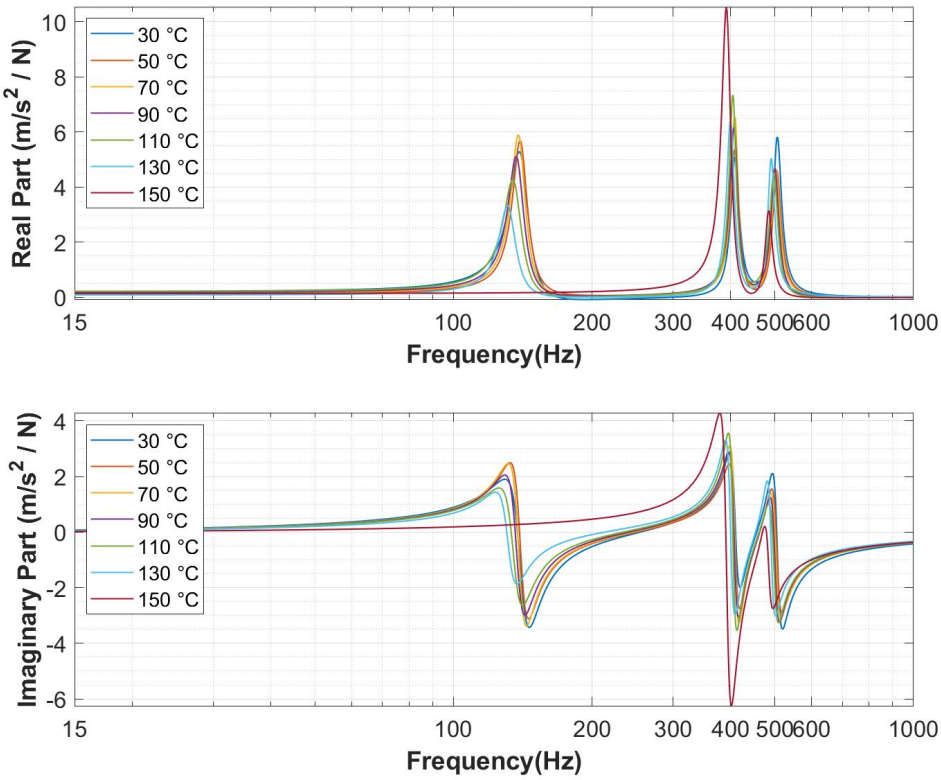

Figure 4.64: The Real and Imaginary Part of FRFs of the Test Plate 5 under Elevated Temperature (2°C/s heating rate)

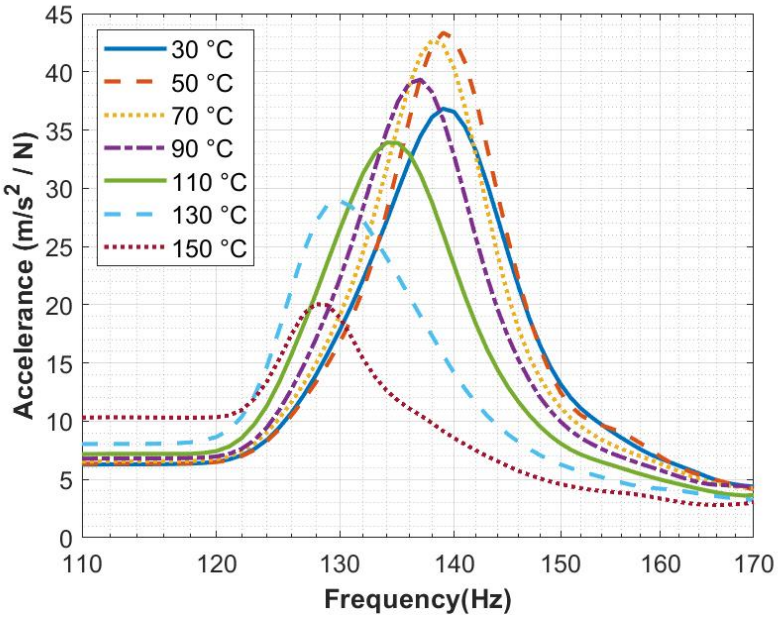

Figure 4.65: The Changes of the First Mode of the Test Plate 5 (2°C/s heating rate)

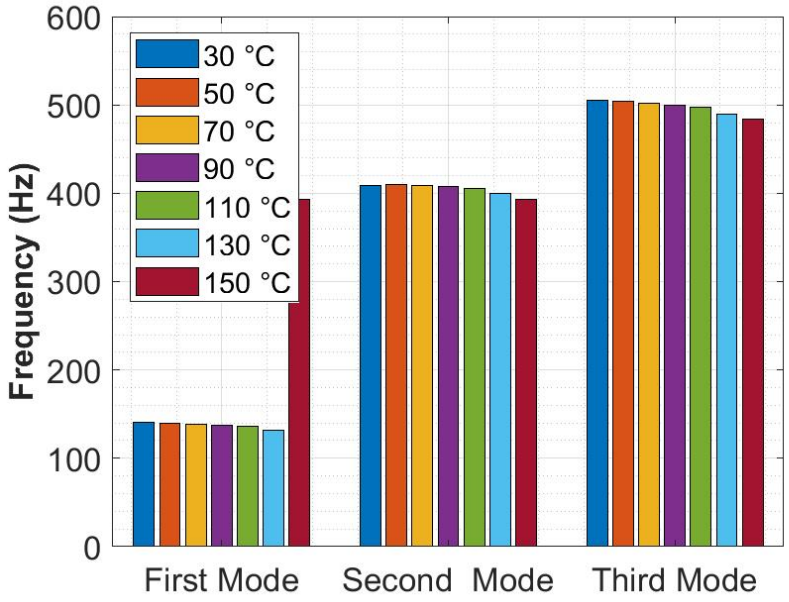

Figure 4.66: The Natural Frequencies of the Test Plate 5 with respect to Temperature (2°C/s heating rate)

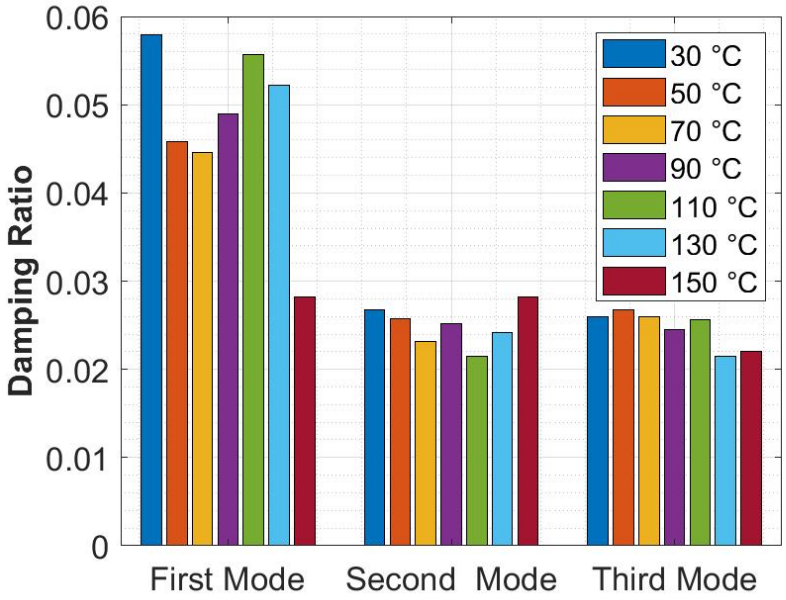

Figure 4.67: The Damping Ratios of the Test Plate 5 with respect to Temperature(2°C/s heating rate)

4.4.1.3 1 °C/s Heating Rate

In this condition, the heated surface heated with 1°C/s heating rate and when the heated surface reaches nearly 160°C the test stopped. The duration of this test condition is 141 seconds. The temperature difference between faces reaches up to 112°C.

During test period, the frequency response functions are calculated for every 20 °C temperature increase and the Figure 4.69 shows the spectrogram of the FRFs.

Figure 4.70 and Figure 4.71 present the changes in the FRFs of the test plate 5 when heated with 1°C/s heating rate.

In Figure 4.72 the change in FRF amplitude of first natural frequency is presented

Table 4.24 shows the values of first three natural freuencies at every 20 °C and Figure 4.73 shows the trend of change in natural frequencies when the test plate 5 is heated with 3 °C/s heating rate. The change rate column shows the percent change of the initial frequency at the end of test period.

The Figure 4.73 presents that the first mode of the test plate dissappered at 150 °C

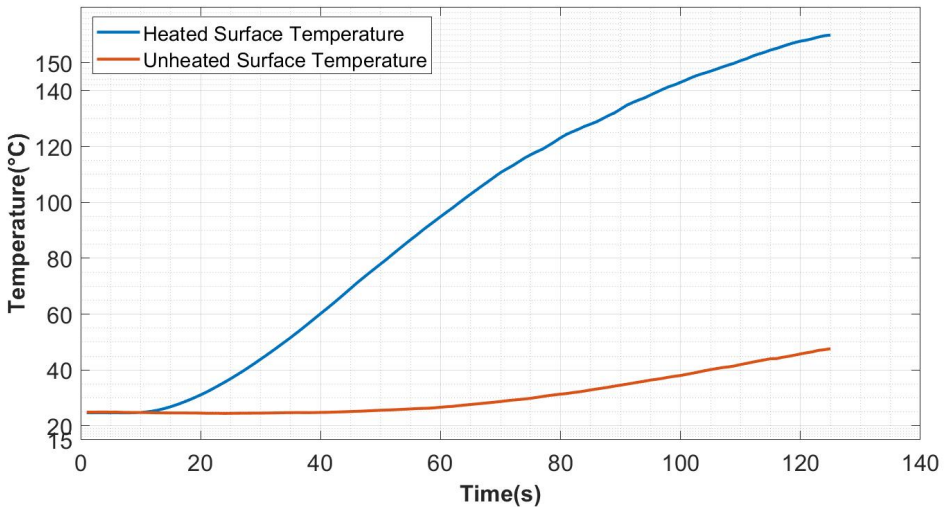

Figure 4.68: The Temperature values of the Test Plate 5 (1°C/s heating rate)

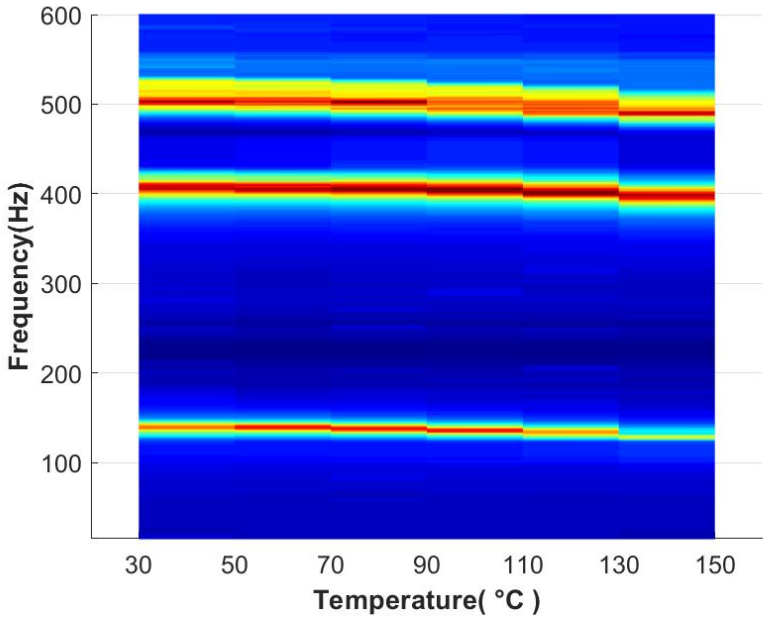

Figure 4.69: The Spectrogram of the Temperature Dependent FRF changes of the Test Plate 5 (1°C/s heating rate)

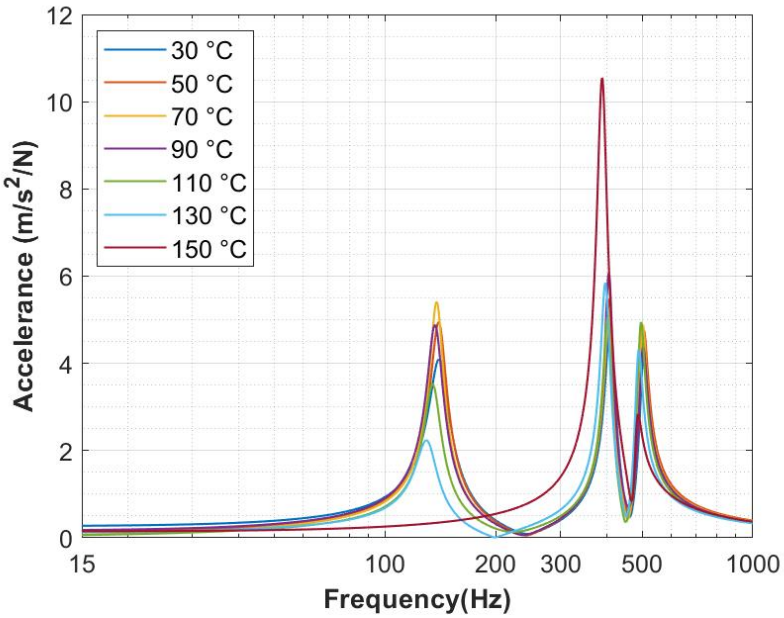

Figure 4.70: The FRFs of the Test Plate 5 under elevated Temperature (1°C/s heating rate)

because of the dramatic decrease in FRF amplitude.

Table 4.24: The Natural Frequencies of the Test Plate 5 with respect to Temperature (1°C/s heating rate)

Natural Frequency (Hz)	**30 °C**	**50 °C**	**70 °C**	**90 °C**	**110 °C**	**130 °C**	**150 °C**	**Change Rate**
First Mode	140.78	140.24	138.38	137.06	135.08	130.34	127.61	-9%
Second Mode	410.48	408.63	406.73	406.60	403.54	397.99	389.61	-5%
Third Mode	504.61	503.32	499.97	501.18	495.09	487.64	482.51	-4%

Table 4.25 and Figure 4.74 present the changes of damping ratios.

Table 4.25: The Damping Ratios of the Test Plate 5 with respect to Temperature(1°C/s heating rate)

1 °C/s	**30 °C**	**50 °C**	**70 °C**	**90 °C**	**110 °C**	**130 °C**	**150 °C**	**Change Rate**
First Mode	0.065	0.051	0.043	0.050	0.053	0.066	0.190	194%
Second Mode	0.030	0.028	0.028	0.026	0.027	0.029	0.032	8%
Third Mode	0.029	0.028	0.026	0.028	0.025	0.025	0.022	-25%

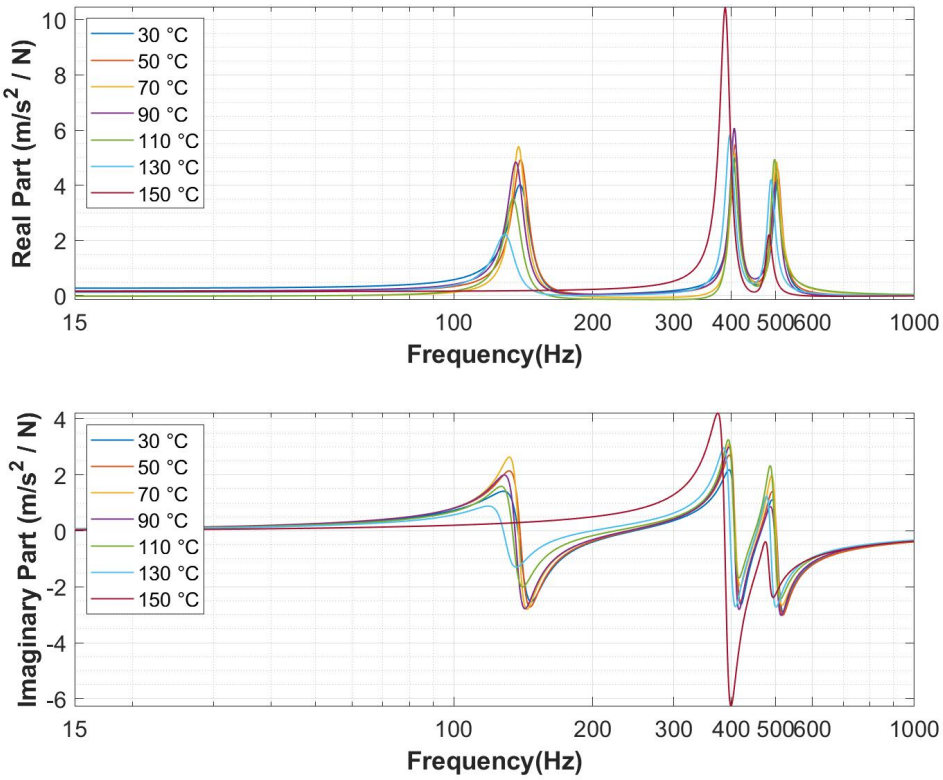

Figure 4.71: The Real and Imaginary Part of FRFs of the Test Plate 5 under Elevated Temperature (1°C/s heating rate)

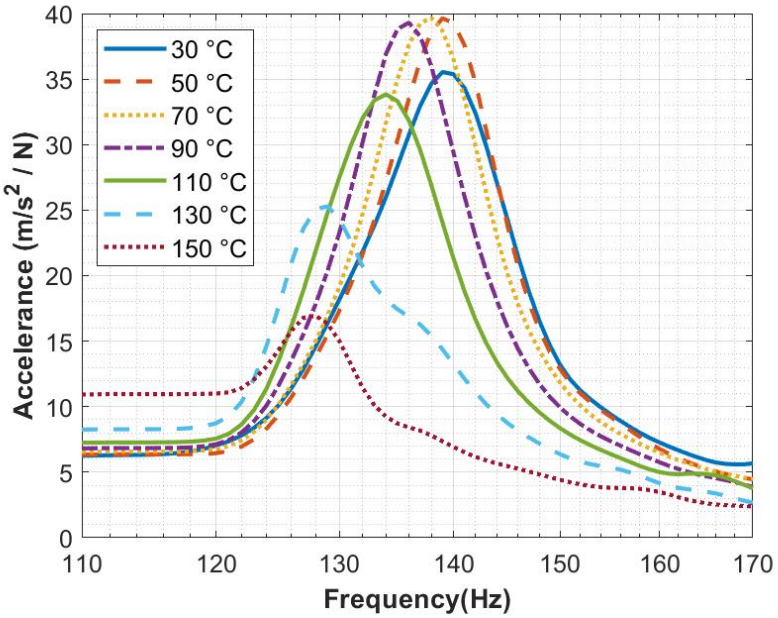

Figure 4.72: The Changes of the First Mode of the Test Plate 5 (1°C/s heating rate)

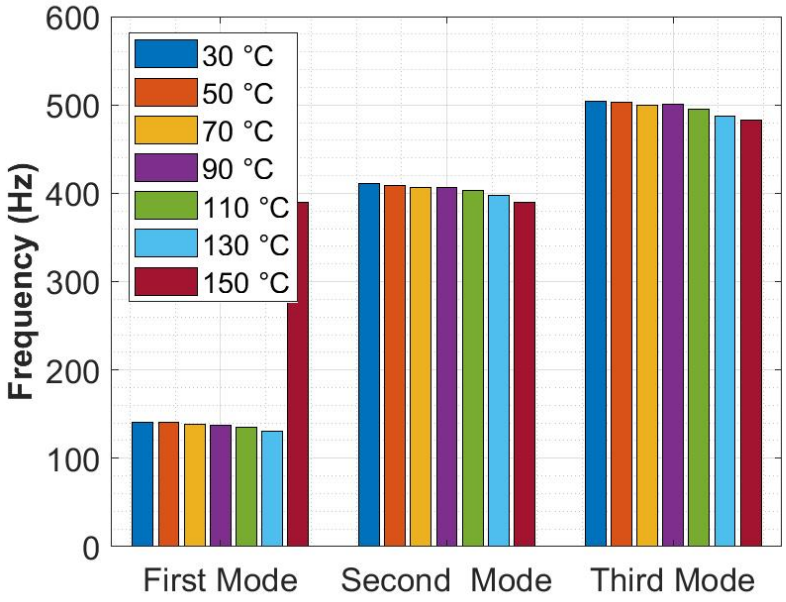

Figure 4.73: The Natural Frequencies of the Test Plate 5 with respect to Temperature (1°C/s heating rate)

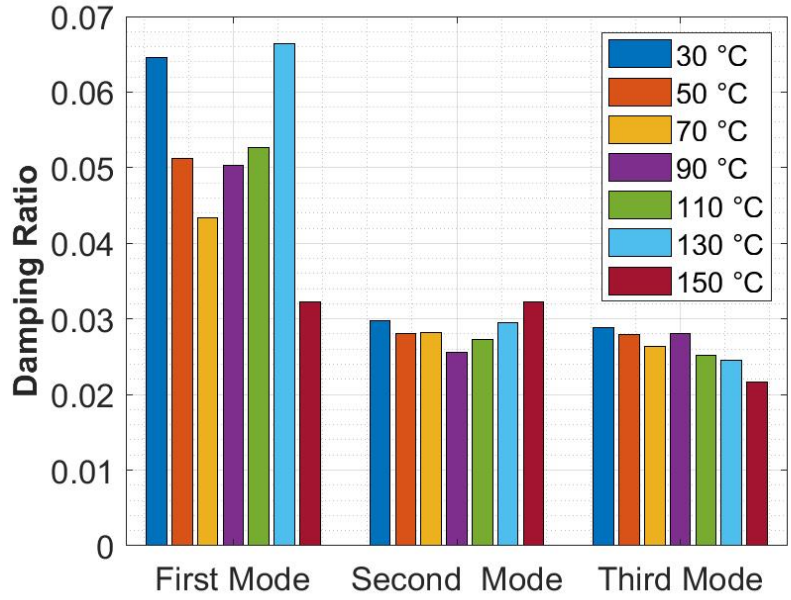

Figure 4.74: The Damping Ratios of the Test Plate 5 with respect to Temperature(1°C/s heating rate)

4.4.2 The Test Results of the Test Plate 6

Figure 4.75 presents the temperature change during the test period.

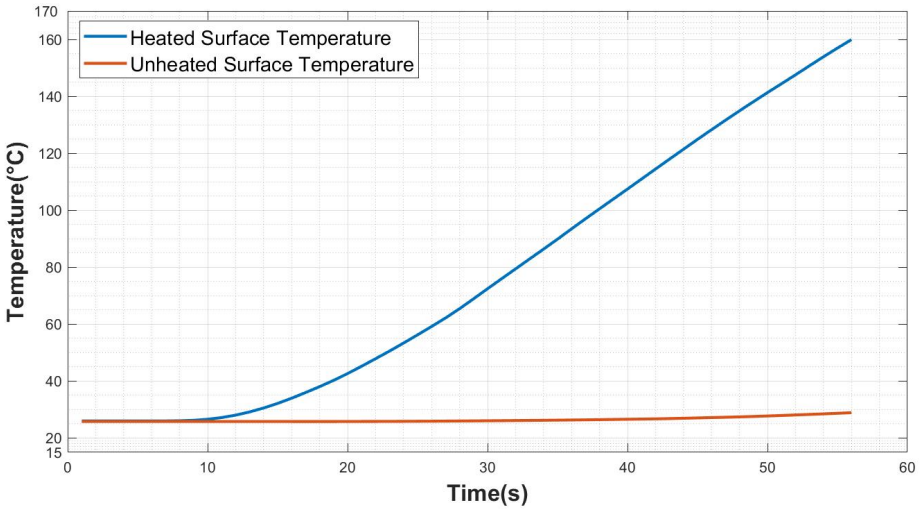

Figure 4.75: The Temperature values of the Test Plate 6 (3 °C/s heating rate)

Table 4.26 and 4.76 shows the first three natural frequencies of the test plate 6.

Table 4.26: The Natural Frequencies of Test Plate 6 under thermal environment

Natural Frequency (Hz)	**30 °C**	**50 °C**	**70 °C**	**90 °C**	**110 °C**	**130 °C**	**150 °C**	**Change Rate**
First Mode	150.91	150.17	148.38	147.07	144.54	142.45	136.89	-9%
Second Mode	429.12	423.00	422.80	426.60	423.31	415.88	408.29	-5%
Third Mode	547.67	543.65	544.51	546.47	539.38	536.82	536.00	-2%

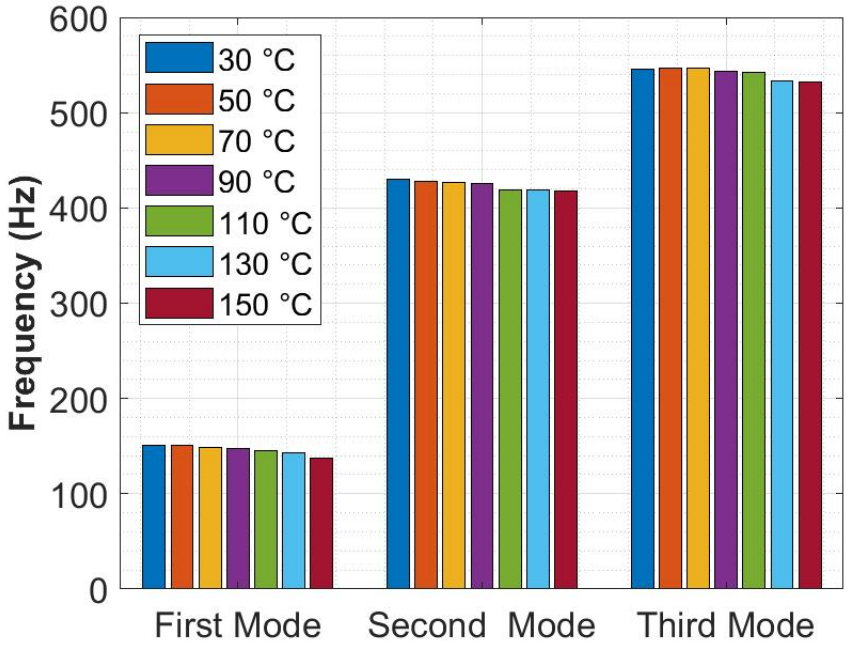

Figure 4.76: The Change of Natural Frequencies of the Test Plate 6 under Thermal Environment

Table 4.27 and Figure 4.77 shows the damping ratios of the test plate 6.

Table 4.27: The Damping Ratios of Test Plate 6 Under the Thermal Environment

3 °C/s	**30 °C**	**50 °C**	**70 °C**	**90 °C**	**110 °C**	**130 °C**	**150 °C**	**Change Rate**
First Mode	0.046	0.050	0.050	0.053	0.052	0.049	0.072	55%
Second Mode	0.034	0.060	0.048	0.026	0.025	0.025	0.034	0%
Third Mode	0.029	0.031	0.021	0.015	0.041	0.024	0.029	-1%

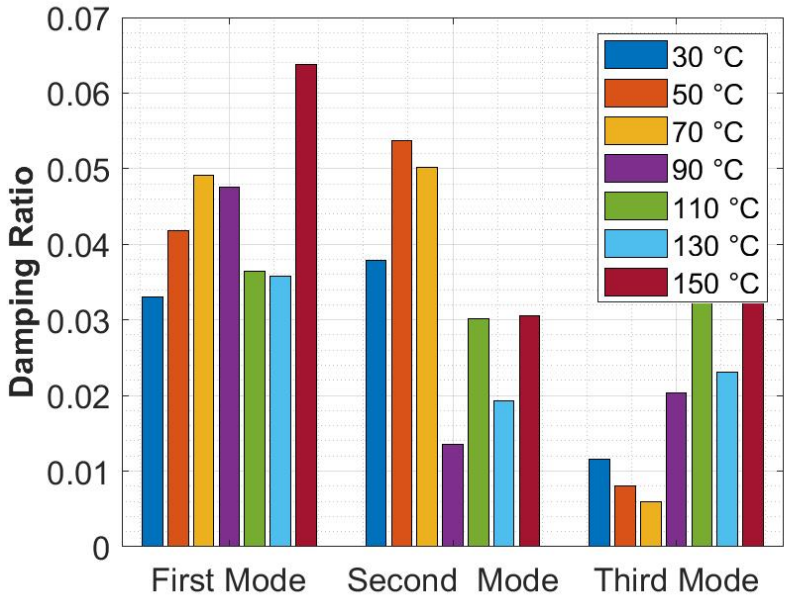

Figure 4.77: The Damping Ratios of the Test Plate 6 with Respect to the Temperature (3°C/s heating rate)

The Figure 4.78 shows the FRF amplitude changes of the first natural frequency of the test plate 6

4.4.3 The Test Results of the Test Plate 7

Figure 4.79 presents the temperature change during the test period.

Table 4.28 and 4.80 shows the first three natural frequencies of the test plate 7.

Table 4.29 and Figure 4.81 shows the damping ratios of the test plate 7.

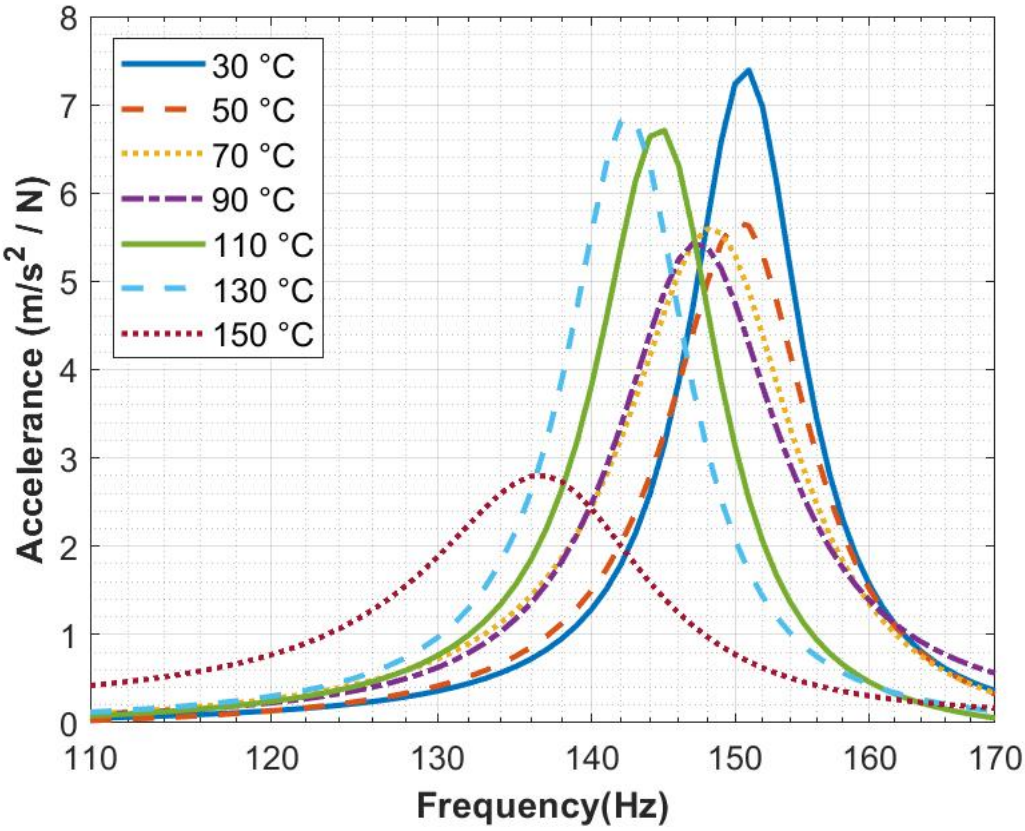

Figure 4.78: The Change of Vibration Response of the Test Plate 6 under Thermal Environment

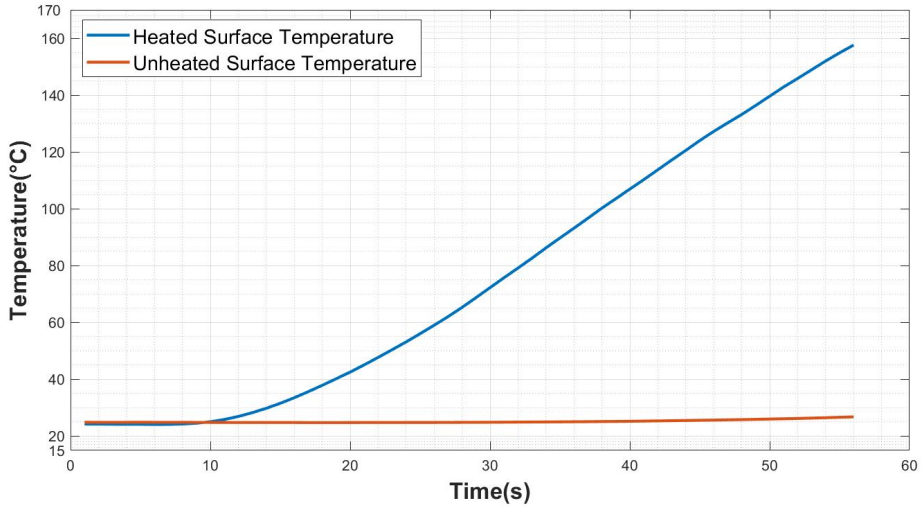

Figure 4.79: The Temperature values of the Test Plate 7 (3 °C/s heating rate)

Table 4.28: The Natural Frequencies of Test Plate 7 under thermal environment

Natural Frequency (Hz)	**30 °C**	**50 °C**	**70 °C**	**90 °C**	**110 °C**	**130 °C**	**150 °C**	**Change Rate**
First Mode	158.04	156.38	154.29	153.15	148.99	143.38	134.37	-15%
Second Mode	445.87	448.64	445.19	445.08	432.73	426.17	416.59	-7%
Third Mode	557.75	558.91	551.93	552.98	542.75	538.24	517.80	-7%

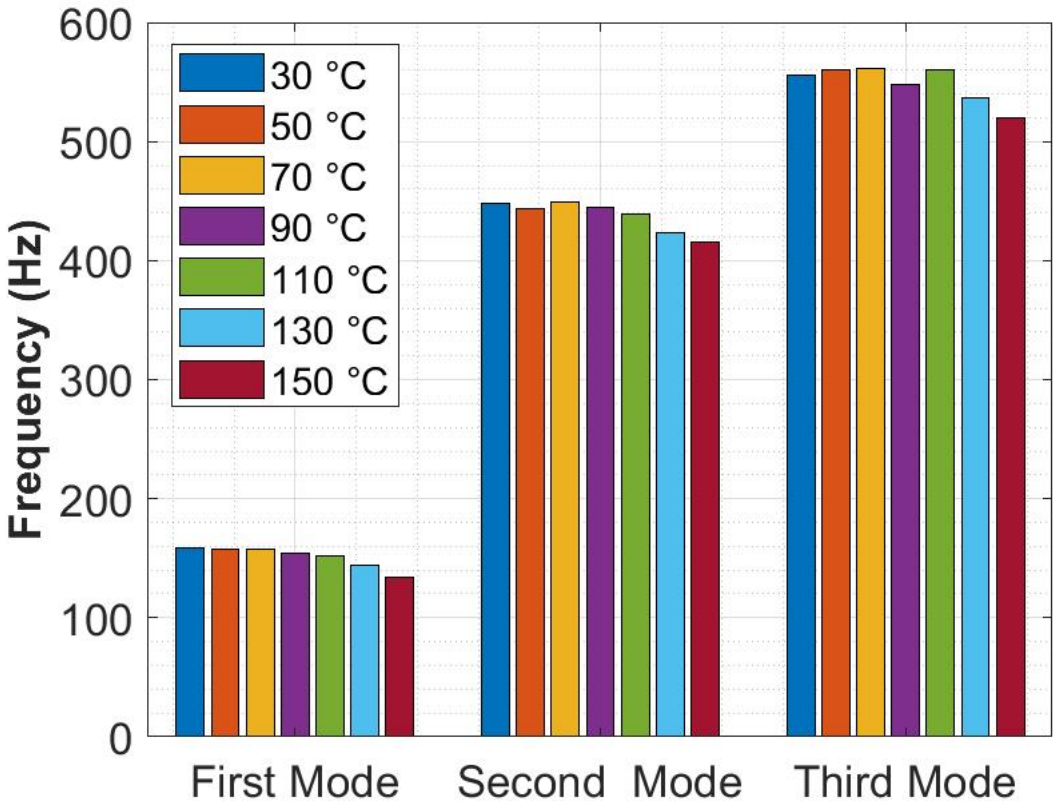

Figure 4.80: The Change of Natural Frequencies of the Test Plate 7 under the Thermal Environment

Table 4.29: The Damping Ratios of Test Plate 7 Under the Thermal Environment

3 °C/s	**30 °C**	**50 °C**	**70 °C**	**90 °C**	**110 °C**	**130 °C**	**150 °C**	**Change Rate**
First Mode	0.040	0.050	0.044	0.047	0.057	0.069	0.090	127%
Second Mode	0.028	0.035	0.042	0.048	0.032	0.035	0.043	52%
Third Mode	0.018	0.027	0.032	0.035	0.014	0.026	0.038	108%

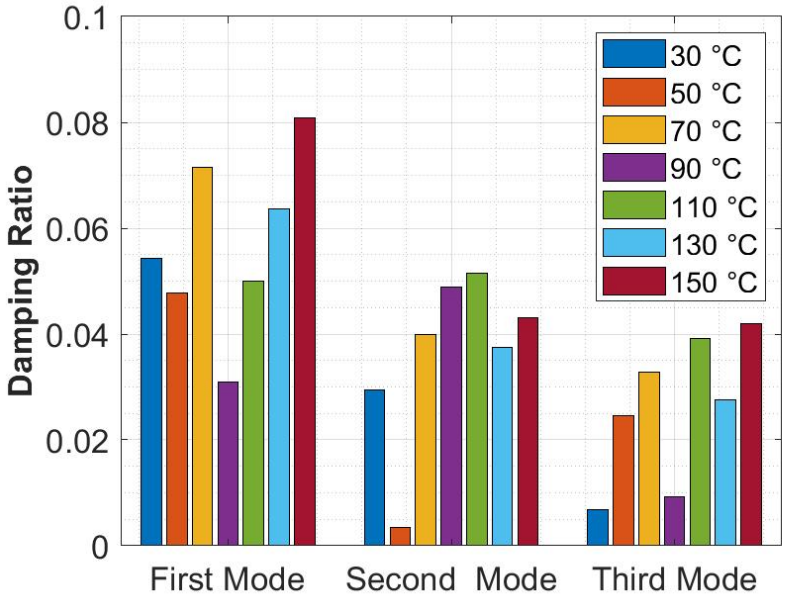

Figure 4.81: The Damping Ratios of the Test Plate 7 with Respect to Temperature (3°C/s heating rate)

The Figure 4.82 shows the FRF amplitude changes of first natural frequency of the test plate 7.

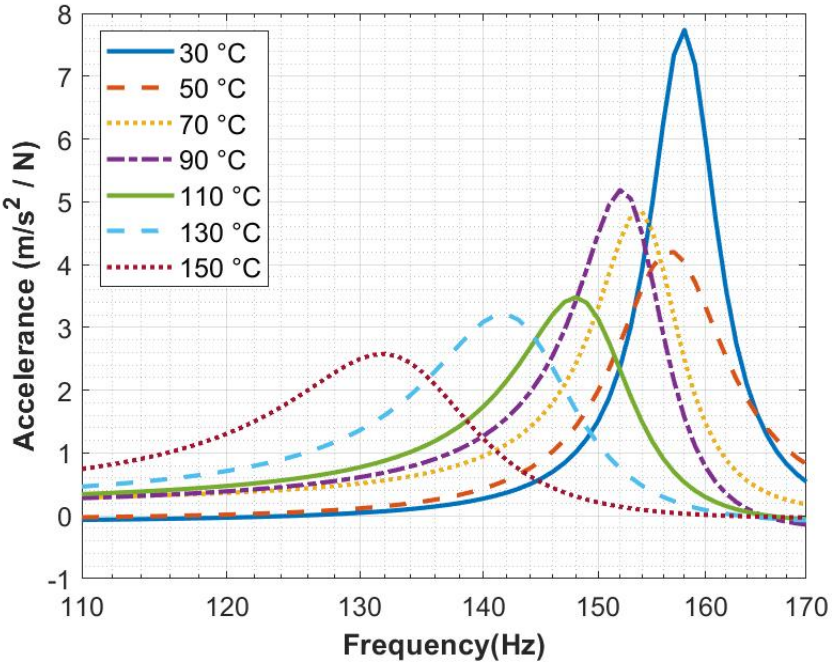

Figure 4.82: The Change of Vibration Response of the Test Plate 7 under Thermal Environment

4.5 The Comparison of The Test Results

In this section, the test results are compared to see effect of core material type, cell size, cell geometry and the core thickness on the modal parameters of sandwich composites under transient thermal environment. The mechanical properties of honeycomb core structures are directly depended on geometrical parameters of core structure. Therefore, the each test plates, which are used in study, have different mass and stiffness values. Therefore, not the values of modal parameters but the changes rates of modal parameters under transient thermal environment is compared to define the effect of different core structures. In the study,

- The test plates with aluminum honeycombs are used in the research of the effect of cell size on modal parameters under the thermal environment.

- The both test plates with Nomex honeycombs are used in the research of the effect of core shape on modal parameters under the thermal environment.

- The each test plates with glassfiber honeycombs are used in the research of the effect of core thickness on modal parameters under the thermal environment.

- The test plates 1, 3 and 5 are used in the research of the effect of core material type on modal parameters under thermal environment. The tests are repeated for different heating rates to see also the effect of the heating rates.

4.5.1 The Effect of Cell Size

The sandwich composite structures conduct heat flow through cell wall and air in cells [16]. The thermal conductivity of air is lower than aluminum and as the core cell size increases, the thermal conductivity of the core through thickness decreases. As a result, the temperature difference between faces become higher in the end of test as the cell size increases. Table 4.30 presents the temperature values and the temperature difference between the faces at the end of the test.

Table 4.30: The Face Temperatures of Test Plates 1 and 2

3 °C/s	Heated Face (°C)	Unheated Face (°C)	Difference (°C)
Test Plate 1	160.00	103.20	56.80
Test Plate 2	160.00	106.30	53.70

The first natural frequency is the most affected mode from the thermal environment for both cell sizes. The first natural frequency of the test plate 2 changes nearly %13 while the test plate 1 changes %7. The difference in the natural frequencies can be seen in Table 4.31.

Table 4.31: The Change Rates of the Natural Frequencies of the Test Plate 1 and 2

Change Rates	First Mode	Second Mode	Third Mode
Test Plate 1	-7%	-2%	-4%
Test Plate 2	-13%	-7%	-8%

Table 4.32 shows the changes in the damping ratios of the test plates with aluminum Cores.

Table 4.32: The Damping Ratios of the Test Plates 1 and 2

3 °C/s	**30 °C**	**50 °C**	**70 °C**	**90 °C**	**110 °C**	**130 °C**	**150 °C**	**Change Rate**
Test Plate 1	0.076	0.068	0.052	0.062	0.085	0.115	0.076	0%
Test Plate 2	0.029	0.027	0.028	0.041	0.054	0.045	0.158	450%

Figure 4.8 and 4.28 presents the FRF of the test plates at different temperature values and the FRF amplitudes have a decreasing trend.

The core with larger cell would have lower stiffness values than smaller cell, but the mass per unit area is also lower than the core with smaller cell. The low mass value would be an advantage for aircraft structures in many aspects like flight performance and fuel consumption. However, if the sandwich composite structure with larger core will be subjected to transient thermal environments, the change rate in natural frequencies would be problem. Therefore, the core with smaller cell size would be preferable in such thermal environments due to its low change rate in natural frequencies.

The cell size of the core structure also influences the damping performance of the composite sandwich structure. One of the reason would be change in contact area between face and core structure. The results show that the damping performance of test plate 2 is more sensitive to the temperature increament.

4.5.2 The Effect of Cell Shape

The effect of cell shape on modal parameters of sandwich composite structure under elevated thermal environment is examined by using two nomex cores with different cell geometries which are the test plates 3 and 4. The cores have identical geometrical parameters except the cell shape.

Table 4.33: The Face Temperatures of Test Plates 3 and 4 at the End of Test Period

3 °C/s	Heated Face (°C)	Unheated Face (°C)	Difference (°C)
Test Plate 3	160.00	32.55	127.45
Test Plate 4	160.00	30.96	130.04

Table 4.34 shows the change rates of the first natural frequencies of the test plates with Nomex cores. The change rates of the first natural frequencies are nearly same for both cores while the second and the third mode have different change rates.

Table 4.34: The Change Rates of the Natural Frequencies of the Test Plate 3 and 4

Change Rates	First Mode	Second Mode	Third Mode
Test Plate 3	-19%	-5%	-5%
Test Plate 4	-18%	0%	-10%

Table 4.35 shows the changes in the damping ratios of the test plates with Nomex Cores.

Table 4.35: The Damping Ratios of the Test Plates 3 and 4 under thermal environment

3 °C/s	**30 °C**	**50 °C**	**70 °C**	**90 °C**	**110 °C**	**130 °C**	**150 °C**	**Change Rate**
Test Plate 3	0.035	0.031	0.042	0.051	0.051	0.078	0.222	536%
Test Plate 4	0.051	0.045	0.053	0.055	0.057	0.082	0.126	147%

Figure 4.33 and 4.53 point out the FRF of the test plates at different temperature values and the FRF amplitudes have a decreasing trend.

The core of the test plate 3 and 4 are manufactured from Nomex with different cell shapes. The OX-Core has the ability of curving or forming in one direction. Therefore, it can be prefferable in curved structures and flat structures while the hexagonal core can be applicable on flat structures. However, the change in natural frequencies showed that, if the OX-Core is preferred instead of hexagonal core in flat structures under transient thermal environment would face with mode coupling of second and third mode. This situation could lead structural failures during operational conditions.

The damping ratio the test plate with Ox-Core is higher than the hexagonal core's at the inital temperature. However, the hexagonal core damping ratio is more sensitive to the thermal environment. At the end of test, the damping ratio of hexagonal core increase nearly 5 times while the OX-Core's increase 1.5 times. The initial damping value of the OX-Core make it more preferrable, but if it will be used in a structure that works under hot environment, the hexagonal cell shape would be more convinient.

4.5.3 The Effect of Core Thickness

Glassfiber core is a good thermal isolator and as the core thickness increases, the temperature difference between the faces increases. Table 4.36 shows the temperature values of the faces at the end of the test.

Table 4.36: The Face Temperatures of Test Plates in the End of Test Period

3 °C/s	Heated Face (°C)	Unheated Face (°C)	Difference (°C)
Test Plate 5	160.00	30.44	129.56
Test Plate 6	160.00	28.90	131.10
Test Plate 7	160.00	26.80	133.20

Table 4.37 presents the change rates of natural frequencies under thermal environment. The results show that, the natural frequencies become more sensitive to the temperature as the core thickness increases. The change rate of the natural frequencies is highest for the thickest core.

Table 4.37: The Change Rates of the Natural Frequencies of the Glassfiber Cores

Change Rates	First Mode	Second Mode	Third Mode
Test Plate 5	-7%	-4%	-5%
Test Plate 6	-9%	-5%	-2%
Test Plate 7	-15%	-7%	-7%

Table 4.38 presents the damping ratios of the first natural frequencies. The results indicate that, at the initial temperature, the damping ratio value and the core thickness have an inverse propertion and the test plate 5 has the highest damping ratio, but the thermal environment influences the damping ratio of the test plates and at the end of the test, the damping ratios become higher as the core thickness increase.

Figure 4.58, 4.78 and 4.82 point out the FRF of the test plates at different temperature values and and the FRF amplitudes have a decreasing trend.

The comparison of the EMA results of the test plates with glassfiber cores are revealed that the thermal environment mostly affects the lowest natural frequency. In design phase of a structure, it seems convinient to increase the core thickness for increasing

Table 4.38: The Damping Ratios of Test Plate 5, 6 and 7 under thermal environment

3 °C/s	**30 °C**	**50 °C**	**70 °C**	**90 °C**	**110 °C**	**130 °C**	**150 °C**	**Change Rate**
Test Plate 5	0.058	0.052	0.053	0.053	0.056	0.063	0.077	34%
Test Plate 6	0.046	0.050	0.050	0.053	0.057	0.064	0.072	55%
Test Plate 7	0.040	0.050	0.044	0.047	0.057	0.069	0.090	127%

the natural frequencies of structure. However, if the sandwich structure is a part of a design that works under high transient thermal conditions like skin panel of an aircraft, the increase in core thickness would not be a sufficient solution to avoid critical frequencies. Therefore, it must be also considered the modal parameters of structure under thermal environment when the core thickness is increased.

The test results show that the thermal environment affects the damping performance of structures. Althought the damping values of the test plates with glassfiber cores, at the last temperature step, the damping ratio of the thickest core become much higher than other cores. Generally, in structural dynamics and aeroelasticity analysis,the frequency dependent damping values are used in calculations. To get more realistic results, the effect of temperature on damping values must also be considered.

4.5.4 The Effect of Core Material Type

Due to high thermal conductivity rate of the aluminum core, when heated with a heating rate lower than 3 °C/s, the cold surface temperature reaches 120 °C before the hot surface reach to 150 °C the comparison between the each test plate is done at 130 °C/s except 3 °C/s heating condition.

Table 4.39: The Change Rate of Natural Frequencies When Heated Up to 130 °C (3°C/s heating rate)

3 °C/s	**Glassfiber Core**	**Nomex Core**	**Aluminum Core**
First Mode	-6.0%	-9.0%	-3.4%
Second Mode	-2.4%	-4.5%	-1.9%
Third Mode	-2.7%	-2.4%	-2.9%

Table 4.39 shows that, the first and second natural frequencies of the test plate with nomex core are influenced more than the other test plates while the change rate of third natural frequency of each test plates are low.

Table 4.40: The Change Rate of Natural Frequencies When Heated Up to 150 °C (3 °C/s heating rate)

3 °C/s	**Glassfiber Core**	**Nomex Core**	**Aluminum Core**
First Mode	-6.9%	-18.5%	-7.1%
Second Mode	-4.4%	-4.8%	-2.3%
Third Mode	-4.8%	-4.7%	-3.6%

Table 4.40 shows that, the temperature step between 130 °C and 150 °C is increased dramatically the first natural frequencies of the test plates with aluminum core and nomex core while the change in first natural frequency of glassfiber core nearly same as Table 4.39.

Table 4.41: The Change Rate of Natural Frequencies When Heated Up to 130 °C (2°C/s heating rate)

2 °C/s	**Glassfiber Core**	**Nomex Core**	**Aluminum Core**
First Mode	-6.2%	-6.4%	-6.6%
Second Mode	-2.2%	-2.8%	-4.1%
Third Mode	-3.1%	-5.6%	-2.7%

Table 4.41 shows that, the reduced heating rate increases the natural frequency change rate of aluminum core while it decreases the change rate of nomex core.

Table 4.42: The Change Rate of Natural Frequencies When Heated Up to 150 °C (2°C/s heating rate)

2 °C/s	**Glassfiber Core**	**Nomex Core**
First Mode	-8.0%	-12.2%
Second Mode	-3.9%	-3.6%
Third Mode	-4.3%	-4.7%

Table 4.42 and Table 4.44 show that, as the heating rate decreases the natural frequency change rate of the glassfiber core increases.

Table 4.43: The Change Rate of Natural Frequencies When Heated Up to 130 °C (1°C/s heating rate)

1 °C/s	**Glassfiber Core**	**Nomex Core**	**Aluminum Core**
First Mode	-7.4%	-8.7%	-10.3%
Second Mode	-3.0%	-1.1%	-10.9%
Third Mode	-3.4%	-0.5%	-2.9%

Table 4.44: The Change Rate of Natural Frequencies When Heated Up to 150 °C (1°C/s heating rate)

1 °C/s	**Glassfiber Core**	**Nomex Core**
First Mode	-9.4%	-13.2%
Second Mode	-5.1%	-1.4%
Third Mode	-4.4%	-2.3%

The test results show that, for each core material samples, each natural frequencies decrease as the temperature increase. The first natural frequency influenced more than the second and third natural frequencies. The decrease in heating rate influences differently each core. As heating rate decreases, the change rates in natural frequency decrease for Nomex, while increase for glassfiber and aluminum core. The change in natural frequency of the glassfiber core is lower than other cores at each heating rate.

The varioation of the temperature also influences the damping performance of the test plates. It is not possible to say that, there is a linear relationship between the temperature and the damping ratio. After 100 °C, the damping ratios are more affected with the increasing in temperature. Figure 4.85 shows that, the damping ratio of each test plates have an growing trend while the plates are heated with 3°C/s. At lower heating rates, the nomex core damping ratio increases while the other test plates fluctuate around the inital value.

Figure 4.83 shows that, the change in damping ratio is very low as temperature increases.

The FRF amplitudes of the test plates also influenced from thermal environment. It is observed that as the temperature increases, the FRF amplitudes are decrease. How-

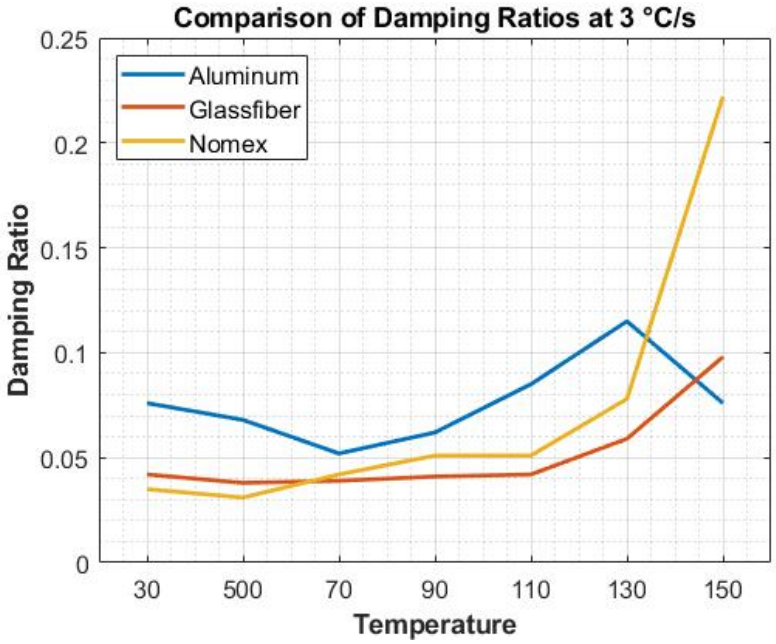

Figure 4.83: The Comparison of Damping Ratios of the Test Plates at 3°C/s Heating Rate

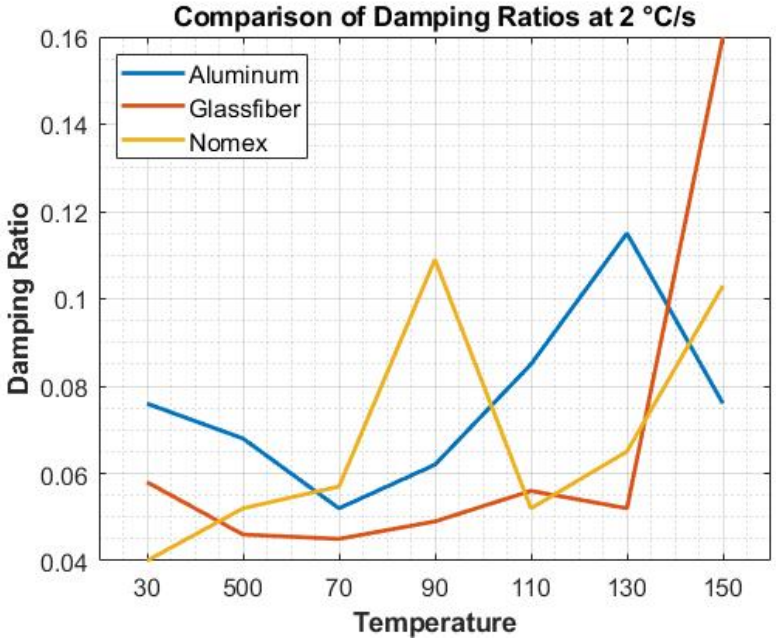

Figure 4.84: The Comparison of Damping Ratios of the Test Plates at 2°C/s Heating Rate

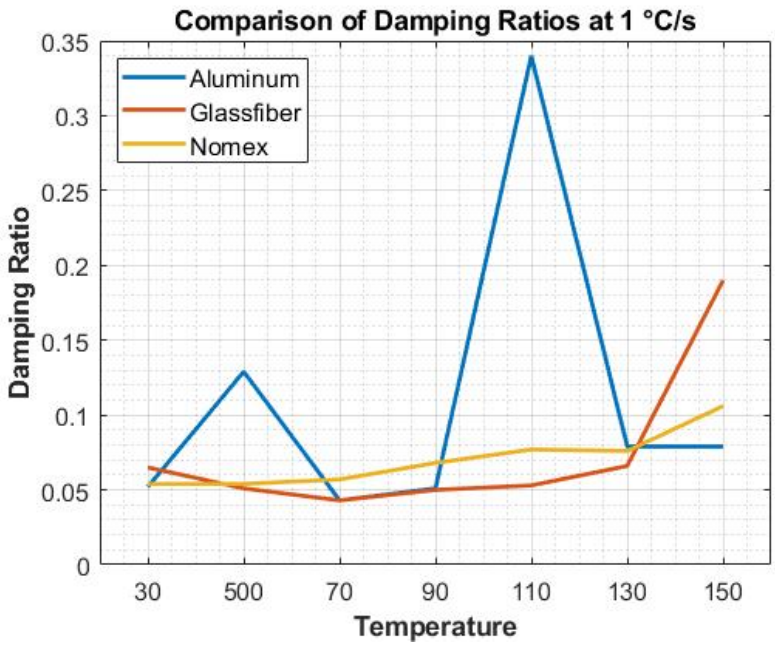

Figure 4.85: The Comparison of Damping Ratios of the Test Plates at 1°C/s Heating Rate

ever, there is no significant result observed to compare the change in FRF amplitudes of the test plates.

The test results showed that the natural frequencies of the each test plate decreased under the effect of thermal environment. The first natural frequency was the most influenced mode for each test plates. The change rate of Nomex core's first natural frequency was higher than the glassfiber core first natural frequency for each heating rates. The damping ratio of the test plate with Nomex core increased while the damping ratio of aluminum and glassfiber increased up to 130°C and decreased after that point. The FRF amplitude of the test plates decreased. The FRF amplitude of the first natural frequency decreased more than the second and the third modes. The frequency bandwidth between the second and the third modes got narrower. As the heating rate decreased, the natural frequency change rate of glassfiber and aluminum core increased while the change rate of nomex core decreased.

CHAPTER 5

DISCUSSION AND CONCLUSION

5.1 Discussion

In this chapter, the limitations and further implications of the test results are discussed.

5.1.1 Discussion on the Test Platform

Experimental Modal Analysis under elevated transient thermal environment has some challanges which must be overcome to get accured results. As an example, the accelerometers was mounted on the surface with special glue that can withstand high temperature. It can provide enough strength to protect rigid connection between test plate and the accelerometers during test period. This strength value was not constant as the temperature value increases. Therefore, the response data of the test plate with aluminum honeycomb had noise at high frequency data. All the test devices and cables were isolated from heat source. Glassfiber and Nomex honeycomb's thermal conductivity is very low and isolate accelerometers from high thermal environment. The aluminum honeycomb was a conductive material. When the hot surface temperature reached to 150 °C, the cold surface temperature, where the accelerometers were mounted, increased up to 120 °C, which was maximum operational temperature value of accelerometers and cables. Therefore, the response data of the test plate with aluminum honeycombs had noise at high frequency data and the maximum temperature value of hot surface was limited to 130 °C for 2 °C/s and 1 °C/s heating rate. During the test period, all instrumentations were isolated as possible as from heat. But, it would be good choice to use laser vibrometer to measure vibration response of the test plates to minimize the effect of heating.

5.1.2 Discussion on the Test Procedure

The EMA was performed under transient thermal environment and to apply same thermal environment, it was important to start test at the same steady-state test plate temperature value. The temperature of the surfaces were measured by thermocouples that placed on the test plates. After each test, the test plate was cooled down to room temperature and waited at least 10 minutes to let core temperature was also have the room temperature value. Because of there was not any placed thermocouple at the core of plate, it was assumed that the waiting time will be enough to perform each test at the room temperature.

5.1.3 Discussion on the Thermal Environment

The test was performed under transient thermal environment with three different heating rates. As the heating rate decreases, the control of heating rate was challenging. The heat array did not have an active control system and the same amount of heat exerted on hot face during the test. As the heating rates decreased, the heat loss from the plate increased at higher temperature values because of the increased test time. Therefore, at higher temperature values, the linear increase trend of the temperature of hot face was slightly reduced at lower heating rates.

The test plates were hanged with bungee cords to minimize thermal stress and simulate free-free boundary conditions. Therefore, no isolation is applied along the thickness of core structure and the heat loss was occurred. This heat loss could lead a non-uniform temperature distribution on the faces but the effect of this situation was assumed negligible.

5.1.4 Discussion on Data Analysis

In the data analysis process, a mathematical modelling program was used to analyze vibration response data and get FRF of the test plates at every 20 °C temperature step. The reason of 20 °C temperature step was to increase time duration of data segments. The lowering the temperature step decreased the testing time between steps and the

shorter testing time would leads statistical error. In data analysis, frequency step is chosen as 1 Hz to observe changes in natural frequency values. Using smaller frequency step in short time test data also increases the statistical error in response functions. However, the statistical error does not shift the natural frequencies. It may cause an unrealistic increase in FRF amplitude.

5.2 Conclusion

In this study, it was aimed to examine the effect of core parameters on the dynamical characteristics of sandwich composite structures under thermal environment by using Experimental Modal Analysis method. The honeycomb cores structures were selected from aluminum, glassfiber and Nomex materials. These core structures were used for manufacturing of the sandwich composite test plates. An unique test platform was designed to apply EMA under thermal environment. Test platform has a heat array that simulates the transient thermal environment while the test plates were tested to see the changes in natural frequencies, damping and FRF responses at every 20°C increasing temperature steps.

The test results showed that, under transient thermal environment, as the core cell size increased, the difference in natural frequency of the test plate increases and the damping of structure became more sensitive to temperature. The first natural frequency of the hexagonal and the OX-Core affected in similar values, however the second mode of the OX-Core was equal to initial value while the third mode decreased more than the third mode of hexagonal core. The damping ratio of the hexagonal core was more sensitive to thermal environment than the Ox-Core damping ratio. The study on the effect of core thickness showed that the dynamic characteristics of sandwich structure became more sensitive to thermal environment as the core thickness increased. The change rate of natural frequencies and damping ratios were the highest for the thickest core. The results also showed that, each core material type affected from thermal environment differently. The dynamic characteristics of the test plate with Nomex core was the most sensitive while the glassfiber core affected less than the other test plates when heated with 3 °C/s heating rate. As the heating rate lowered, the change rates in natural frequency decrease for Nomex while increase for glassfiber and aluminum

core. The difference in glassfiber core is lower than other cores at each heating rate. The FRF responses of each test plates decreased under the effect of transient thermal environment.

It is important to consider the effect of heating on the change of dynamic characteristics of sandwich composite structures that works under thermal and vibration environments to avoid any vibration based structural failures. In design phase, the effect of selected core material on dynamic behavior of structure under thermal environment should to be considered as a selection criterion, and proper core structure must be preferred.

5.3 Future Works

The study results showed that the importance of core parameters on dynamic characteristics of sandwich composite structures under thermal environments. To develop the study further, the future works are planned and

- The effect of curvature on sandwich structures,
- The effect of constrain and boundary conditions,
- The development of a FEA solution that simulates the behavior of sandwich composite plates under transient thermal environments

will be studied.

REFERENCES

[1] B. Piquet, "FAST (Flight Airworthiness Support Technology)"Special Edition A350XWB," *Airbus Technical Magazine*, no. June, pp. 1–25, 2013.

[2] M. J. Grayson, Charles E.; French, Mary; O'Brien, *Traditional Archery from Six Continents*. Columbia and London: University of Missouri Press, 2007.

[3] D. Daniel, "Composing Composites," Last visit on June 15, 2020.

[4] "Composite Structures – Fiber Forms and Types of Fiber," Last visit on June 15, 2020.

[5] HEXCEL, "HexWeb® Honeycomb Sandwich Design Technology," Tech. Rep. AGU 075b, 2000.

[6] HEXCEL, "Typical Products for Jets," Last visit on June 15, 2020.

[7] Hexcel Composites, "HexWeb® Honeycomb Attributes and Properties," tech. rep., HEXCEL, 1999.

[8] P. Avitabile, *Modal Testing: A Practitioner's Guide*. The Society for Experimental Mechanics and John Wiley & Sons Ltd, 2018.

[9] V. V. Vasiliev and E. V. Morozov, *Advanced Mechanics of Composite Materials*. Great Britain: Elsevier Ltd, 2007.

[10] SAE, *Composite Materials Handbook - Vol.6 Structural Sandwich Composites*, vol. 6. 2013.

[11] J. Kaye, "The Transient Temperature Distribution in a Wing Flying at Supersonic Speeds," *Journal of the Aeronautical Sciences*, vol. 17, no. 12, pp. 787–807, 1950.

[12] R. J. Monaghan, "Formulae and Approximations for Aerodynamic Heating Rates in high speed flight," Tech. Rep. 360, AERONAUTICAL RESEARCH COUNCIL, LONDON, 1957.

[13] E. R. van Driest, "The Problem of Aerodynamic Heating," *AERONAUTICAL ENGINEERING REVIEW*, pp. 26–41, 1956.

[14] J. Rohacs, I. Jankovics, I. Gal, J. Bakunowicz, G. Mingione, and A. Carozza, "Small Aircraft Infrared Radiation Measurements Supporting the Engine Airframe Aero-thermal Integration," *Periodica Polytechnica Transportation Engineering*, 2018.

[15] K. Daryabeigi, "Heat Transfer in Adhesively Bonded Honeycomb Core Panels," *Journal of Thermophysics and Heat Transfer*, vol. 16, no. 2, 2002.

[16] J. Fatemi and M. H. Lemmen, "Effective Thermal/Mechanical Properties of Honeycomb Core Panels for Hot Structure Applications," *Journal of Spacecraft and Rockets*, vol. 46, no. 3, pp. 514–525, 2009.

[17] J. D. D. Melo and D. W. Radford, "Time and temperature dependence of the viscoelastic properties of PEEK/IM7," *Journal of Composite Materials*, vol. 38, no. 20, pp. 1815–1830, 2004.

[18] J. D. D. Melo and D. W. Radford, "Time and temperature dependence of the viscoelastic properties of CFRP by dynamic mechanical analysis," *Composite Structures*, vol. 70, pp. 240–253, 2005.

[19] Q. Liu and Y. Zhao, "Role of Anisotropic Core in Vibration Properties of Honeycomb Sandwich Panels," *Journal of Thermoplastic Composite Materials*, vol. 15, no. 1, 2002.

[20] G. Aklilu, S. Adali, and G. Bright, "Temperature Effect on Mechanical Properties of Carbon, Glass and Hybrid Polymer Composite Specimens," *International Journal of Engineering Research in Africa*, vol. 39, pp. 119–138, 2018.

[21] K. E. Vosteen, Louis F. ; Fuller, "BEHAVIOR OF A CANTILEVER PLATE UNDER RAPID-HEATING CONDITIONS," tech. rep., 1955.

[22] R. T. L.F. Vosteen, R.R. McWhitney, "Effect of Transient Heating on Vibration Frequencies of Simple Wing Structures," tech. rep., National Advisory Committee for Aeronautics, WASHINGTON, 1957.

[23] H. L. Dryden and J. E. Duberg, "AEROELASTIC EFFECTS OF AERODYNAMIC HEATING," *ADVISORY GROUP FOR AERONAUTICAL RESEARCH AND DEVELOPMENT*, 1955.

[24] H. L. Runyan and N. H. Jones, "EFFECT OF AERODYNAMIC HEATING ON THE FLUTTER OF A RECTANGULAR WING AT A MACH NUMBER OF 2," Tech. Rep. 411, NATIONAL ADVISORY COMMITTEE FOR AERONAUTICS, WASHINGTON, 1958.

[25] M. W. Kehoe and V. C. Deaton, "Correlation of Analytical and Experimental Hot Structure Vibration Results," tech. rep., NASA, 1993.

[26] H. T. Snyder and M. W. Kehoe, "Determination of the Effects of Heating on Modal Characteristics of an Aluminum Plate with Application to Hypersonic Vehicles," tech. rep., NASA Technical Memorandum, 1991.

[27] Y. W. Kim, "Temperature dependent vibration analysis of functionally graded rectangular plates," *Journal of Sound and Vibration*, vol. 284, no. 3-5, pp. 531–549, 2005.

[28] P. Vangipuram and N. Ganesan, "Buckling and vibration of rectangular composite viscoelastic sandwich plates under thermal loads," *Composite Structures*, vol. 77, pp. 419–429, 2007.

[29] P. Jeyaraj, C. Padmanabhan, and N. Ganesan, "Vibration and Acoustic Response of an Isotropic Plate in a Thermal Environment," *Journal of Vibration and Acoustics*, vol. 130, no. 5, pp. 051005–1 – 051005–6, 2008.

[30] P. Jeyaraj, N. Ganesan, and C. Padmanabhan, "Vibration and acoustic response of a composite plate with inherent material damping in a thermal environment," *Journal of Sound and Vibration*, vol. 320, no. 1-2, pp. 322–338, 2009.

[31] Y. Liu and Y. Li, "Vibration and acoustic response of rectangular sandwich plate under thermal environment," *Shock and Vibration*, vol. 20, no. 5, pp. 1011–1030, 2013.

[32] H. Liu, X. Li, and F. Liu, "Thermal Modal Analysis of Wing Considering Aerodynamic Heating," in *Proceedings - 6th International Symposium on Computational Intelligence and Design, ISCID 2013*, vol. 2, pp. 372–375, 2013.

[33] Q. Geng, H. Li, and Y. Li, "Dynamic and acoustic response of a clamped rectangular plate in thermal environments: Experiment and numerical simulation," *The Journal of the Acoustical Society of America*, vol. 135, no. 5, pp. 2674–2682, 2014.

[34] S. Zhao, Y. Wang, D. Wu, Y. Pu, and L. Shang, "Experimental Research on Thermal-Vibration for Composite Trilaminated Wing Structure," *Advanced Materials Research*, vol. 1061-1062, pp. 799–805, 2014.

[35] X. Zhang, K. Yu, Y. Bai, and R. Zhao, "Thermal vibration characteristics of fiber-reinforced mullite sandwich structure with ceramic foams core," *Composite Structures*, vol. 131, pp. 99–106, 2015.

[36] H. Cheng, H. Li, W. Zhang, B. Liu, Z. Wu, and F. Kong, "Effects of Radiation Heating on Modal Characteristics of Panel Structures," *Journal of Spacecraft and Rockets*, vol. 52, no. 4, pp. 1228–1235, 2015.

[37] X. Li and K. Yu, "Vibration and acoustic responses of composite and sandwich panels under thermal environment," *Composite Structures*, vol. 131, pp. 1040–1049, 2015.

[38] M. Du, Q. Geng, and Y. ming Li, "Vibrational and acoustic responses of a laminated plate with temperature gradient along the thickness," *Composite Structures*, vol. 157, pp. 483–493, 2016.

[39] G. Vio, D. Munk, and D. Verstraete, "Transient Temperature Effects on the Aerothermoelastic Response of a Simple Wing," *Aerospace*, vol. 5, 2018.

[40] Y. Bai, K. Yu, J. Zhao, and R. Zhao, "Experimental and Simulation Investigation of Temperature Effects on Modal Characteristics of Composite Honeycomb Structure," *Composite Structures*, vol. 201, pp. 816–827, 2018.

[41] T. Johnson, "History of Composites," Last visit on June 15, 2020.

[42] M. C.-Y. Niu, *Composite Airframe Structures*. Hong Kong Conmilit Press Ltd., 3 ed., 2010.

[43] J. Reddy, *Mechanics of Laminated Composite Plates and Shells Theory and Analysis*. CRC Press, 2003.

[44] W. S. Burton and A. K. Noor, "Assessment of continuum models for sandwich panel honeycomb cores," *Computer Methods in Applied Mechanics and Engineering*, vol. 145, pp. 341–360, 1997.

[45] Dynamic Testing Agency, *Handbook on Modal Testing*. 1993.

[46] O. Døssing and Bruel & Kjaer, "Structural Testing Part 2:Modal Analysis and Simulation," tech. rep., 1998.

[47] D. J. Ewins, *Modal Testing: Theory, Practice and Application*. 2001.

[48] PLASCORE, "PAMG-XR1 5056 Aluminum Honeycomb," tech. rep.

[49] EURO-COMPOSITES, "Mechanical Properties of ECG Honeycomb," tech. rep.

[50] HEXCEL, "HexWeb ® HRH-10 Aramid Fibre/Phenolic Honeycomb," tech. rep., 2017.

[51] J. S. Bendat and A. G. Piersol, *Random Data Analysis and Measurement Procedures*. 2010.

[52] C. Lalanne, *Mechanical Vibration and Shock Analysis: Third edition*, vol. 3. 2014.

APPENDIX B

PUBLICATIONS DERIVED FROM THE THESIS STUDY

- KISA, Enes Erkan; SÜMER, Bilsay "THE EFFECTS OF HONEYCOMB CORE THICKNESS ON DYNAMIC RESPONSE CHANGE RATE OF THE SANDWICH COMPOSITE STRUCTURE UNDER THERMAL ENVIRONMENT" 27th International Congress on Sound and Vibration (ICSV27) Prague, July 2021 (accepted)
- KISA, Enes Erkan; SÜMER, Bilsay; KOÇ, İlker Murat; ARPACI, Alaittin Arpacı "The Effects of Honeycomb Cell Size on Dynamic Response of Sandwich Composite Structure under Thermal Environment" 11th International Conference on Structural Dynamics (EURODYN2020) Athena, November 2021 (accepted)